2022. 02. 10. 물리학회 원자분자분과 겨울학교

레이저 주파수 안정화

한국표준과학연구원 (KRISS)

이원규

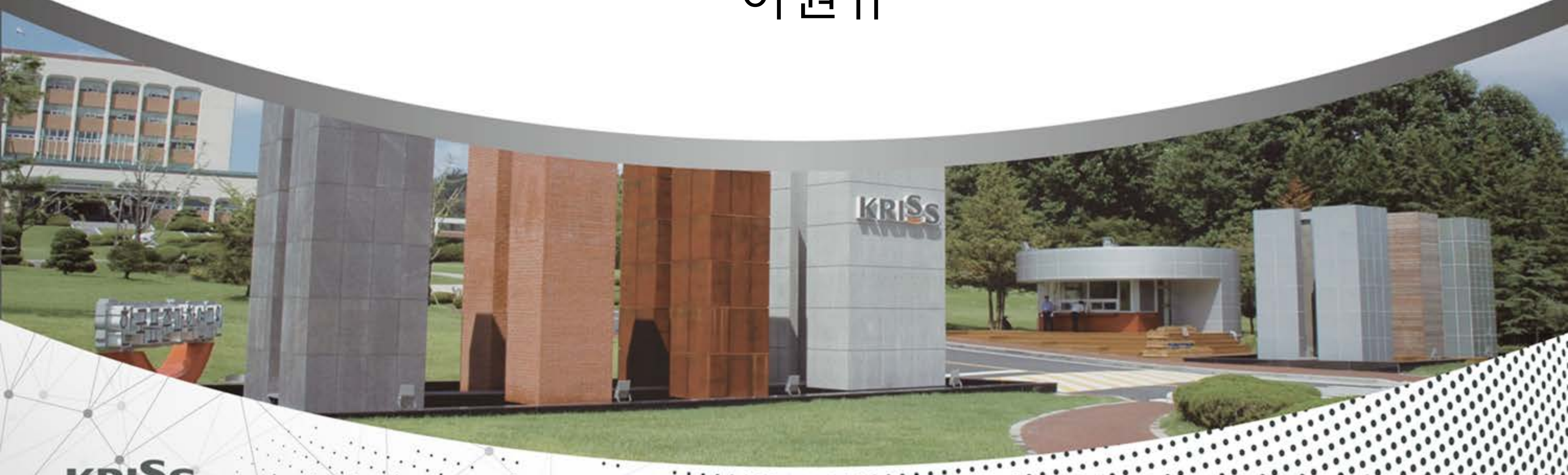

주파수는 가장 정확히 잴 수 있는 측정량

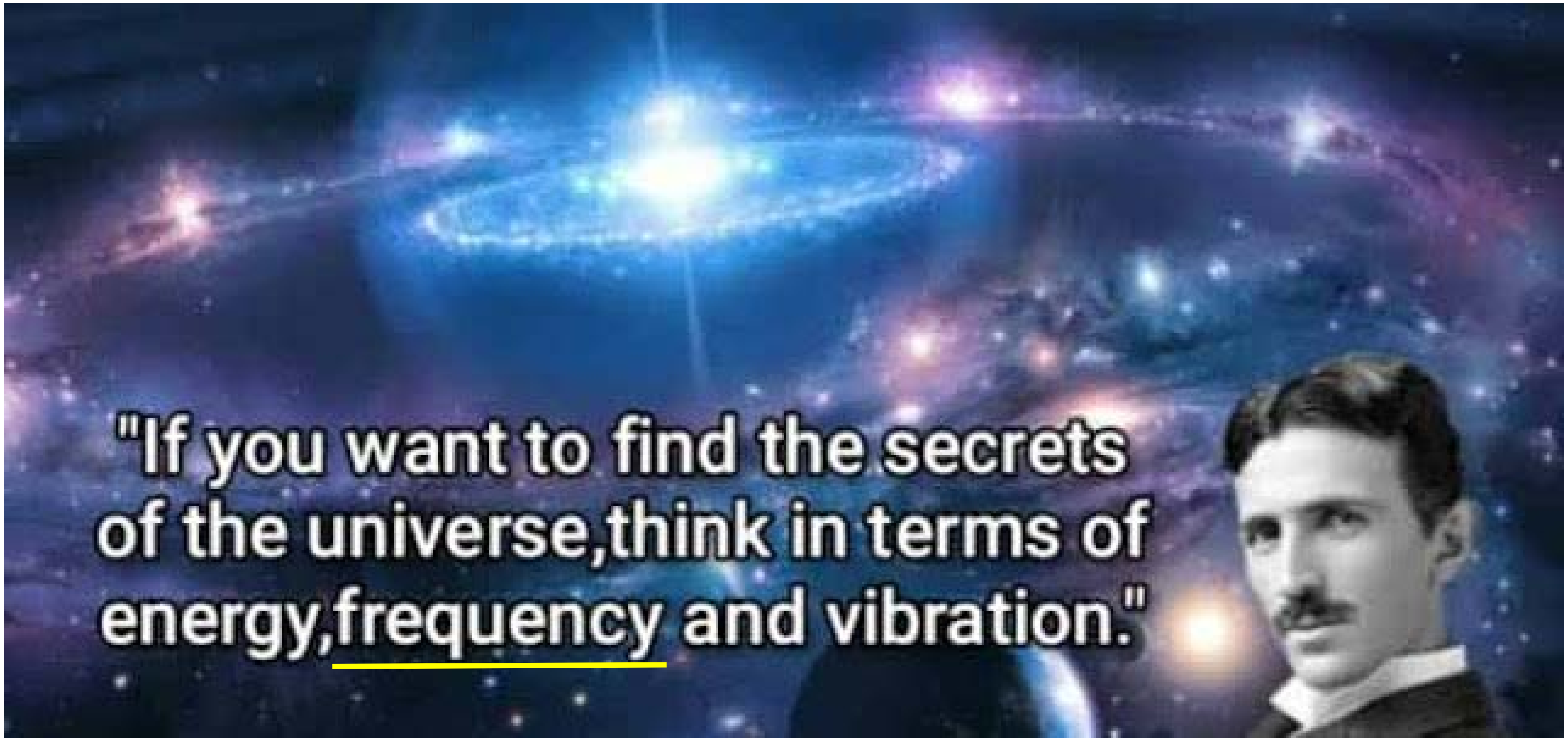

Nikola Tesla (1856~1943)

https://1001inspiringquotes.blogspot.com/2019/05/if-you-want-to-find-secrets-of.html

주파수는 가장 정확히 잴 수 있는 측정량

Uncertainties of Physical Realizations of the Base SI Units

Physical Quantity	SI base unit	Uncertainties of physical realization
luminous intensity	cd	4×10^{-5}
thermodynamic temperature	K	3×10^{-7}
amount of substance	mol	2×10^{-8}
electric current	A	1×10^{-8}
mass	kg	1×10^{-8}
length	m	1×10^{-12}
time	s	1.5×10^{-16}

Cs fountain clock

https://www.bipm.org/en/publications/mises-en-pratique

주파수는 가장 정확히 잴 수 있는 측정량

❖ Frequency ratio of Yb lattice clock and Sr lattice clock (18-digit accuracy)

= 1.207 507 039 343 337 8482(82) [1]

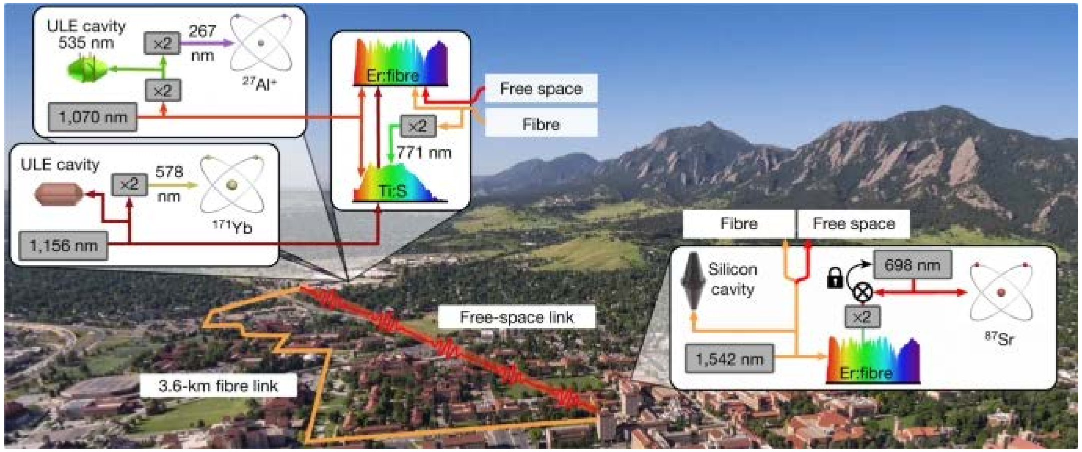

❖ CODATA (committee on data) fundamental constants recommended values [2]

- Rydberg frequency ; 3.289 841 960 2508(64)×10^{15} Hz (1.9×10^{-12})
- 양성자-전자 질량비 ; 1836.152 673 43(11) (6.0×10^{-11})
- 진공 유전율 ; 8.854 187 8128(13)×10^{-12} Fm^{-1} (1.5×10^{-10})
- ……
- 만유인력상수 ; 6.674 30(15)×10^{-11} $m^3kg^{-1}s^{-2}$ (2.2×10^{-5})

[1] Nature volume 591, 564–569 (2021)
[2] RevModPhys.93.025010(2021)-CODATA recommended values of the fundamental physical constants: 2018

레이저 주파수의 시간에 따른 변화

Linewidth? frequency noise? Jitter? Drift?
Short-term noise?
Long-term noise?

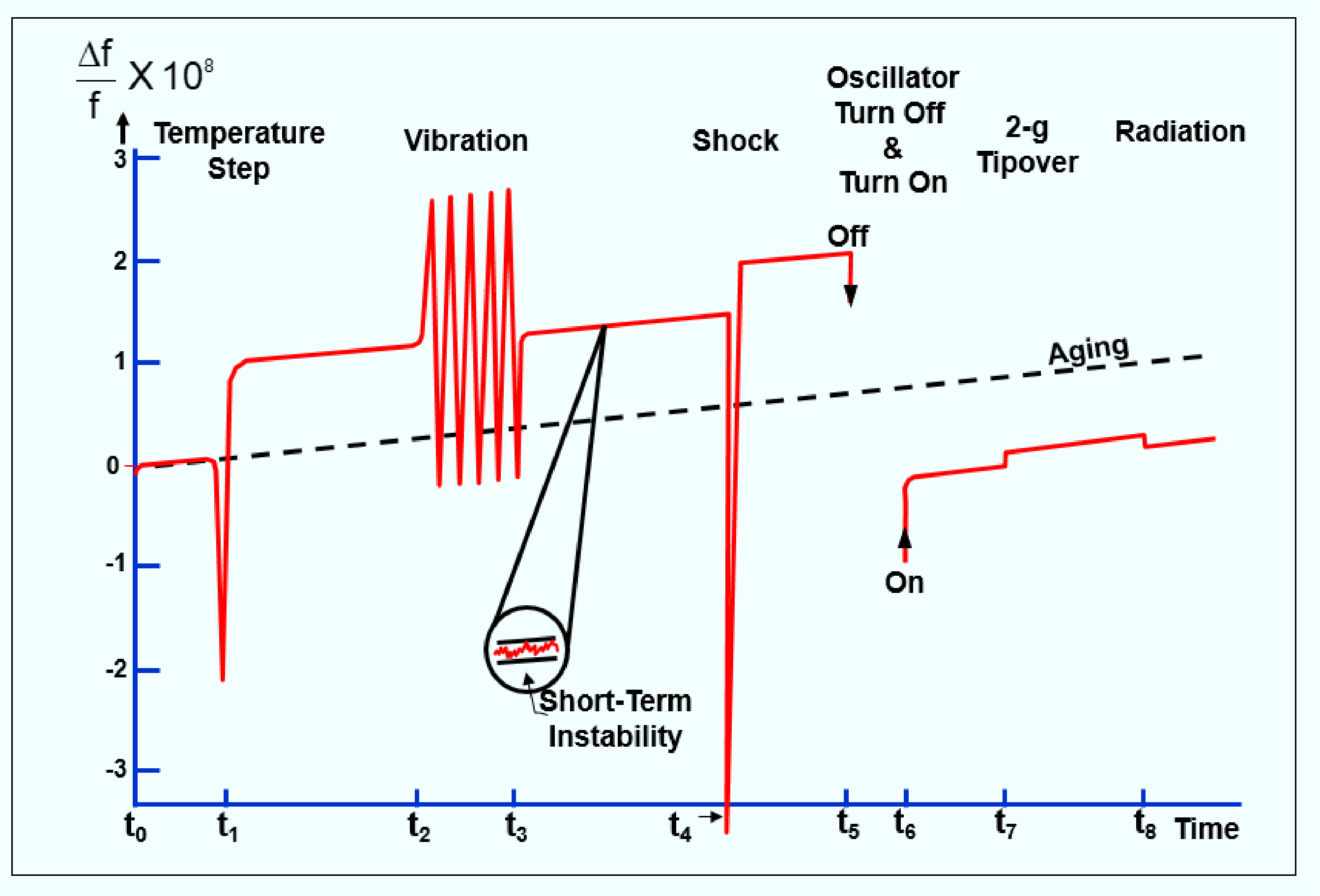

J.R. Vig 2014-10-Quartz Crystal Resonators and Oscillators - For Frequency Control and Timing Applications - A Tutorial

Accuracy, Precision, and Stability

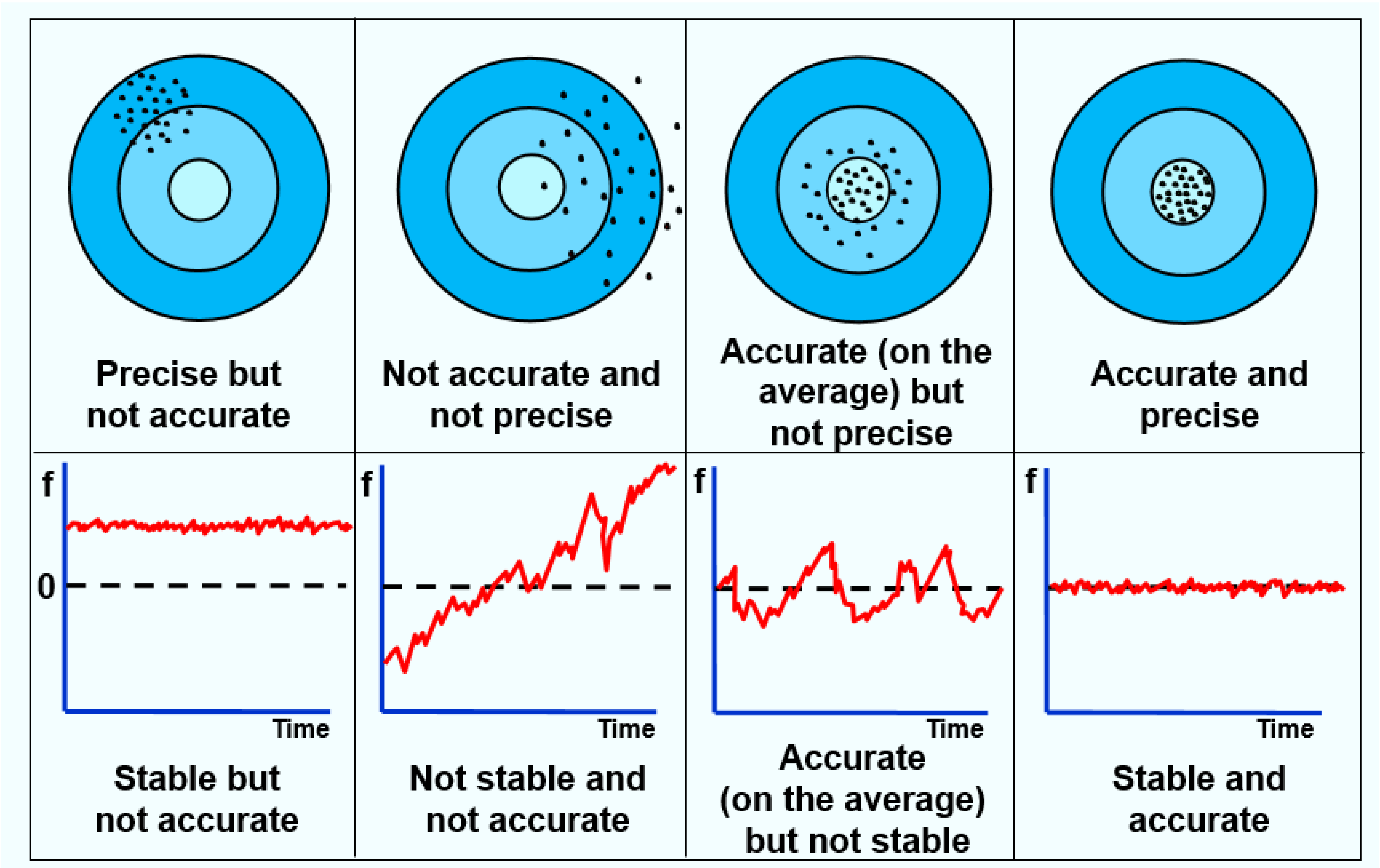

Short-term 안정도의 world-record

PRL 118, 263202 (2017) PHYSICAL REVIEW LETTERS week ending 30 JUNE 2017

1.5 μm Lasers with Sub-10 mHz Linewidth

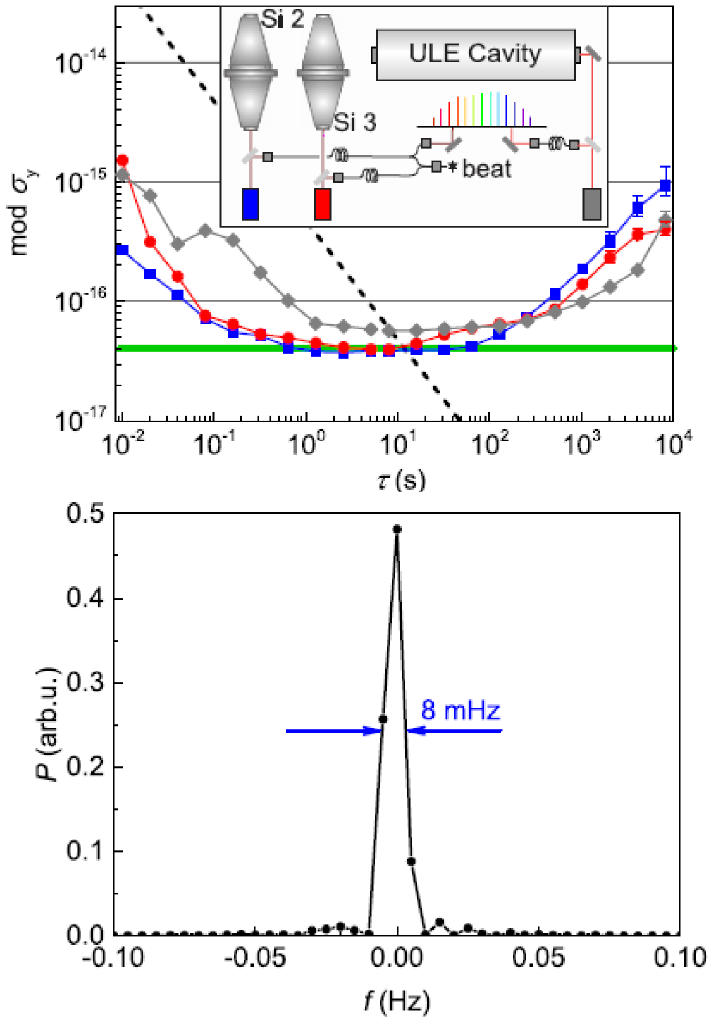

nature photonics ARTICLES
PUBLISHED ONLINE: 9 SEPTEMBER 2012 | DOI: 10.1038/NPHOTON.2012.217

A sub-40-mHz-linewidth laser based on a silicon single-crystal optical cavity

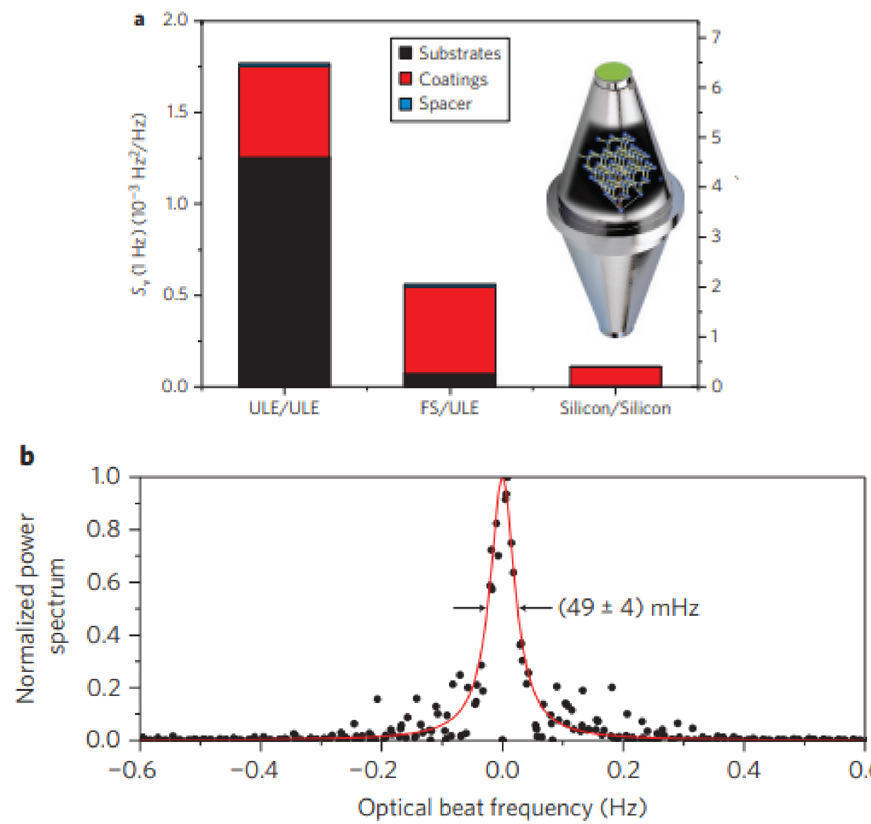

[1] PhysRevLett.118.263202(2017)1.5 μm Lasers with Sub-10 mHz Linewidth
[2] Nat. Photon. 6, 687(2012) A sub-40 mHz linewidth laser based on a silicon single-crystal optical cavity

Long-term 안정도, 정확도의 world-record

LETTER

https://doi.org/10.1038/s41586-018-0738-2

Atomic clock performance enabling geodesy below the centimetre level

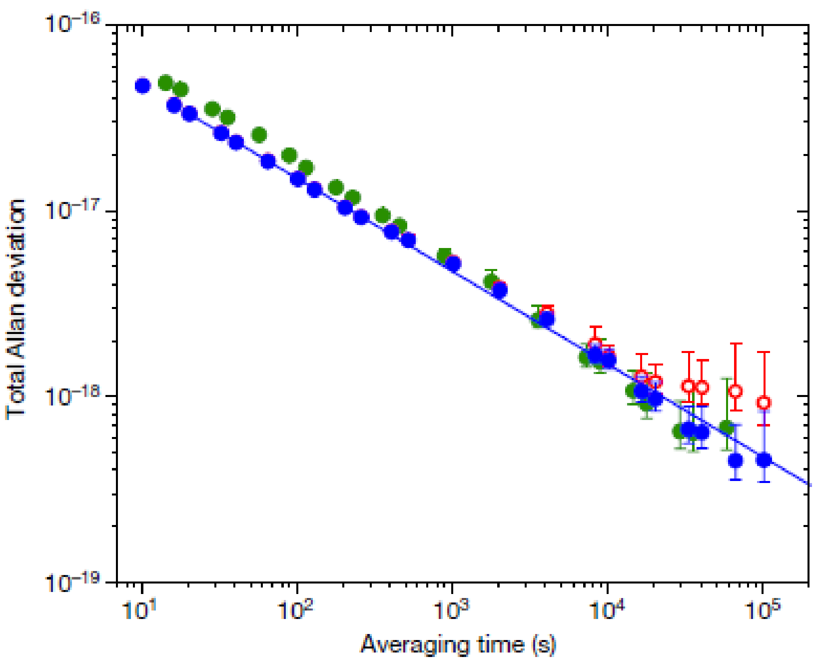

Measurement instability of 3.2×10^{-19}

Table 1 | Characteristic clock uncertainty budget

Shift	Yb-1 shift	Yb-1 uncertainty
Background gas collisions	−5.5	0.5
Spin polarization	0	<0.3
Cold collisions[a]	−0.21	0.07
Doppler	0	<0.02
BBR[a]	−2,361.2	0.9
Lattice light (model)	0	0.3
Travelling wave contamination	0	<0.1
Lattice light (experimental)	−1.5	0.8
Second-order Zeeman[a]	−118.1	0.2
DC Stark	0	<0.07
Probe Stark	0.02	0.01
Line pulling	0	<0.1
Tunnelling	0	<0.001
Servo error	0.03	0.05
Optical frequency synthesis	0	<0.1
Total	**−2,486.5**	**1.4**
Gravity shift from TT reference surface	180,819	6
Total shift from TT reference surface	**178,333**	**6**

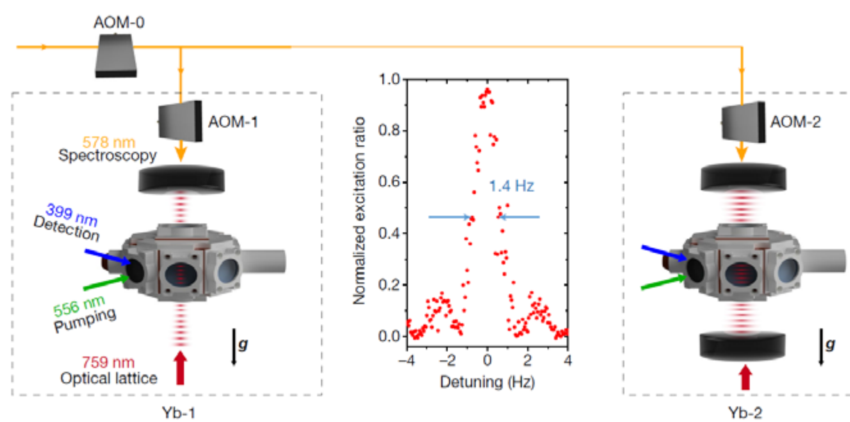

[1] nature564-87(2018)Atomic clock performance enabling geodesy below the centimetre level

레이저 주파수 안정화

Frequency stabilization of a laser:

Transfer of the frequency stability from an optical frequency reference to the laser source

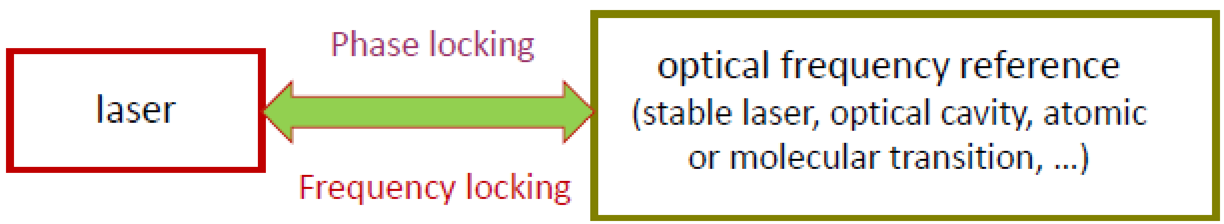

→ Servo systems

Frédéric Du Burck – The servo loop, the mean to reach stability transfer

레이저 주파수 안정화

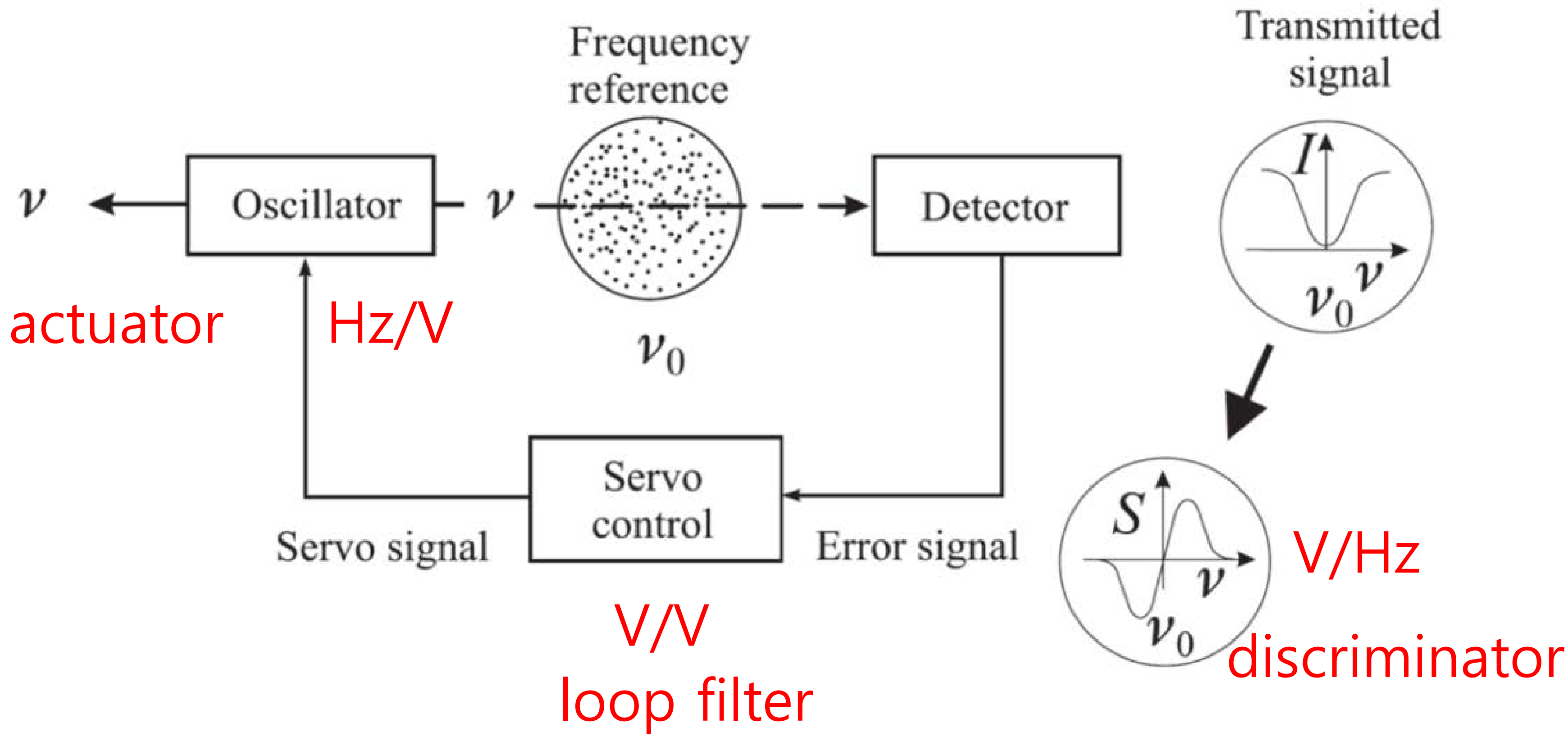

F. Riehle, Frequency standards: basics and applications (John Wiley & Sons, 2006).

레이저 주파수 안정화

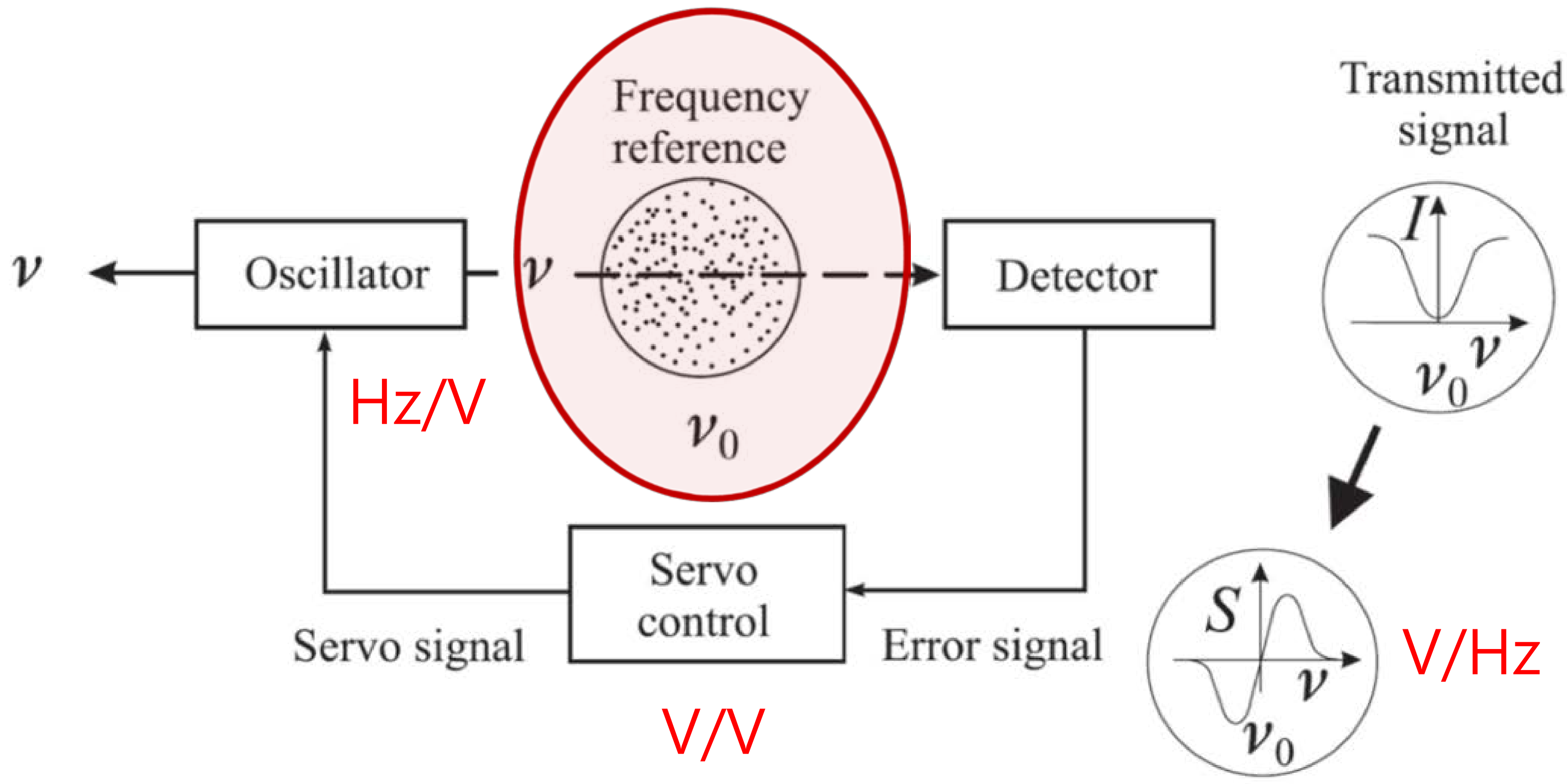

F. Riehle, Frequency standards: basics and applications (John Wiley & Sons, 2006).

Locking to a reference

		Stability
Reference:	Wavemeter	< 10 – 100 MHz (1 hr)
	Gas cell	< 1 MHz (1 hr)
	Cavity (scanning)	< 10 – 100 kHz (1 hr)
	Cavity (fixed)	< 100 Hz – 1 kHz (1 hr)
		< 1 Hz (1 s)
	Laser (phase-lock)	< 1 rad

레이저 주파수 안정화

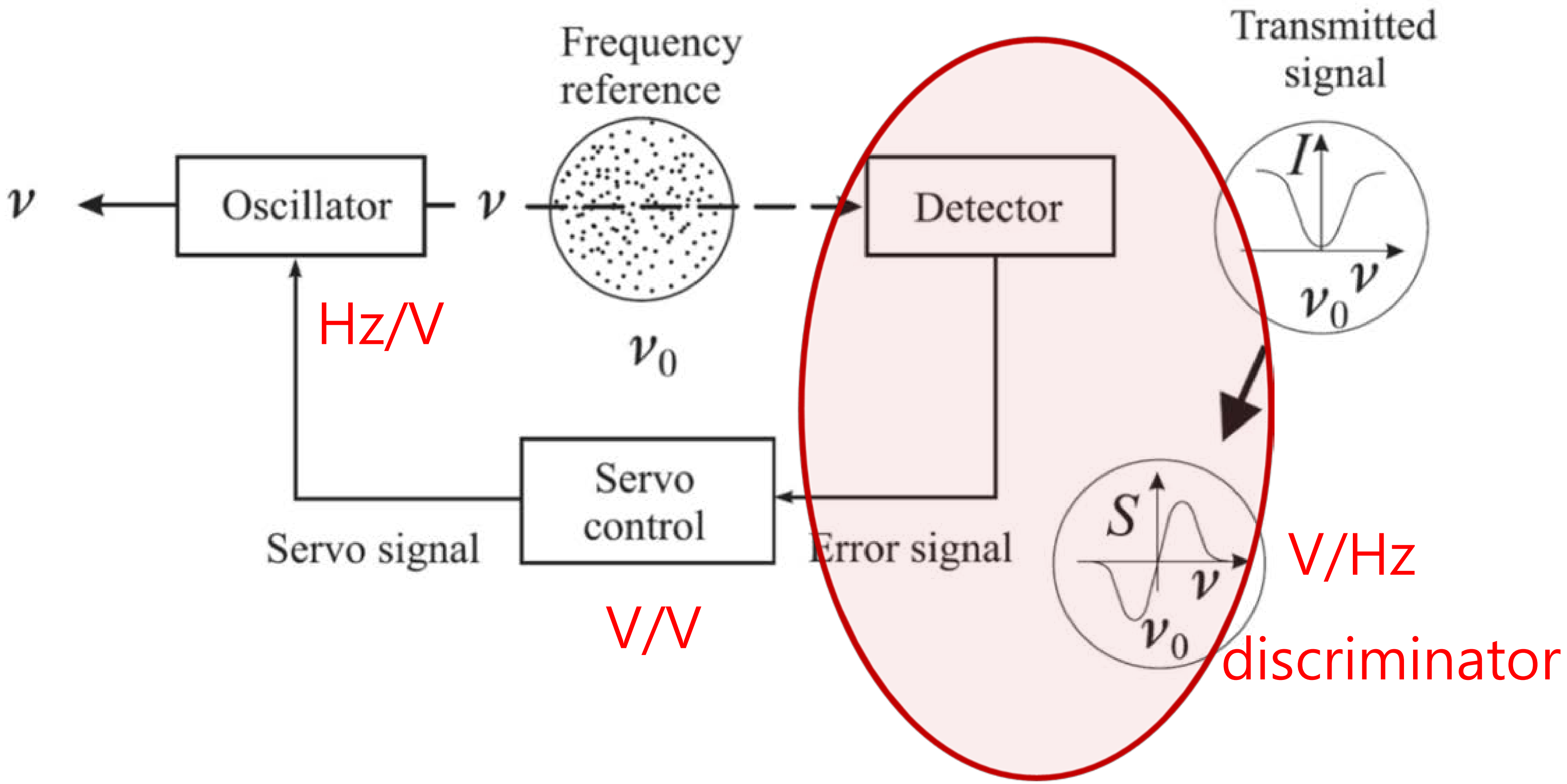

F. Riehle, Frequency standards: basics and applications (John Wiley & Sons, 2006).

레이저 주파수 안정화

Side-of-fringe locking

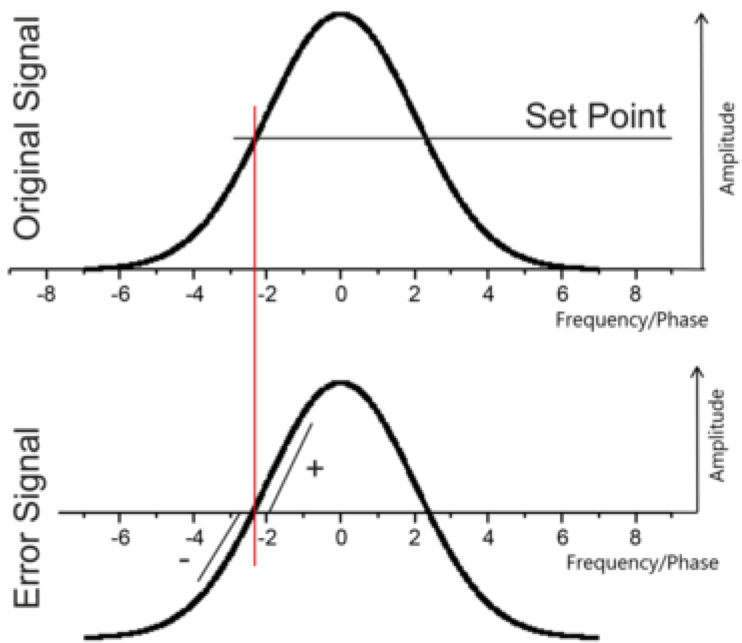

Top-of-fringe locking
FM spectroscopy

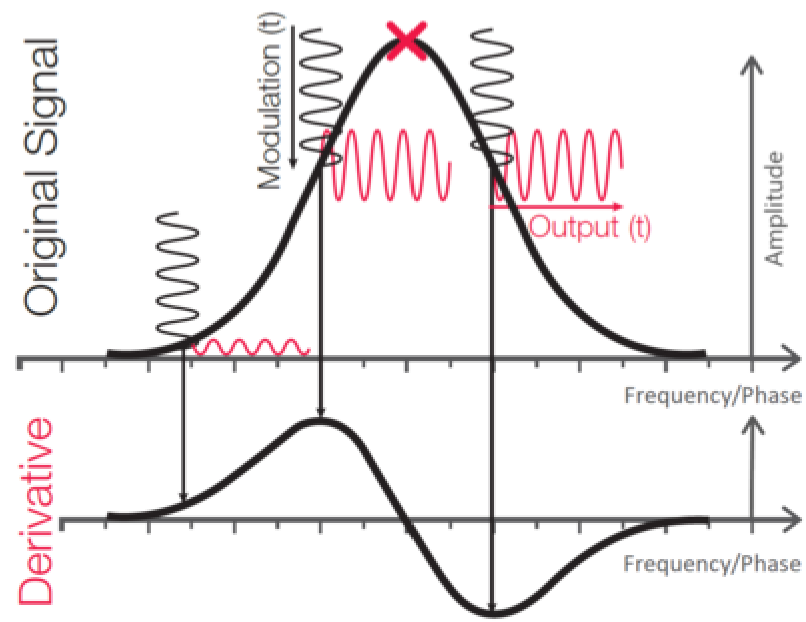

https://www.toptica.com/application-notes/phase-and-frequency-locking-of-diode-lasers/error-signal-generation/general-error-signal-generation-schemes

레이저 주파수 안정화

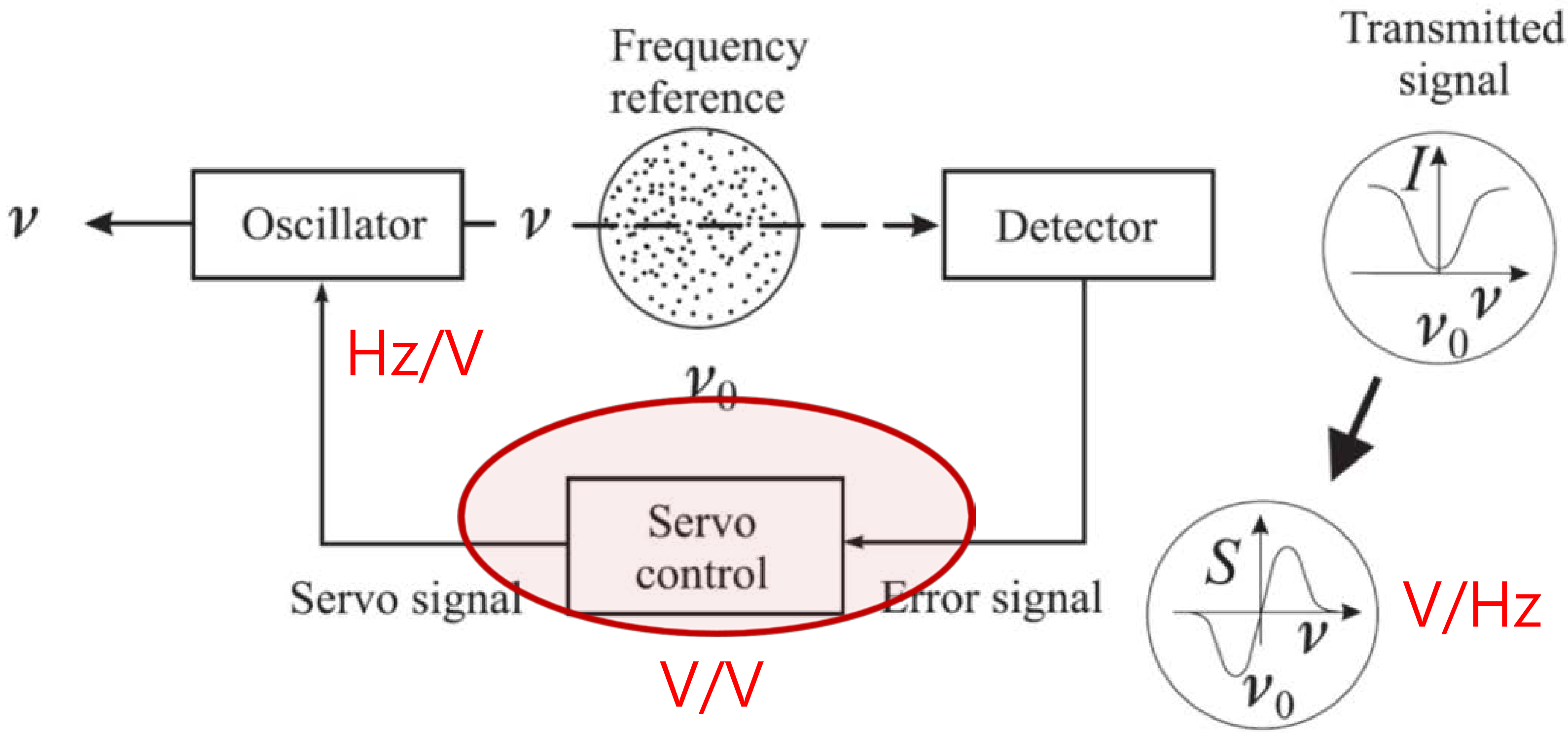

F. Riehle, Frequency standards: basics and applications (John Wiley & Sons, 2006).

Feedback control loop

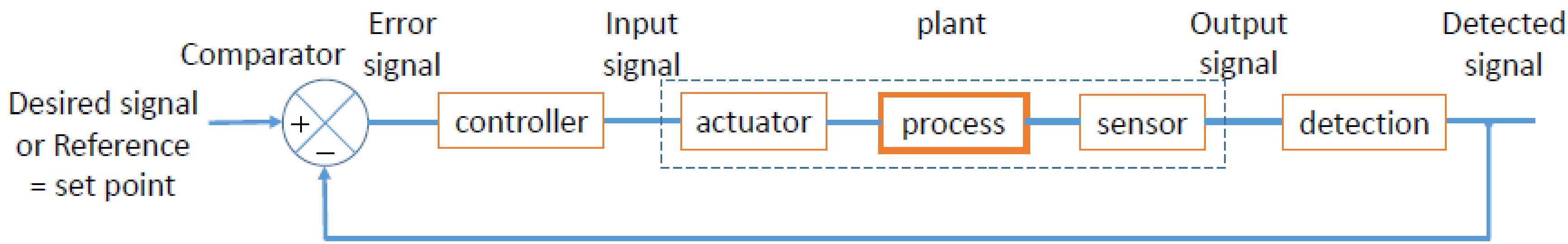

The PID feedback

(Proportional – Integral – Derivative)

$$u(t) = K\left(e(t) + \frac{1}{\tau_I}\int_0^t e(t')\,dt' + \tau_D\,\frac{de}{dt}\right) \Rightarrow C(s) = \frac{U(s)}{E(s)} = K\left(1 + \frac{1}{\tau_I\, s} + \tau_D\, s\right)$$

Proportional Integral Derivative

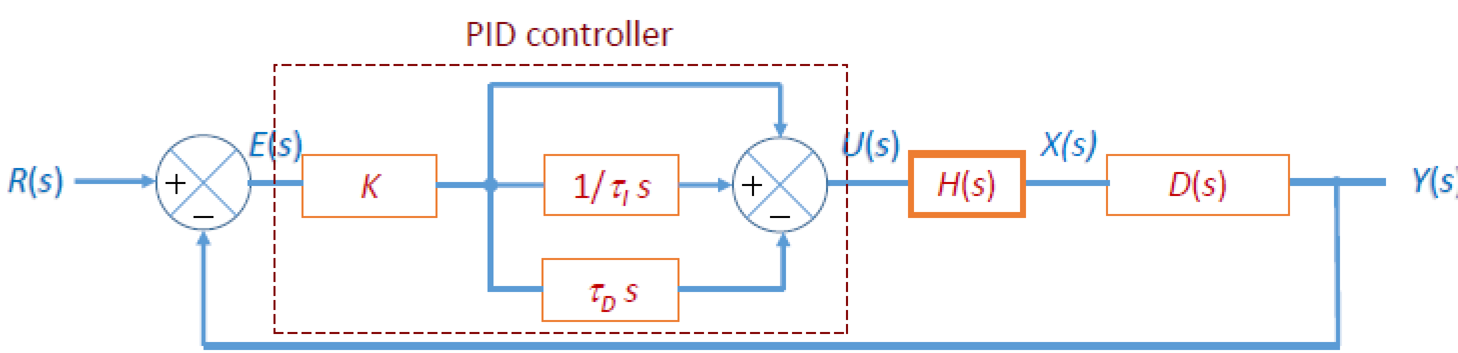

Frédéric Du Burck – The servo loop, the mean to reach stability transfer

레이저 주파수 안정화

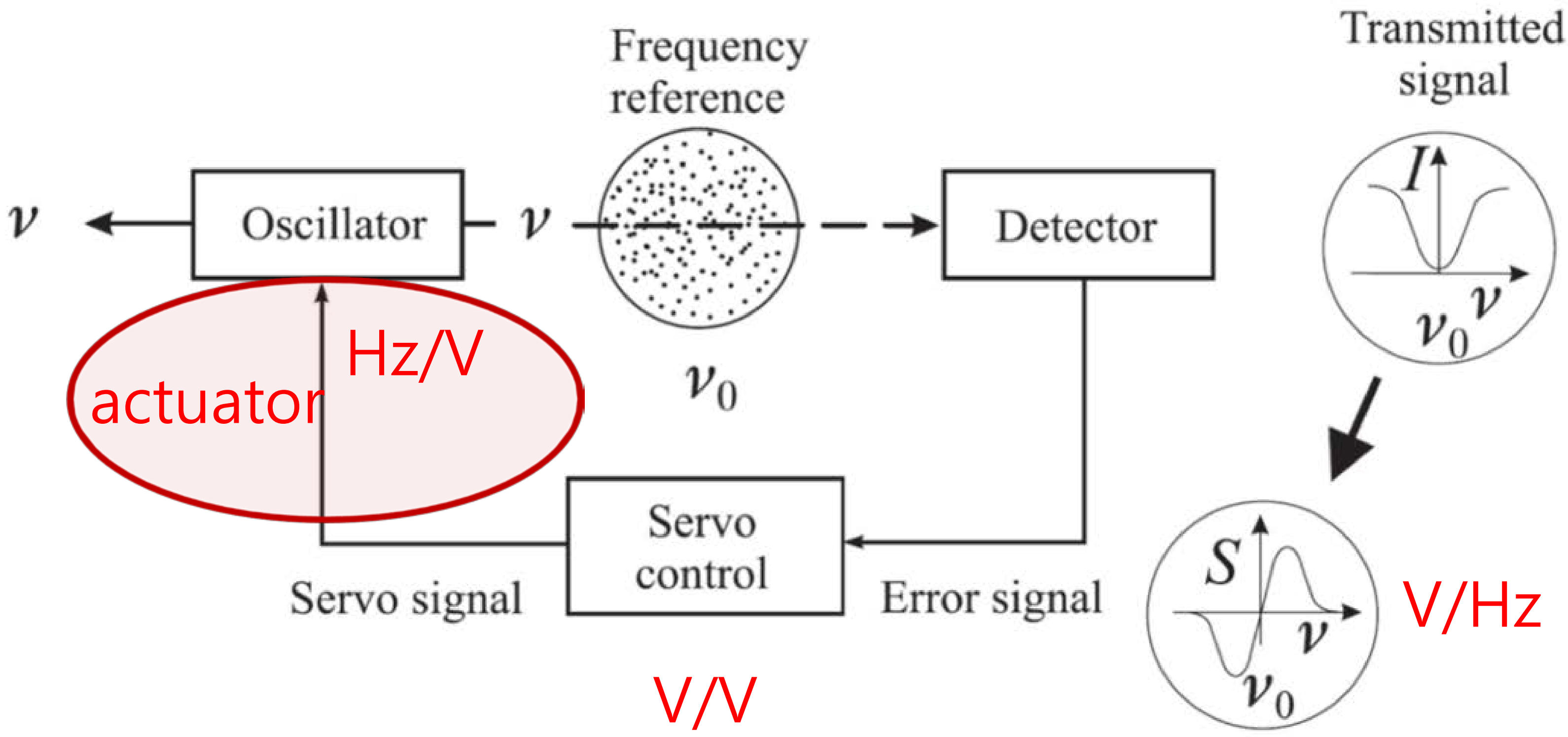

F. Riehle, Frequency standards: basics and applications (John Wiley & Sons, 2006).

Actuator

		Bandwidth
Actuator:	galvo plates	< 100 Hz
	Long piezo stack	< 1 kHz
	Fast piezo	< 100 kHz
	AOM	< 300 kHz
	current	< 3 MHz
	intra-cavity EOM	< 10 MHz

AOM

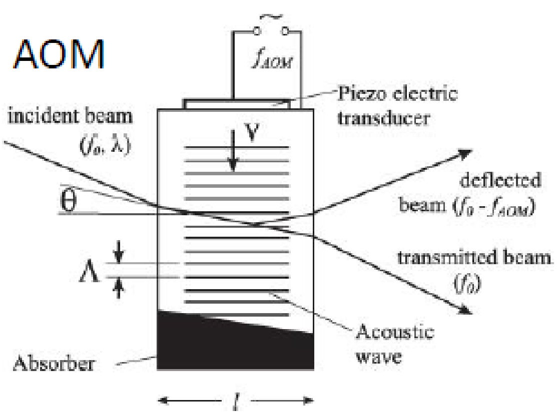

EOM

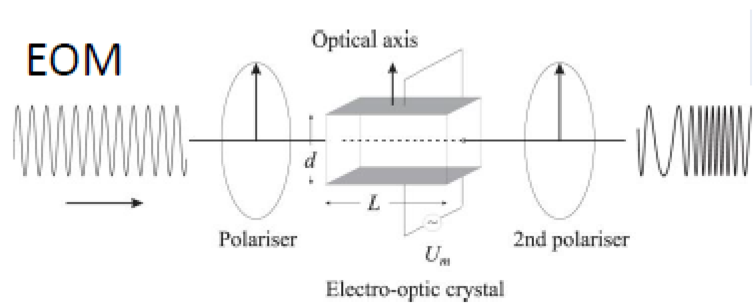

Servo Bump

out-of loop error spectrum

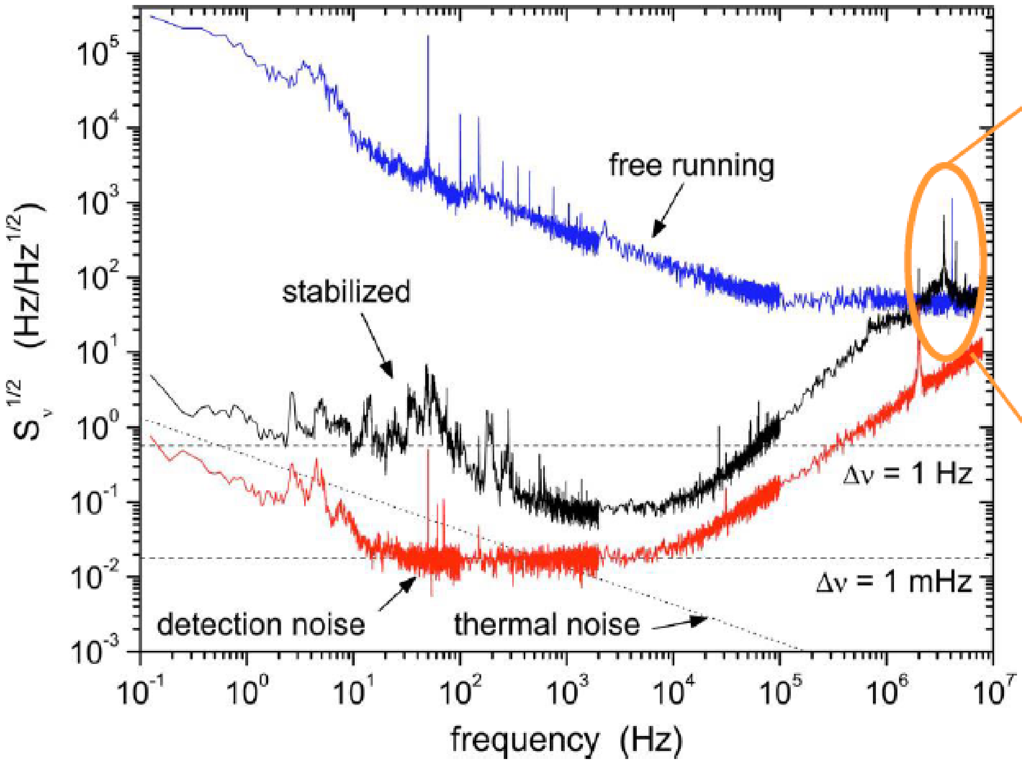

"Servo Bump"

noise increases
around unit-gain frequency

noise will further increase
and finally system oscillates
there with increasing gain

H. Stoehr, F. Mensing, J. Helmcke and U. Sterr, *Diode Laser with 1 Hz Linewidth,* Opt. Lett. **31**, 736-738 (2006)

레이저 주파수 안정화 - 원자물리에서의 응용

- Atmospheric physics
- Atom interferometry, rotation & acceleration
- Atom lithography and optical dipole traps
- Atomic fountains
- Bose Einstein condensate
- Coherent manipulation of ions
- Degenerate Fermi gas
- Degenerate gases in optical lattices simulating solid state physics
- Dipole interaction and dipole blockade
- Doppler cooling
- Electric field measurement
- Fundamental constants and tests of fundamental theories
- Ion traps
- Ionization of neutral atoms
- Laser cooling of trapped ions
- Magneto-cardiography
- Magneto-encephalography
- Magneto-optical trapping (MOT)
- Molecular and atomic spectroscopy
- Non-linear magneto-optical rotation for B-field measurement
- Optical pumping
- Quantum computing
- Quantum cryptography
- Quantum teleportation
- Raman cooling and exotic laser cooling schemes
- Rydberg excitation for quantum optics
- Sisyphus / polarization gradient cooling & optical molasses
- Sources for single or entangled photons
- Time & frequency
- Tuning interactions in degenerate gases
- ……

https://vescent.com/kr/technology-innovations/applications/laser-frequency-stabilization.html

Laser requirements for optical clocks

Photo-ionisation (ions)	< 100 MHz
Cooling laser	100 kHz – 1 MHz
Auxiliary lasers (repumping, optical pumping)	100 kHz – 1 MHz
Lattice laser (atoms)	1 kHz
Probe (clock) laser	10 mHz – 1 Hz

- Diode laser
- Solid-state laser: Ti:Sapphire, Nd:YAG
- Fibre laser
- Dye laser

Frequency double/triple/quadruple to reach blue/uv

Free-running linewidth, 1 – 10,000 kHz

Lock to reference: wavemeter, gas cell, cavity, laser

레이저 주파수 안정화 – 이터븀 광격자 시계에서의 응용

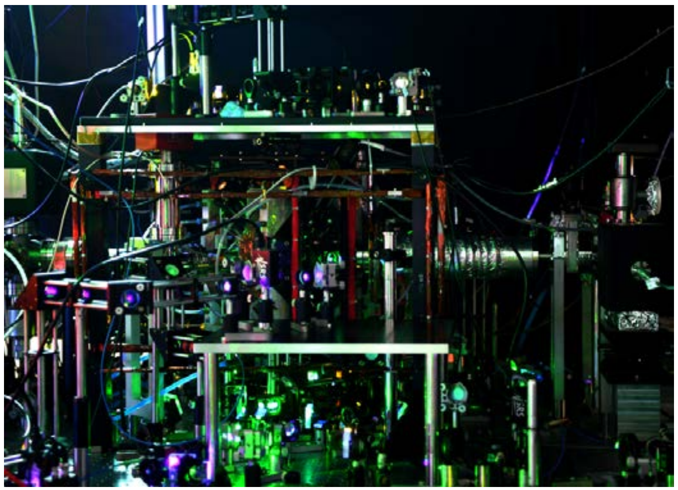

<KRISS-Yb1>

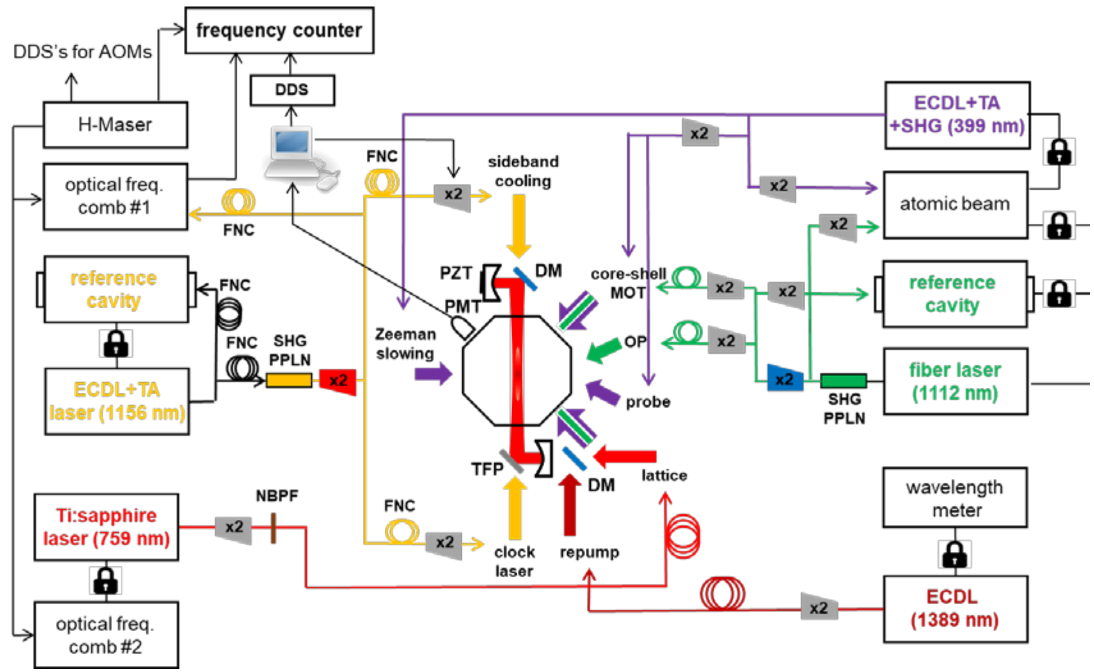

- 399 nm blue MOT laser – frequency-locked to atomic beam
- 556 nm green MOT laser – frequency-locked to atomic beam and reference cavity
- 578 nm clock laser – frequency-locked to reference cavity
- 578 nm clock laser – fiber frequency noise cancellation
- 759 nm lattice laser – phase-locked to optical frequency comb
- 1389 nm repumping laser – frequency-locked to wavemeter
- 578 nm clock laser – frequency-steered to Yb atom resonance
- ……

Metrologia_58_055007(2021)Absolute frequency measurement of the 171Yb optical lattice clock at KRISS using TAI for over a year.pdf

레이저 주파수 안정화 – 이터븀 광격자 시계에서의 응용

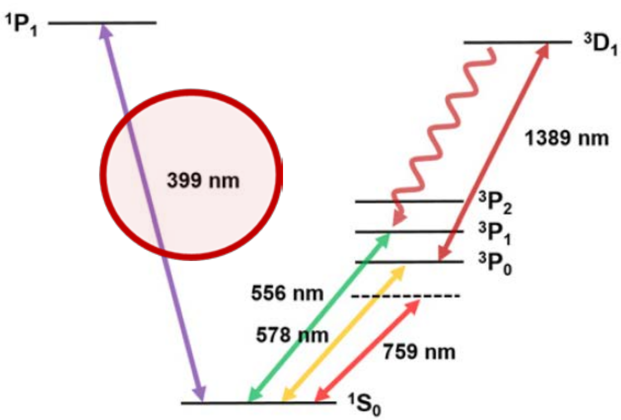

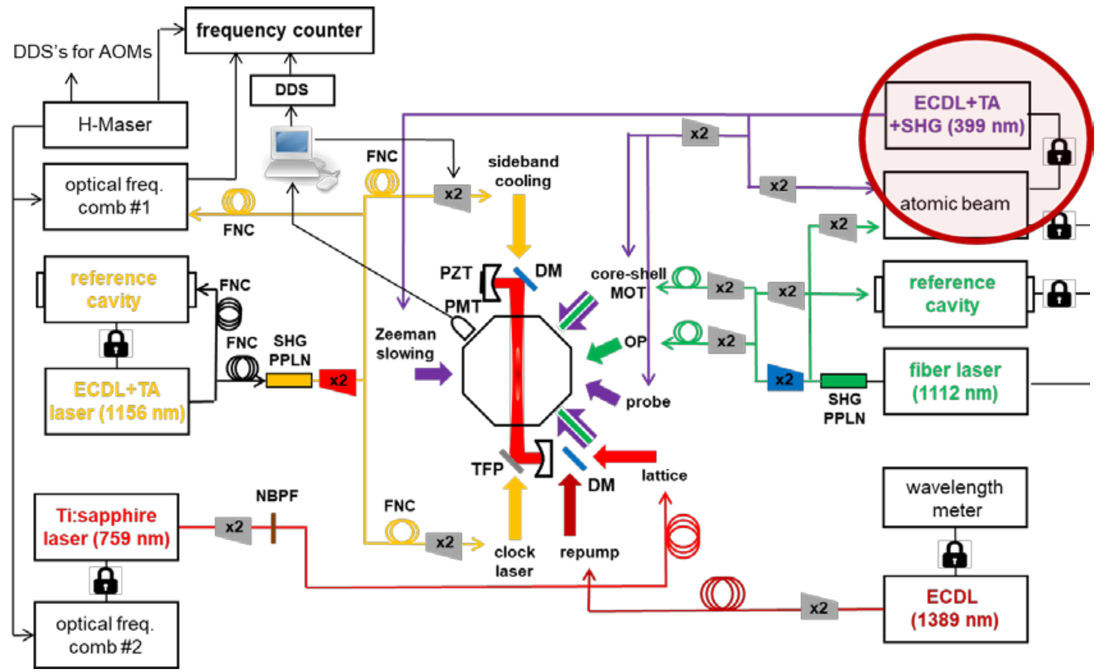

- 399 nm blue MOT laser – frequency-locked to atomic beam (전이선폭 28 MHz)
- 556 nm green MOT laser – frequency-locked to atomic beam and reference cavity
- 578 nm clock laser – frequency-locked to reference cavity
- 578 nm clock laser – fiber frequency noise cancellation
- 759 nm lattice laser – phase-locked to optical frequency comb
- 1389 nm repumping laser – frequency-locked to wavemeter
- 578 nm clock laser – frequency-steered to Yb atom resonance
- ......

Metrologia_58_055007(2021)Absolute frequency measurement of the 171Yb optical lattice clock at KRISS using TAI for over a year.pdf

이터븀 광격자 시계 – 1차,2차 자기광포획

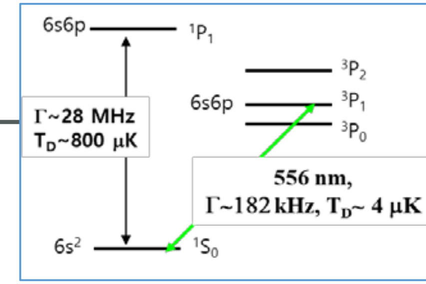

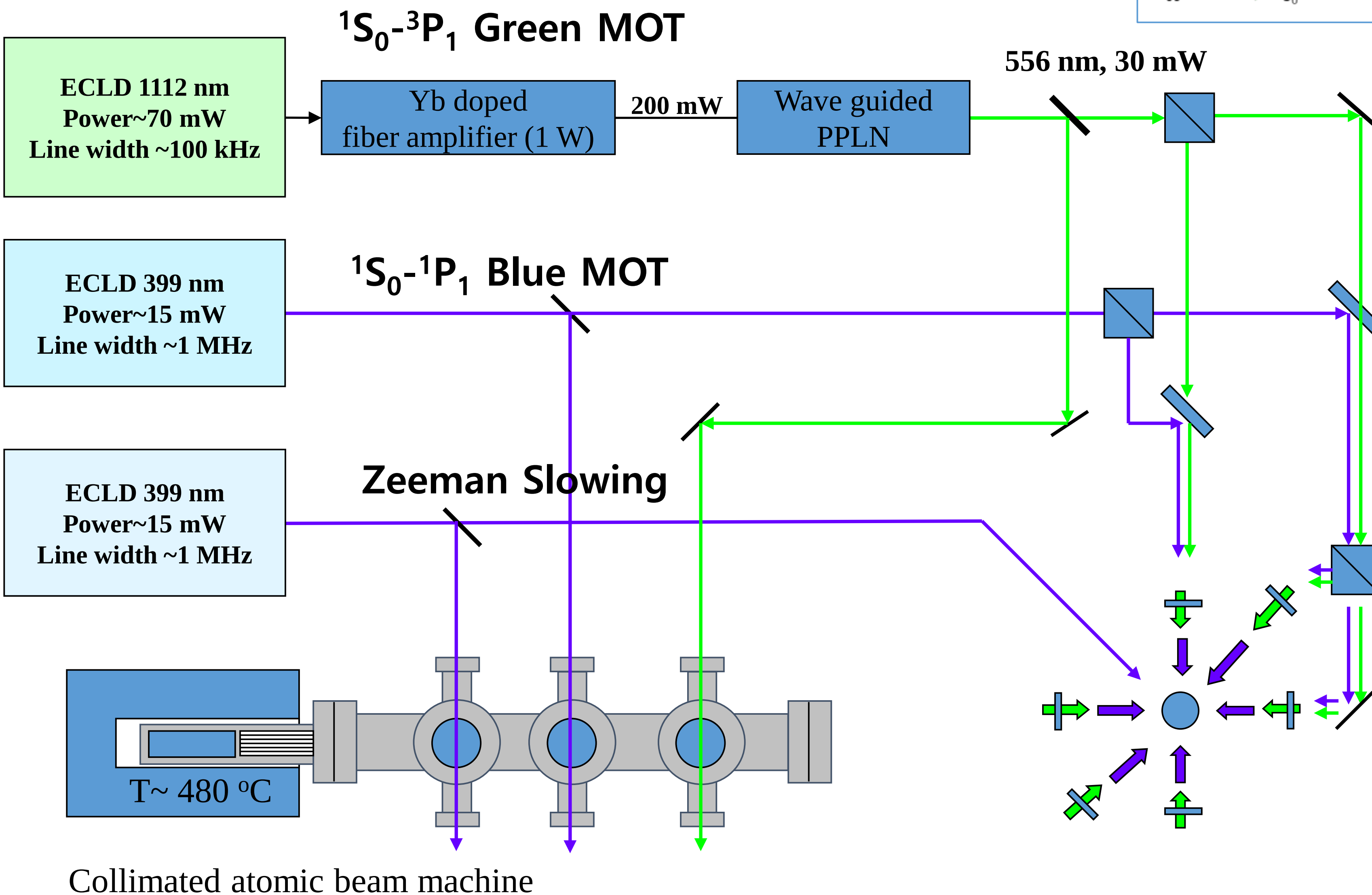

Saturated Absorption Spectroscopy

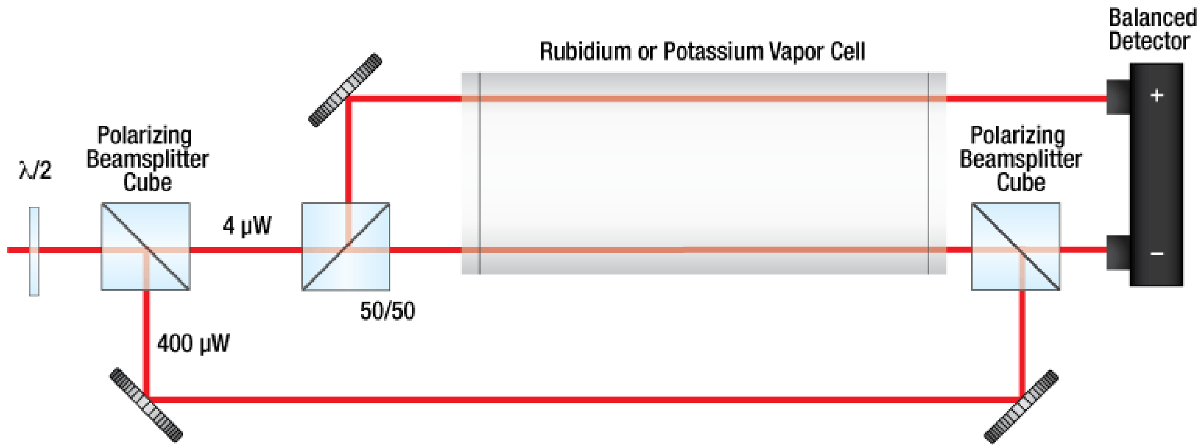

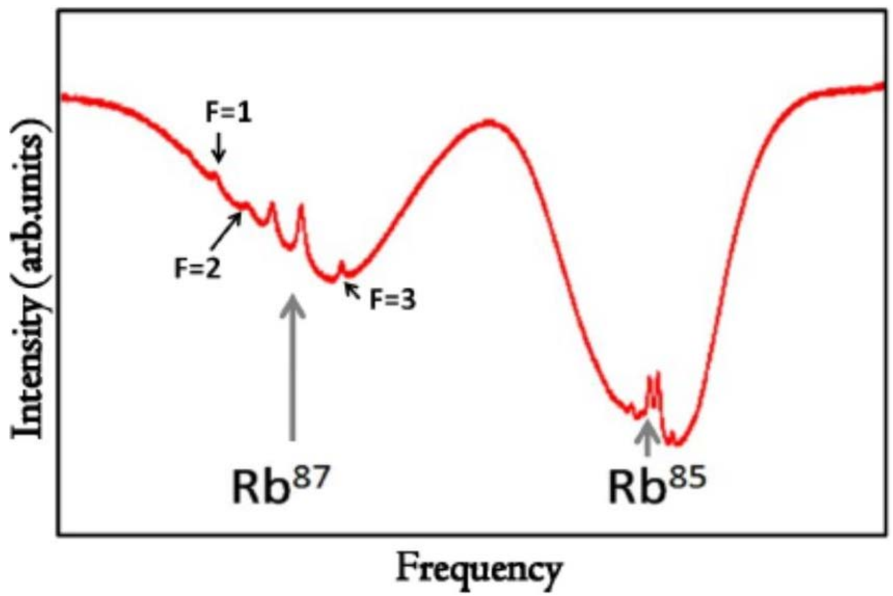

https://www.thorlabs.com/newgrouppage9.cfm?objectgroup_ID=5616

Saturated Absorption Spectroscopy

- Acetylene Stabilized LD (KRISS-Ace1)

For $^{13}C_2H_2$, P(16) ($\nu_1 + \nu_3$)

BIPM : f = 194 369 569.4 MHz ± 5.2 x 10^{-10}

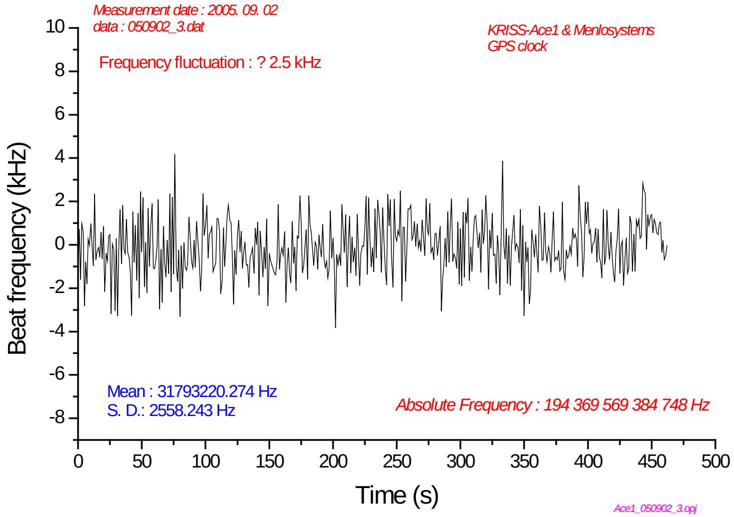

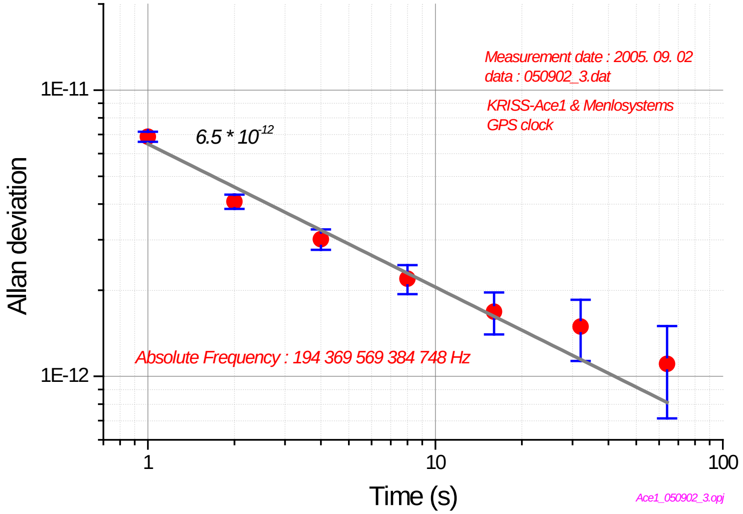

f = 194 369 569 384.7 (± 2.6) kHz

frequency stability (1 s) = 6.5 x 10^{-12}

Cf. 399 nm blue MOT laser – frequency-locked to atomic beam (전이선폭 28 MHz)

레이저 주파수 안정화 – 이터븀 광격자 시계에서의 응용

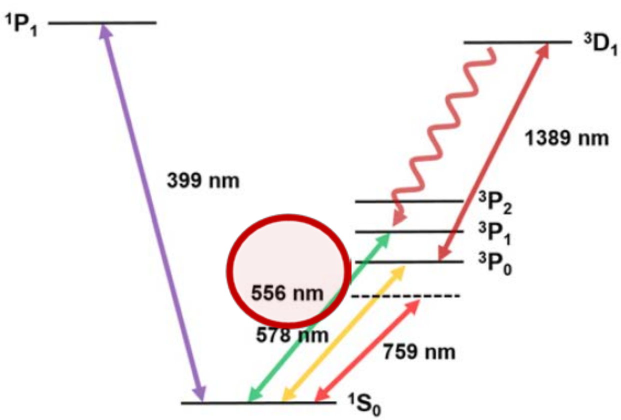

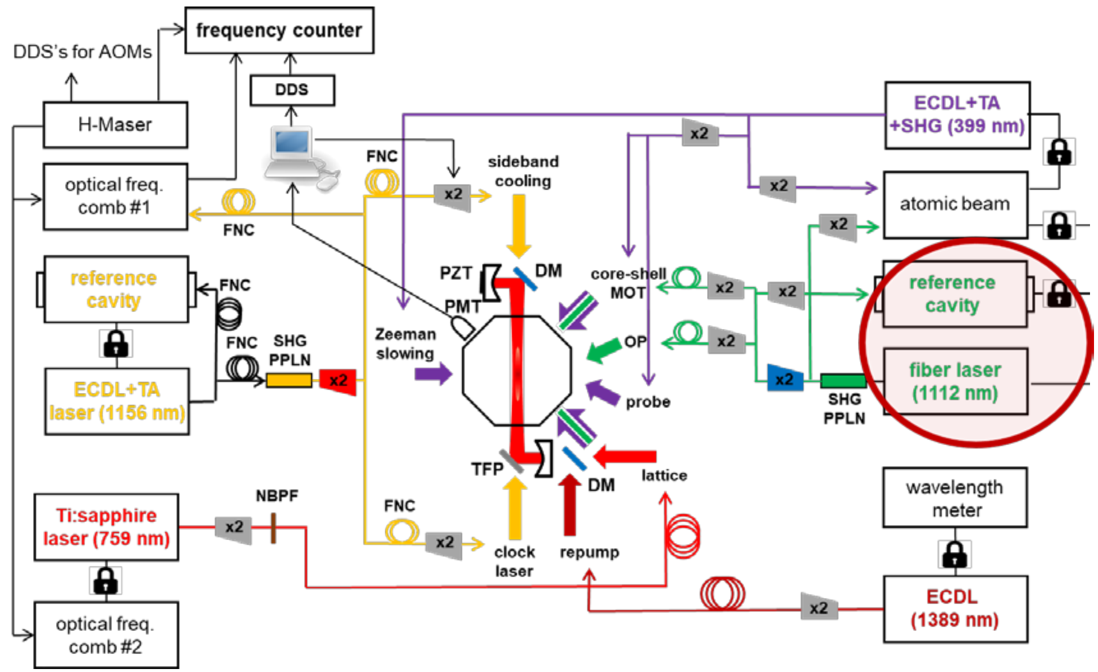

- 399 nm blue MOT laser – frequency-locked to atomic beam
- 556 nm green MOT laser – frequency-locked to atomic beam and reference cavity
- 578 nm clock laser – frequency-locked to reference cavity
- 578 nm clock laser – fiber frequency noise cancellation
- 759 nm lattice laser – phase-locked to optical frequency comb
- 1389 nm repumping laser – frequency-locked to wavemeter
- 578 nm clock laser – frequency-steered to Yb atom resonance
- ……

Metrologia_58_055007(2021)Absolute frequency measurement of the 171Yb optical lattice clock at KRISS using TAI for over a year.pdf

PDH (Pound-Drever-Hall) Locking

556 nm 전이선폭 182 kHz - 원자빔 FM 안정화로 불충분

556 nm green MOT laser – frequency-locked to atomic beam and reference cavity

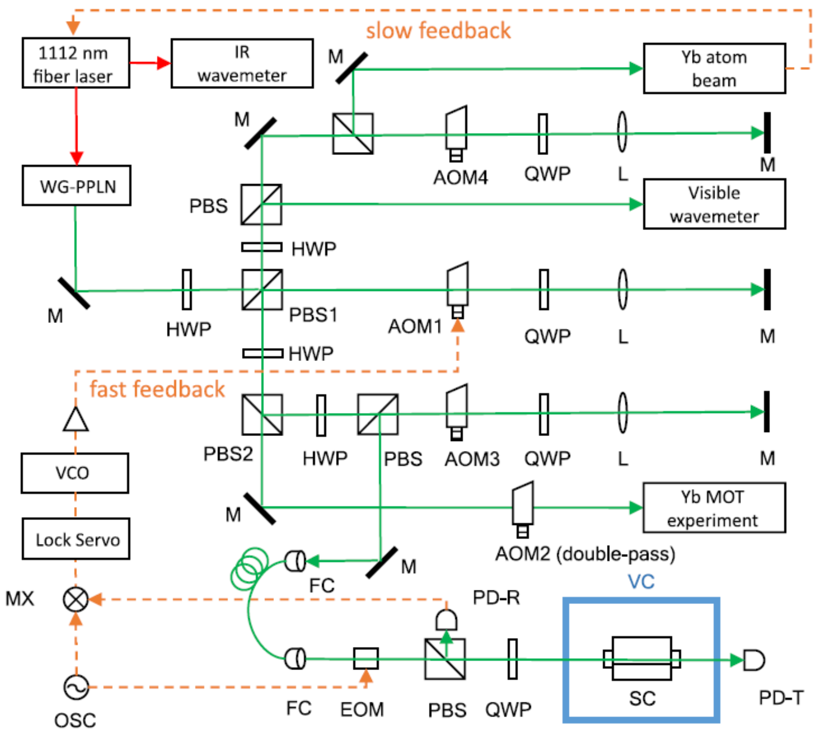

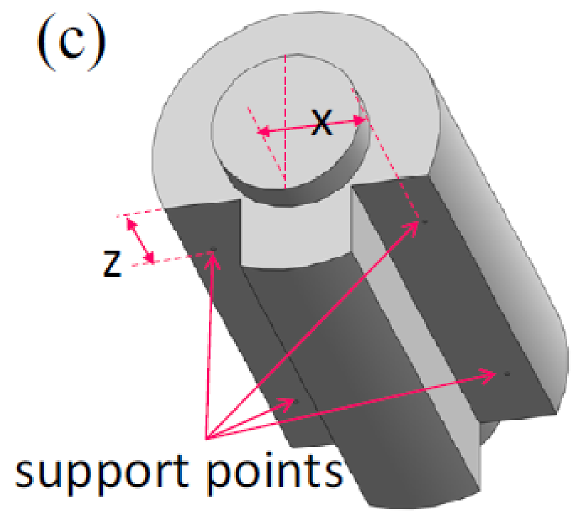

An experimental method is developed for robust frequency stabilization using a high-finesse cavity when the laser exhibits large intermittent frequency jumps. This is accomplished by applying an additional slow feedback signal from Doppler-free fluorescence spectroscopy in an atomic beam with increased frequency locking range.

ao-59-28-8918(2020)
COPP-3(2)128(2019)

PDH (Pound-Drever-Hall) Locking

Drever *et al.*, Appl. Phys. B 31, 97 (1983)

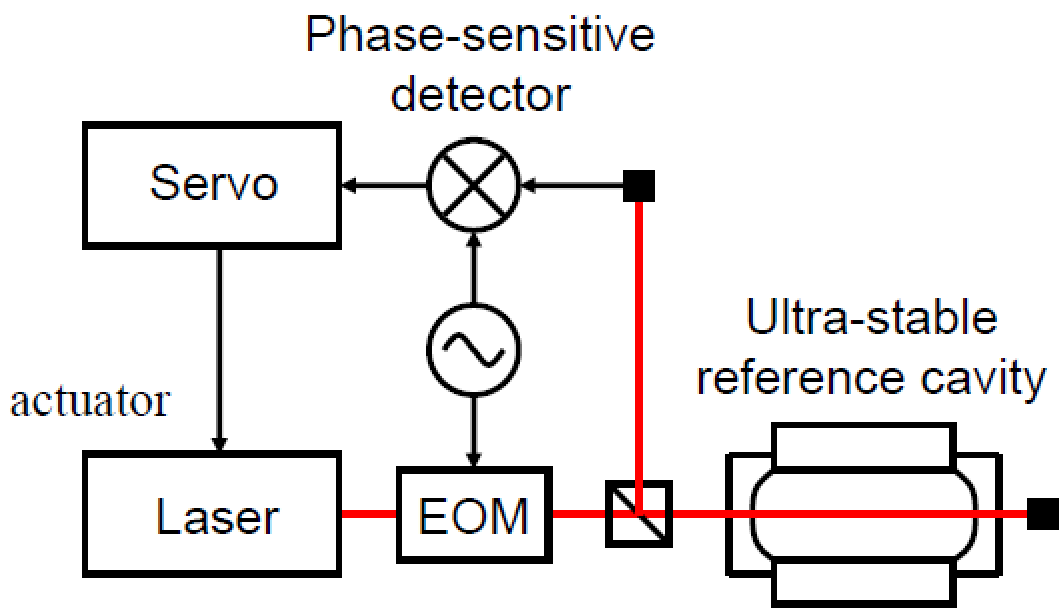

Modulate: Electro-Optic Modulator (EOM)
Detect reflection from cavity at modulation frequency
Generate error signal/discriminant: phase-sensitive detector
Actuator: piezoelectric transducer, current, external acousto-optic modulator

PDH (Pound-Drever-Hall) Locking

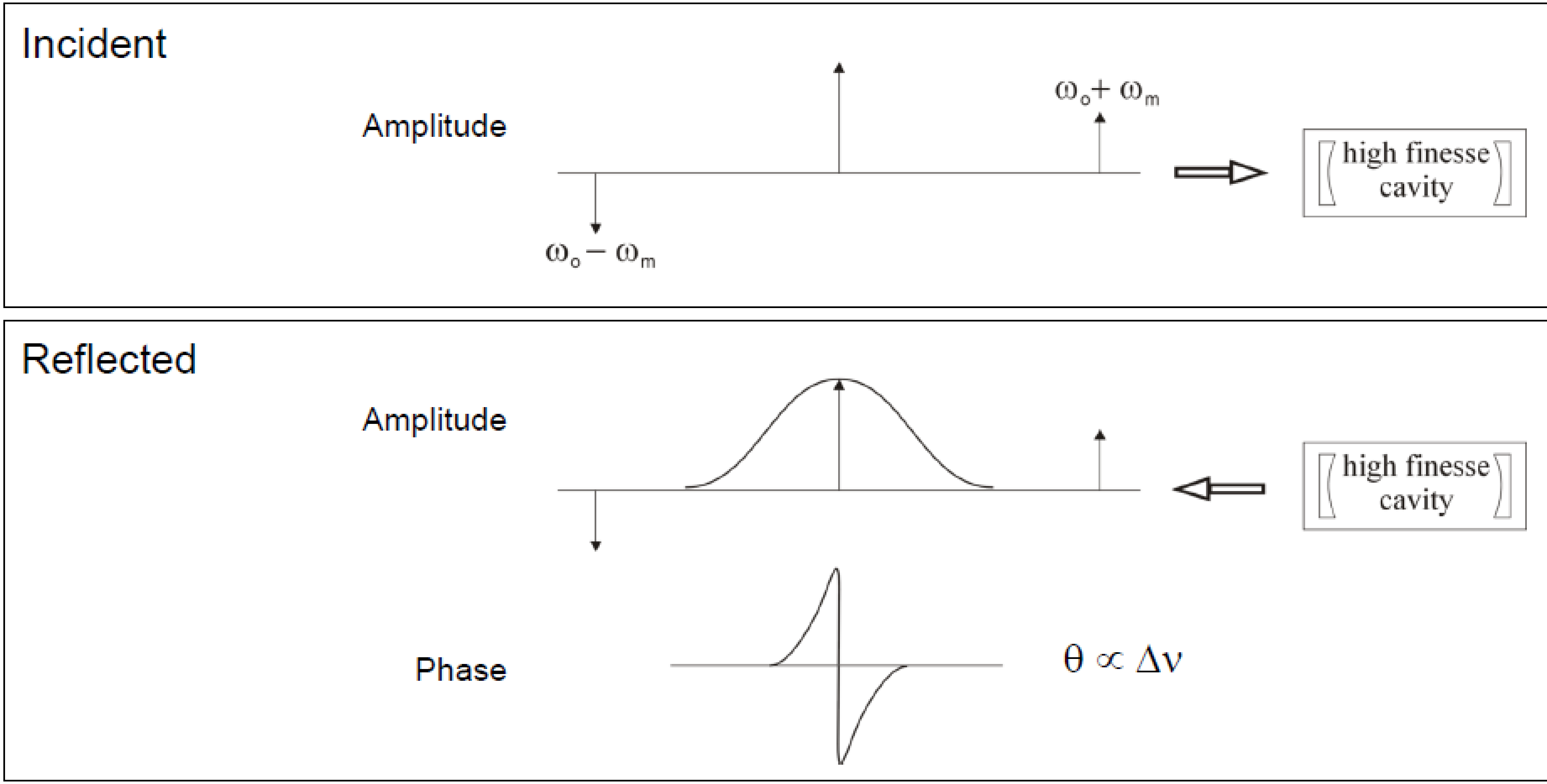

S. Webster-EFTF2016 Tutorial-Lasers for Optical Frequency Standards

PDH (Pound-Drever-Hall) Locking

PDH error signal:

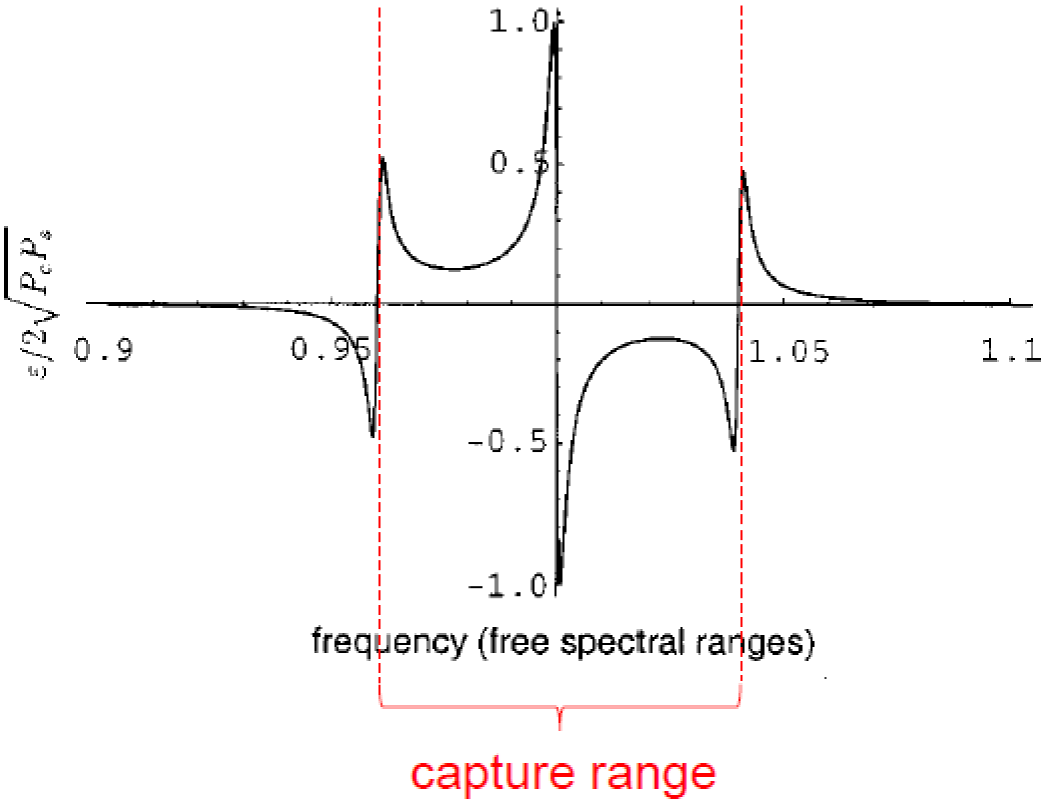

레이저 주파수 안정화 – 이터븀 광격자 시계에서의 응용

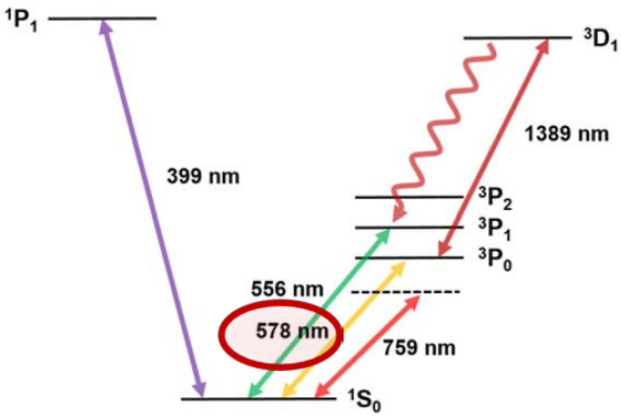

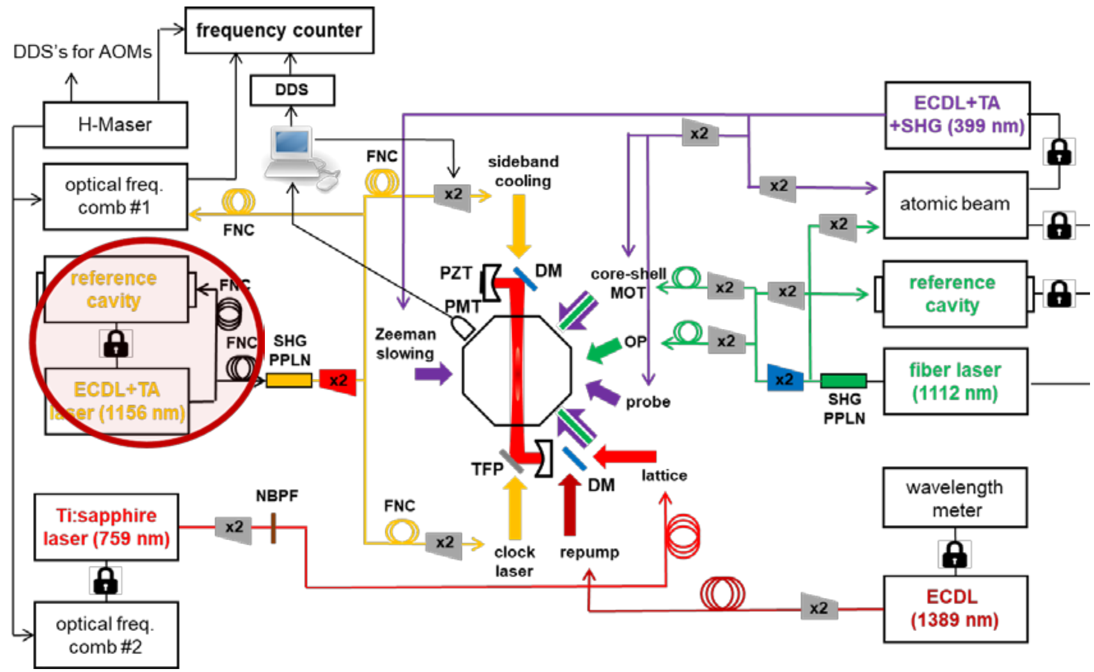

- 399 nm blue MOT laser – frequency-locked to atomic beam
- 556 nm green MOT laser – frequency-locked to atomic beam and reference cavity
- 578 nm clock laser – frequency-locked to reference cavity
- 578 nm clock laser – fiber frequency noise cancellation
- 759 nm lattice laser – phase-locked to optical frequency comb
- 1389 nm repumping laser – frequency-locked to wavemeter
- 578 nm clock laser – frequency-steered to Yb atom resonance
- ……

Metrologia_58_055007(2021)Absolute frequency measurement of the 171Yb optical lattice clock at KRISS using TAI for over a year.pdf

Ultra-narrow linewidth laser locking by PDH method

578 nm 전이선폭 10 mHz - ULE cavity 이용

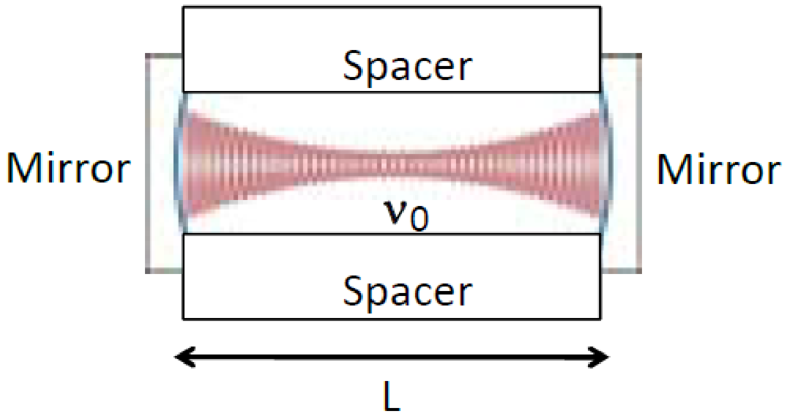

Length changes in the cavity cause frequency changes of the laser locked to the cavity

$$\frac{\Delta \nu}{\nu_0} = \frac{\Delta L}{L}$$

5 Hz → ~ 1 fm or 1 nuclear radius !!!

... If the spacer for an optical cavity were the Earth, a human hair added to the diameter would cause a frequency shift of about 300 Hz!

J. C. Bergquist

Noise Factors in Ultra-narrow Lasers

Low-frequency noise

- acoustic and seismic noise
- temperature fluctuations
- optical feedback
- Brownian motion

High-frequency noise

- quantum fluctuations in lasers
- Schawlow-Townes Limit
- limited servo gain
- index fluctuations in fibers

방음

제진대

온도제어

AR코팅

spectral filtering & injection lock

진공

캐비티 민감도 소거

광섬유 잡음 제거

Cavity spacer material

ULE Zero crossing temperature에 온도 안정화

Material

Thermal Expansion Coefficient (α) must be small.

Material	a [K^{-1}]	Creep $\Delta L/L$ (at 1 sec)
Super-Inver	~10^{-7}	
ULE	~10^{-8}	0.2~0.5 x 10^{-15} (smooth)
Zerodur	~10^{-8}	2~4 x 10^{-15} (random jumps)
sapphire @ room temp.	~10^{-6}	
sapphire @ 3~4 K	~10^{-11}	

Ultra Low Expansion Glass (ULE)

Young's Modulus	67 GPa
Poisson Ratio	0.17
density	2200 kg/m^3
Coefficient of thermal expansion[specification]	0.00 ±0.03 × 10^{-6} K^{-1}(5 to 35°C)

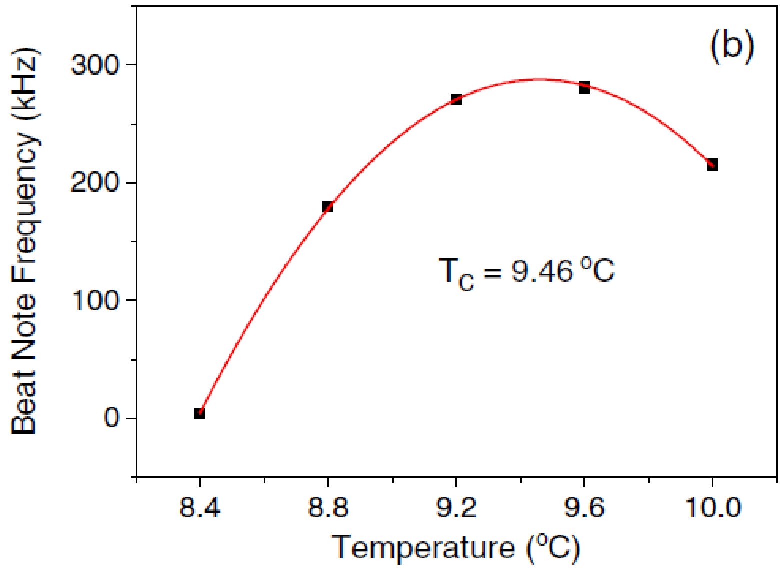

ao-59-28-8918(2020)
COPP-3(2)128(2019)

Vibration-Insensitive Cavity

Horizontal Cavity

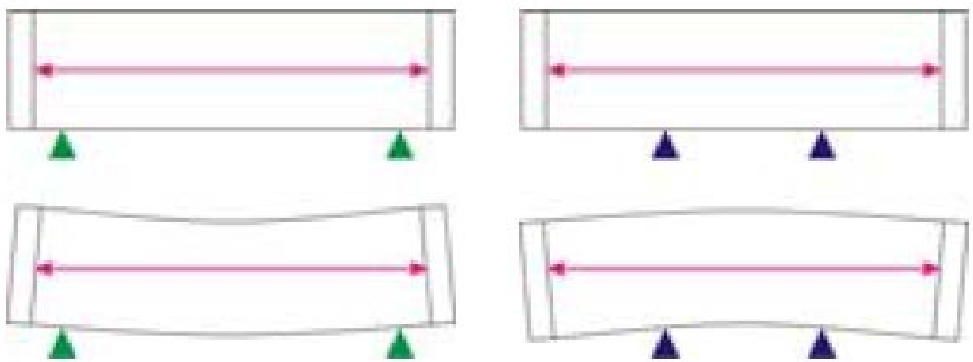

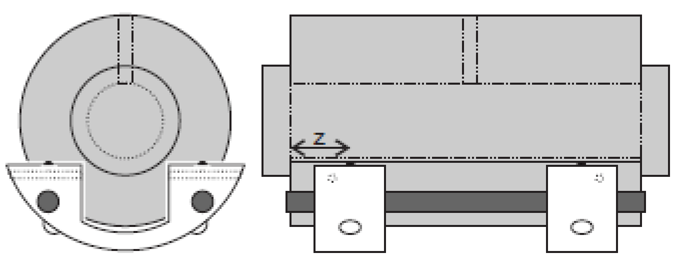

FIG. 4. Cutout cavity on mount. The cavity is supported at four points on 3 mm diameter rubber spheres which are located within “yokes,” shown in white.

PRA 77, 033847 (2008)

Vertical Cavity

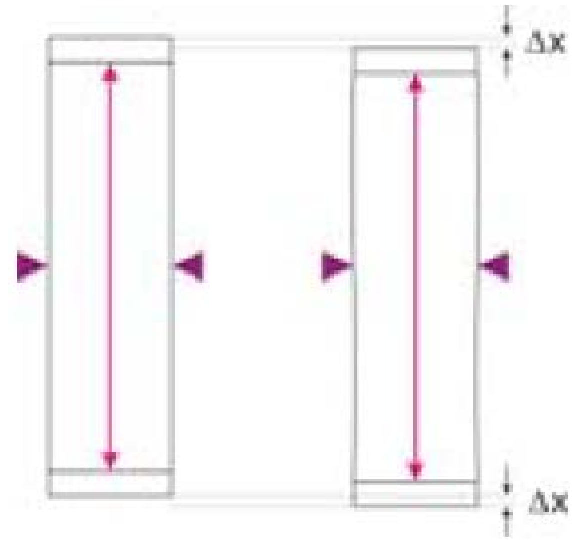

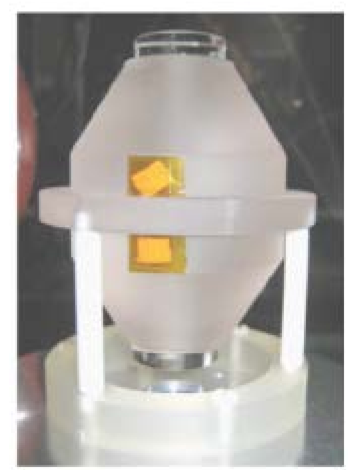

OL 32, 641 (2007)

Thermal noise

Mechanical thermal fluctuation

$m\ddot{x} + \gamma\dot{x} + kx = f_n$ Langevin equation

f_n : thermal fluctuation

Power spectrum of Brownian motion $\propto \sqrt{\frac{T}{Q}}$

➡ Low T & high Q

Q : mechanical quality factor

Spacer

$$S_{spacer}(f) = \frac{4k_B T}{\omega} \frac{L}{3\pi R^2 E} \phi_{spacer}$$

ϕ : mechanical loss $\phi = 1/Q$

k_B : Boltzmann constant

T : temperature

R : radius

Mirror

$$S_{mirror}(f) = \frac{4k_B T}{\omega} \frac{1-\rho^2}{\sqrt{\pi} E w_0} \phi_{sub} \left(1 + \frac{2}{\sqrt{\pi}} \frac{1-2\rho}{1-\rho} \frac{\phi_{coat}}{\phi_{sub}} \frac{d}{w_0}\right)$$

ρ : Poisson ratio

w_0 : beam radius

d : coating thickness

$\sqrt{S_{spacer}} = 5.6 \times 10^{-18}\, m/\sqrt{Hz}$ @ 1Hz

$\sqrt{S_{mirror}} = 4.3 \times 10^{-17}\, m/\sqrt{Hz}$ @ 1Hz

➡ $\sqrt{S_{total}} = 6.2 \times 10^{-17}\, m/\sqrt{Hz}$ ➡ $\sqrt{S_{\nu}} = 0.43\, Hz/\sqrt{Hz}$ ➡ $\sigma_y \cong 1 \times 10^{-15}$

How to improve?

$$\sigma_{\text{therm}} = \sqrt{\ln 2 \frac{8k_B T}{\pi^{3/2}} \frac{1-\sigma^2}{E w_0 L^2} \left(\phi_{\text{sub}} + \phi_{\text{coat}} \frac{2}{\sqrt{\pi}} \frac{1-2\sigma}{1-\sigma} \frac{d}{w_0} \right)}$$

(1) lower temperatures

(2) longer cavities

(3) larger beam waist

(4) substrate and dielectric coating materials with lower mechanical loss.

[2] Nat. Photon. 6, 687(2012) A sub-40 mHz linewidth laser based on a silicon single-crystal optical cavity

Linewidth record by cryogenic Si single crystal cavity

<Advantages of single silicon crystal>

- ❖ High Q -> reduced thermal noise
- ❖ Large Young's modulus (superior stiffness) -> reduced vibration sensitivity
- ❖ No aging-related frequency drifts
- ❖ Large thermal conductivity -> homogeneous temperature

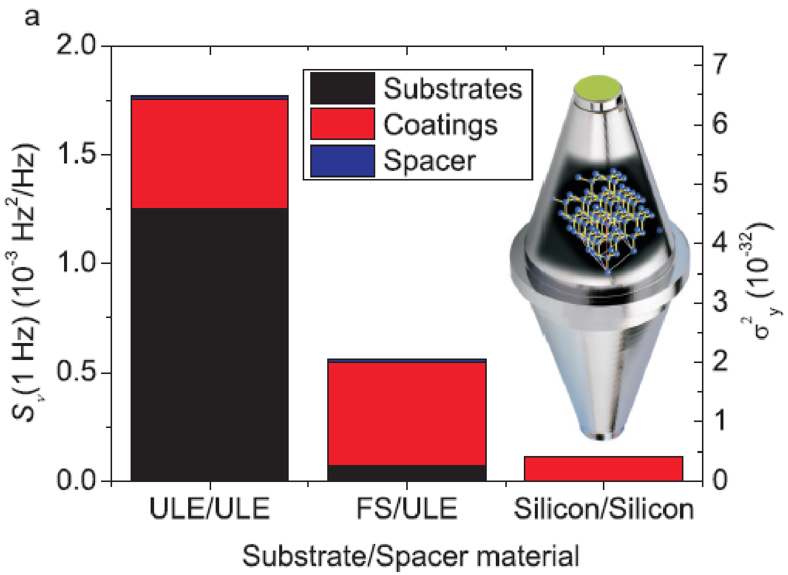

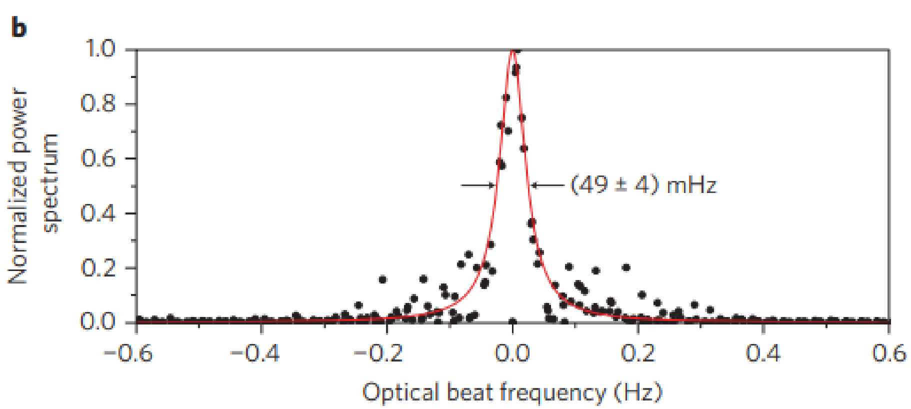

[2] Nat. Photon. 6, 687(2012) A sub-40 mHz linewidth laser based on a silicon single-crystal optical cavity

Low noise crystalline coating

KRISS – new clock laser

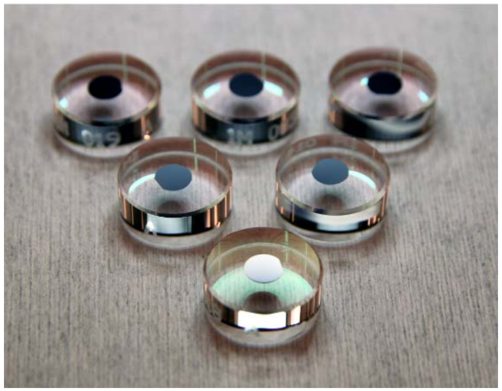

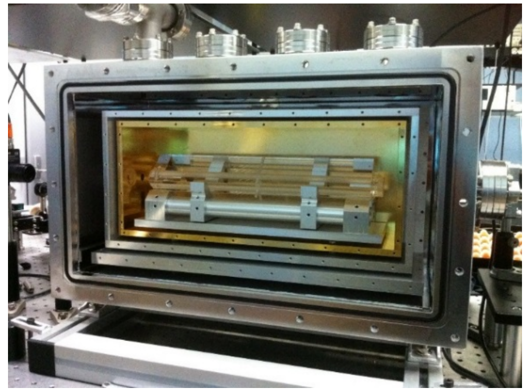

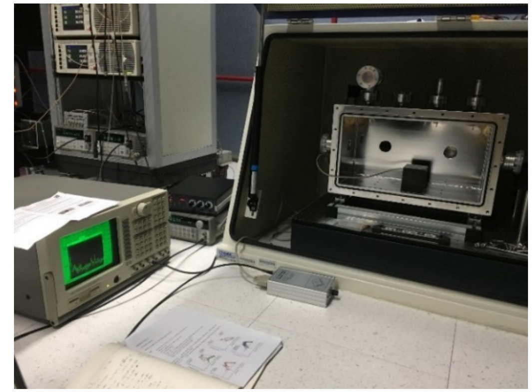

- 광격자시계 불확도 평가에 소요되는 시간을 획기적으로 줄일 수 있음 (10000초에 10^{-18}의 불확도 평가).
- 크리스탈 성장 방식으로 제작된 캐비티 미러를 사용하여 열적요동으로 인한 한계가 $4.3\text{x}10^{-17}$으로 기대됨.
- 개발 성공시 상온에서 동작하는 clock laser 중 세계에서 가장 좋은 안정도를 보일 것으로 기대됨.
- 크리스탈 미러를 도입하고 30 cm 길이의 캐비티 두 개를 제작.

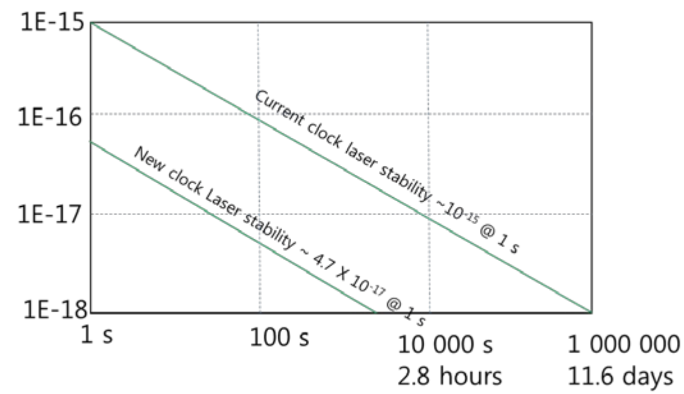

레이저 주파수 안정화 – 이터븀 광격자 시계에서의 응용

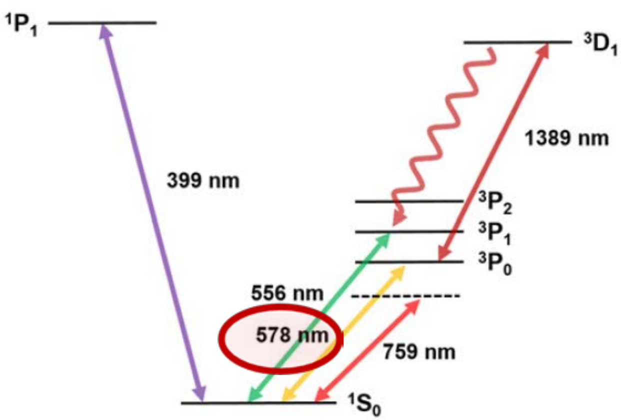

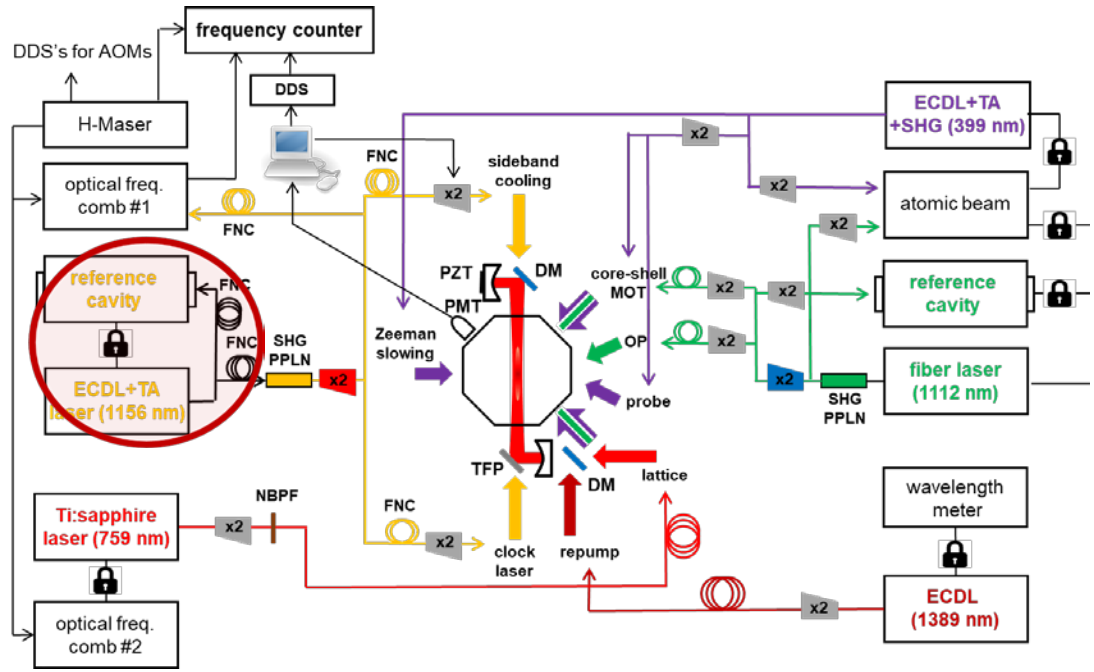

- 399 nm blue MOT laser – frequency-locked to atomic beam
- 556 nm green MOT laser – frequency-locked to atomic beam and reference cavity
- 578 nm clock laser – frequency-locked to reference cavity
- 578 nm clock laser – fiber frequency noise cancellation
- 759 nm lattice laser – phase-locked to optical frequency comb
- 1389 nm repumping laser – frequency-locked to wavemeter
- 578 nm clock laser – frequency-steered to Yb atom resonance
- ……

Metrologia_58_055007(2021)Absolute frequency measurement of the 171Yb optical lattice clock at KRISS using TAI for over a year.pdf

Fiber noise cancellation

Phase Coherent Transmission of Optical Standard

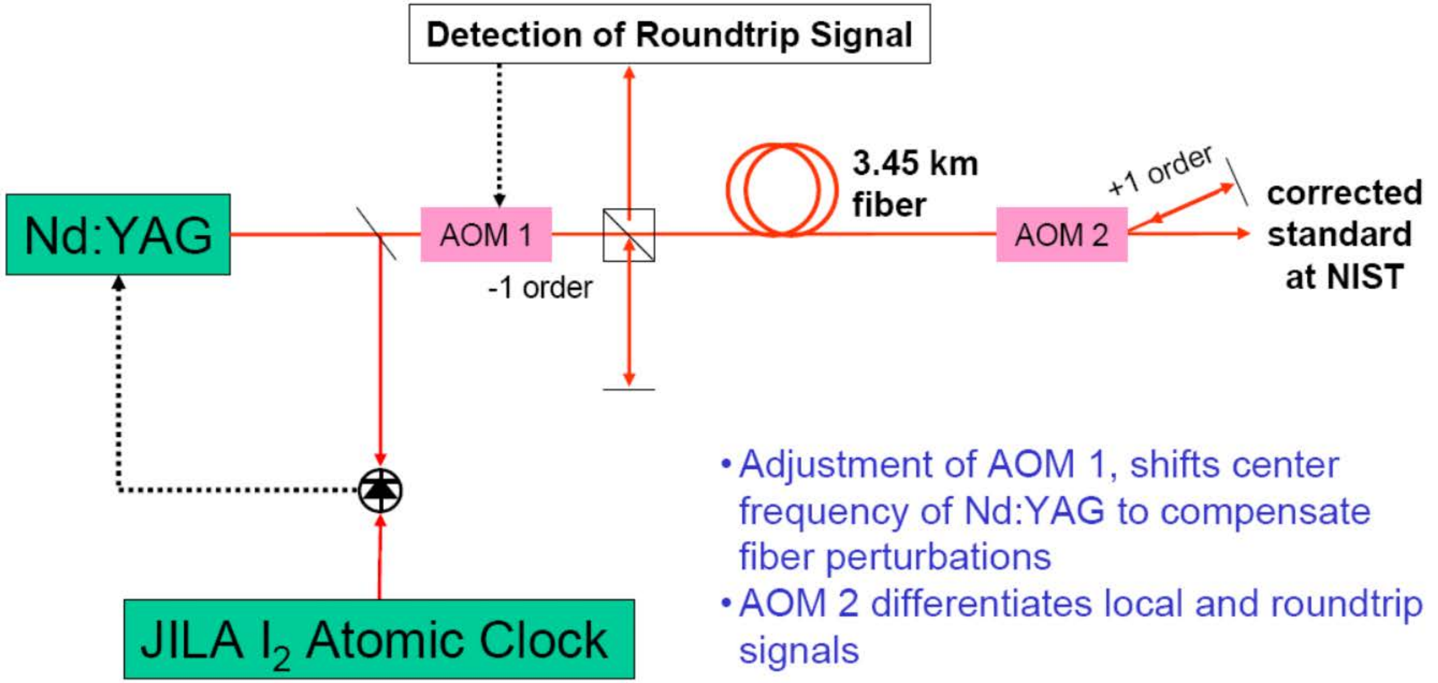

- Adjustment of AOM 1, shifts center frequency of Nd:YAG to compensate fiber perturbations
- AOM 2 differentiates local and roundtrip signals

Ref. JILA-NIST

레이저 주파수 안정화 – 이터븀 광격자 시계에서의 응용

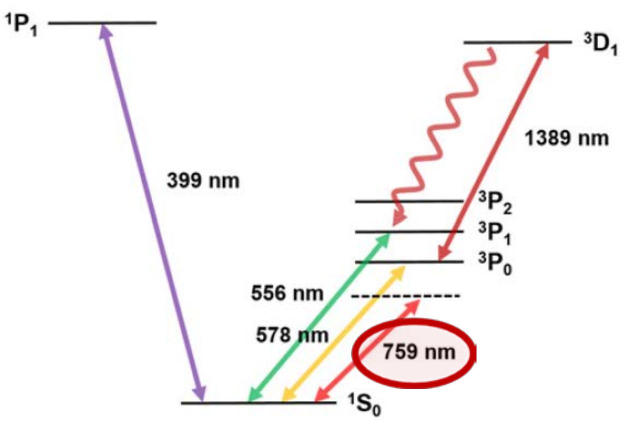

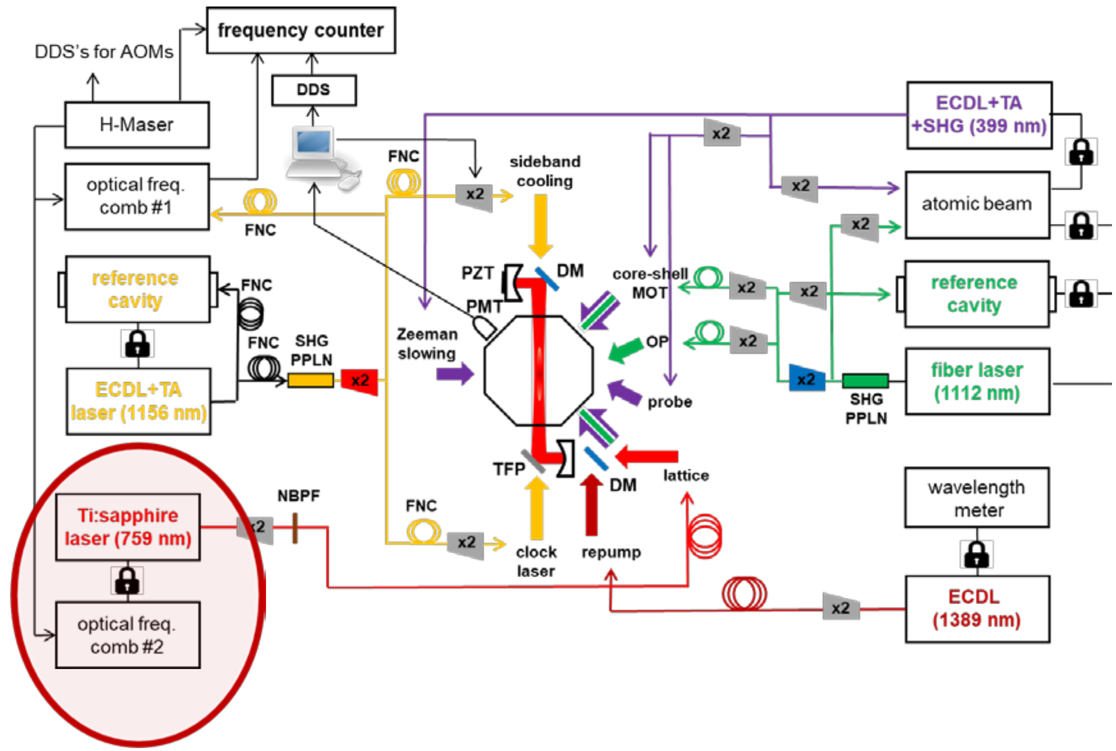

- 399 nm blue MOT laser – frequency-locked to atomic beam
- 556 nm green MOT laser – frequency-locked to atomic beam and reference cavity
- 578 nm clock laser – frequency-locked to reference cavity
- 578 nm clock laser – fiber frequency noise cancellation
- 759 nm lattice laser – phase-locked to optical frequency comb
- 1389 nm repumping laser – frequency-locked to wavemeter
- 578 nm clock laser – frequency-steered to Yb atom resonance
- ……

Metrologia_58_055007(2021)Absolute frequency measurement of the 171Yb optical lattice clock at KRISS using TAI for over a year.pdf

Heterodyne beat

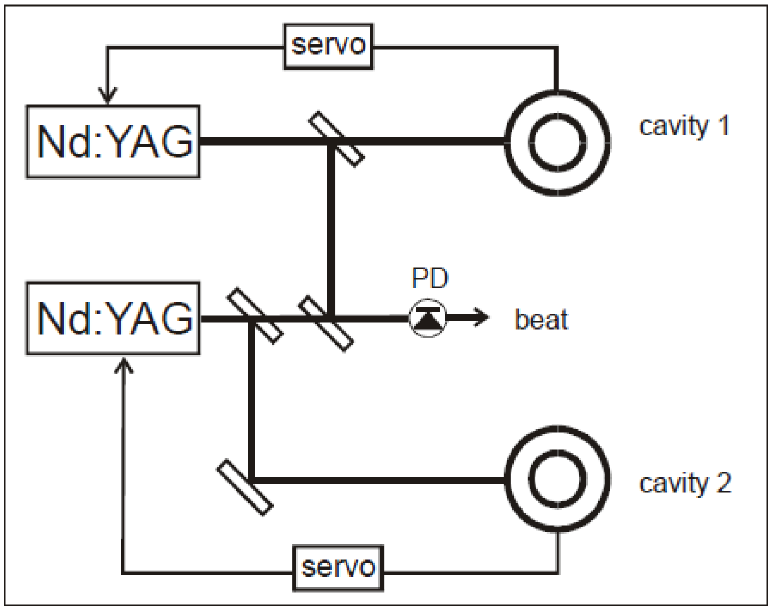

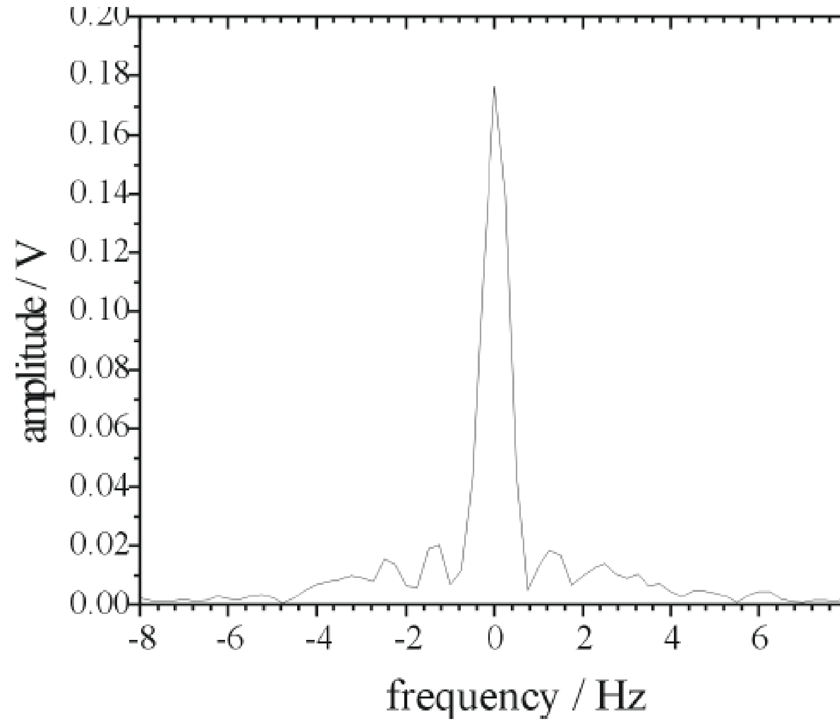

$\delta\nu = 0.7$ Hz (after removal of instrumental bandwidth of 0.25 Hz)
$\delta\nu = 0.5$ Hz (for at least one system)

"Subhertz-linewidth Nd:YAG laser", Webster *et al.*, Opt. Lett. **29** 1497 (2004)

Optical phase lock

- Optical phase lock between two lasers

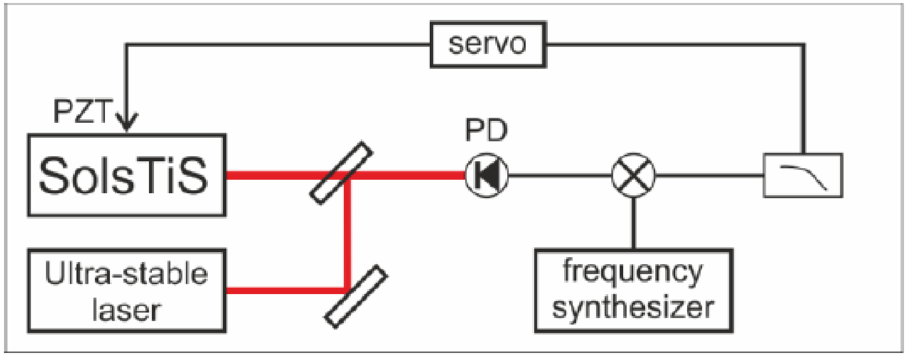

Phase-lock to ultra-stable laser
Feedback to PZT

- 759 nm lattice laser – phase-locked to optical frequency comb

Optical frequency comb phase locking to microwave reference

f_{rep} lock

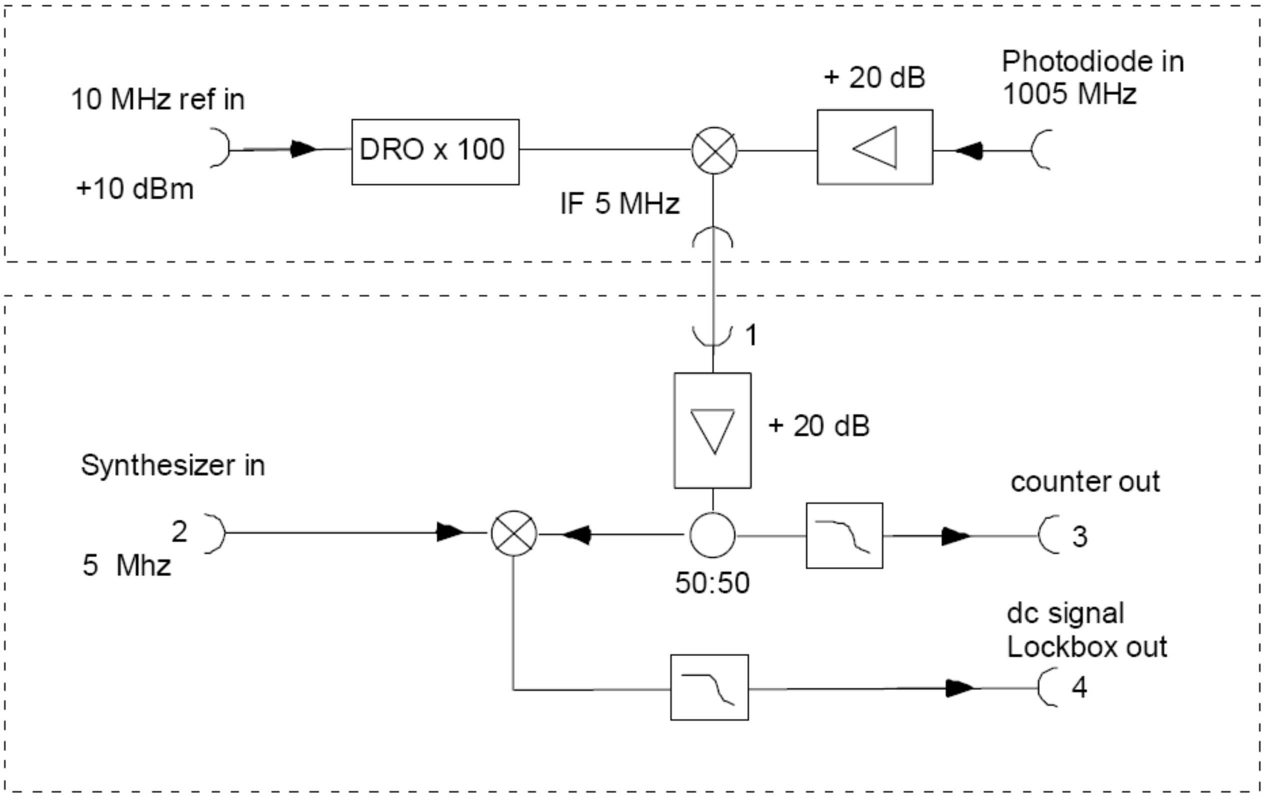

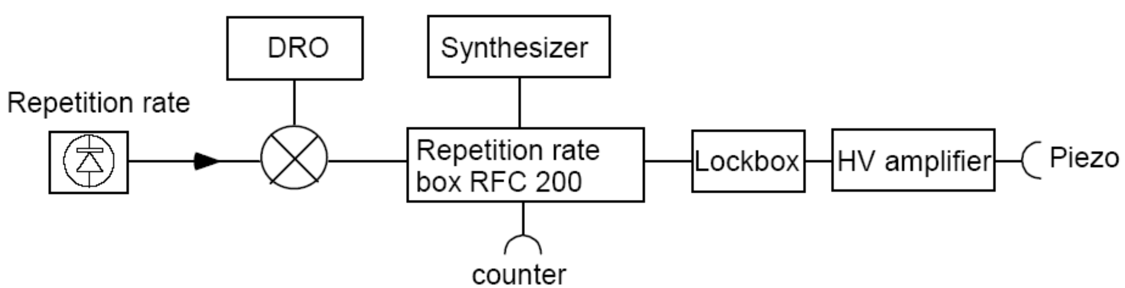

Optical frequency comb phase locking to microwave reference

f_{CEO} lock

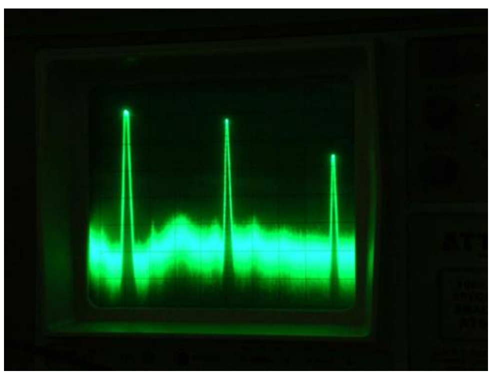

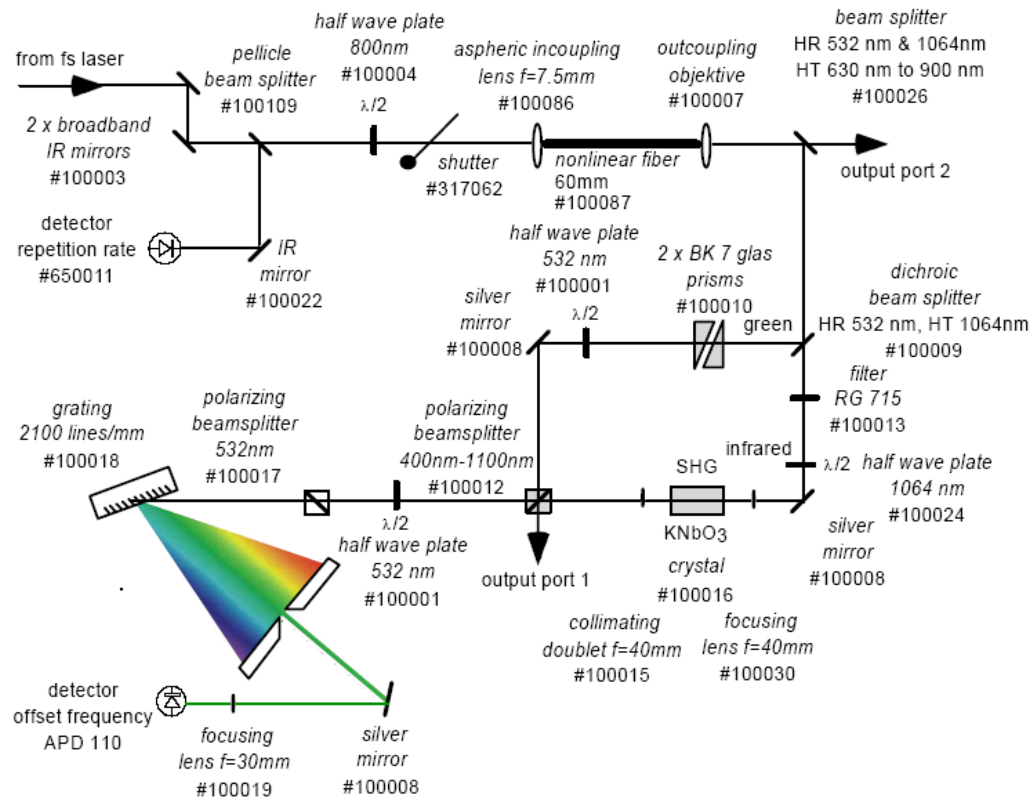

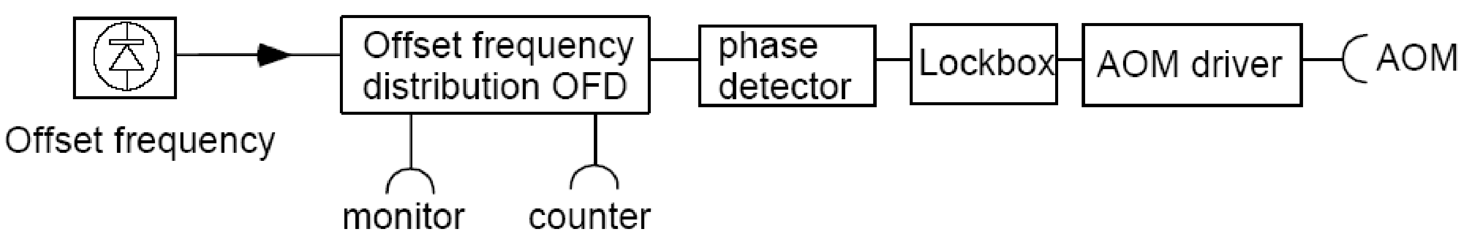

레이저 주파수 안정화 – 이터븀 광격자 시계에서의 응용

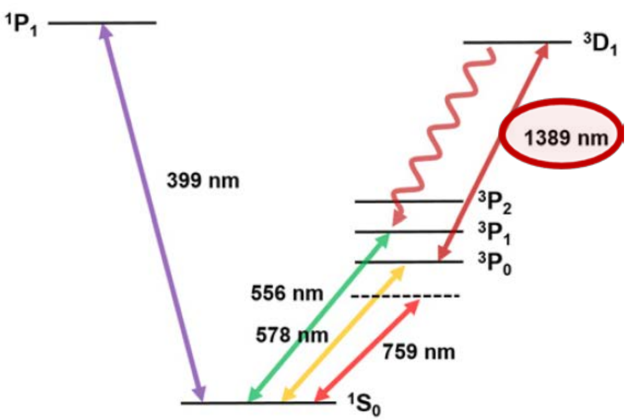

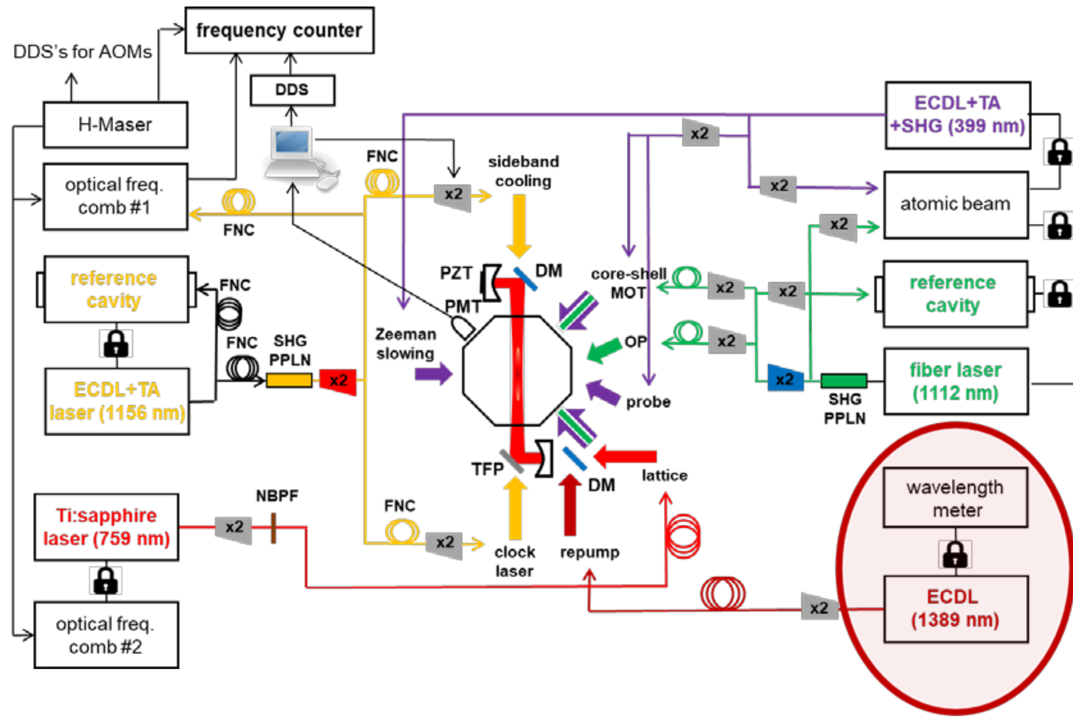

- 399 nm blue MOT laser – frequency-locked to atomic beam
- 556 nm green MOT laser – frequency-locked to atomic beam and reference cavity
- 578 nm clock laser – frequency-locked to reference cavity
- 578 nm clock laser – fiber frequency noise cancellation
- 759 nm lattice laser – phase-locked to optical frequency comb
- 1389 nm repumping laser – frequency-locked to wavemeter
- 578 nm clock laser – frequency-steered to Yb atom resonance
- ……

Metrologia_58_055007(2021)Absolute frequency measurement of the 171Yb optical lattice clock at KRISS using TAI for over a year.pdf

파장계를 이용한 레이저 주파수 안정화

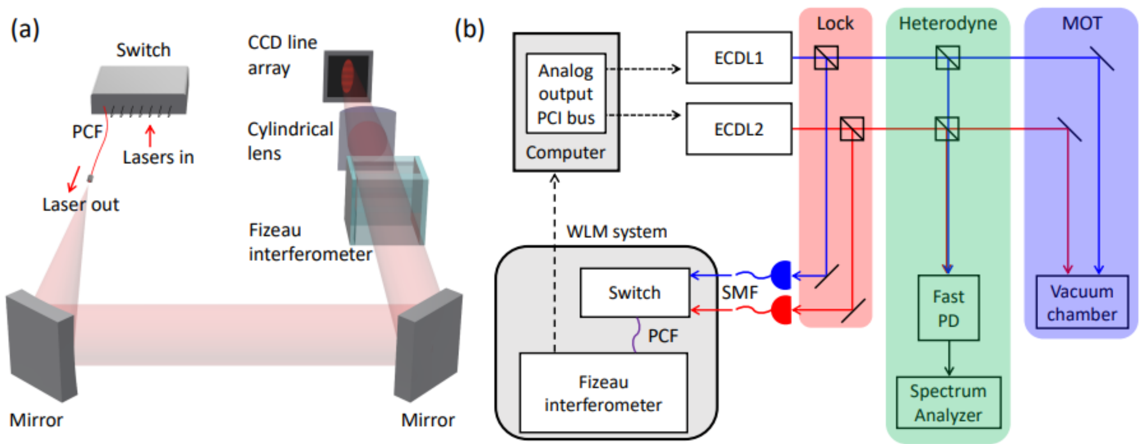

The frequency drift of the WLM is measured to be about 2.0(4) MHz over 36 h.

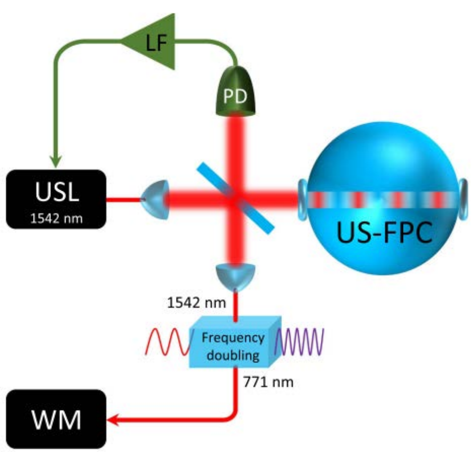

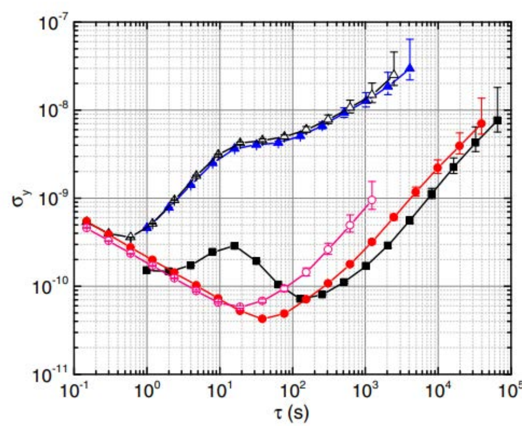

Blue: free-running
Red: 파장계 한계
Black: 파장계로 안정화된 레이저
(16초 bump 원인은 레이저 문제)

Ref.1. **Moonjoo Lee** - Sensors 21-6255(2021)-Locking Multi-Laser Frequencies to a Precision Wavelength Meter- Application to Cold Atoms
Ref.2. ao-54-32-9446(2015)Frequency stability of a wavelength meter and applications to laser frequency stabilization

Accuracy, Precision, and Stability

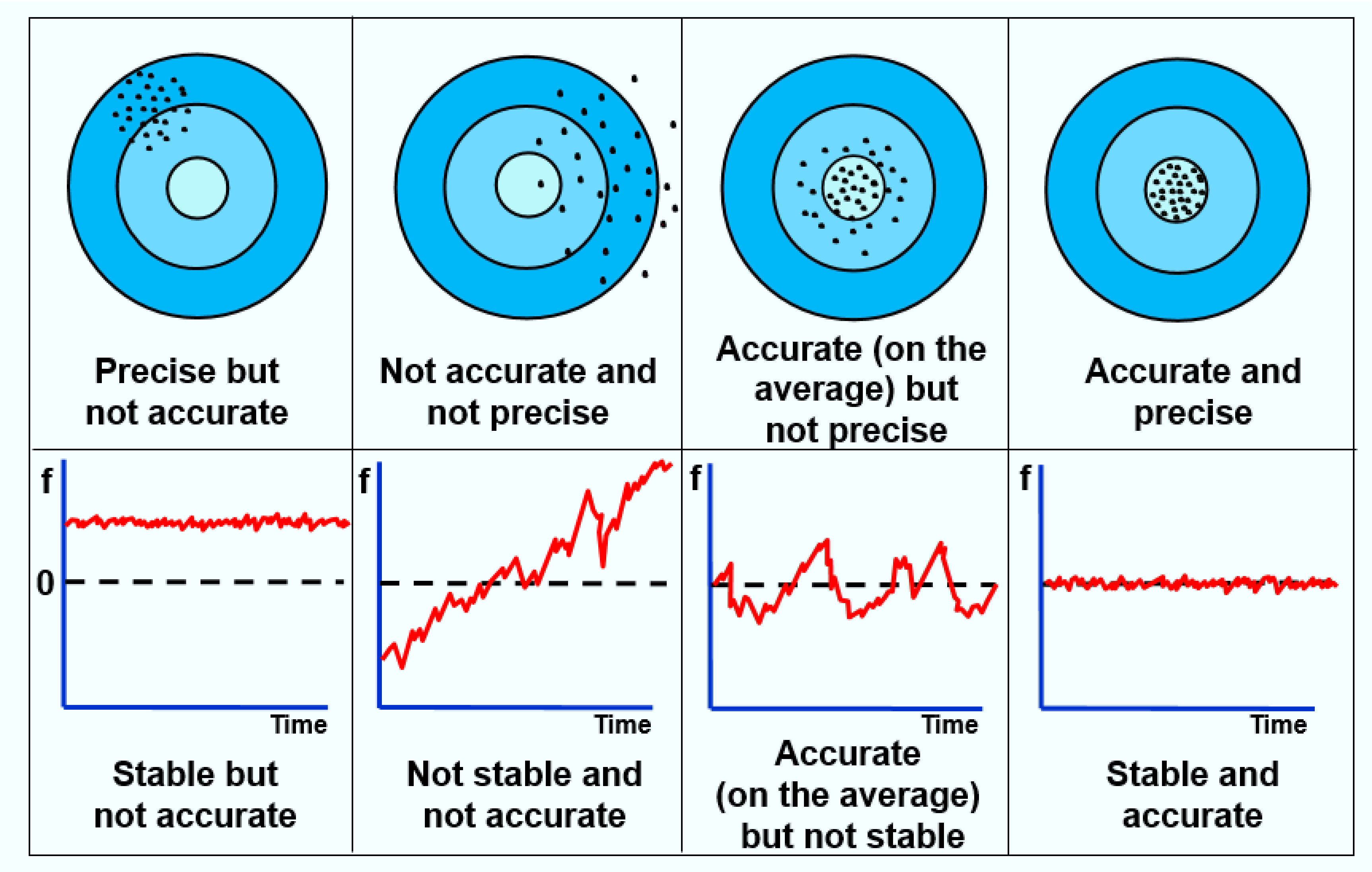

Short Term Instability (Noise)

Stable Frequency (Ideal Oscillator)

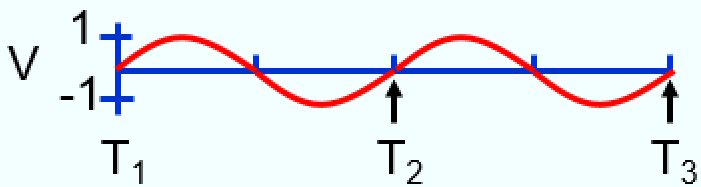

$V(t) = V_0 \sin(2\pi\nu_0 t)$

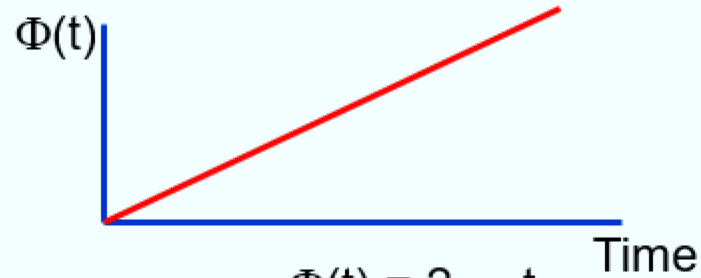

$\Phi(t) = 2\pi\nu_0 t$

Unstable Frequency (Real Oscillator)

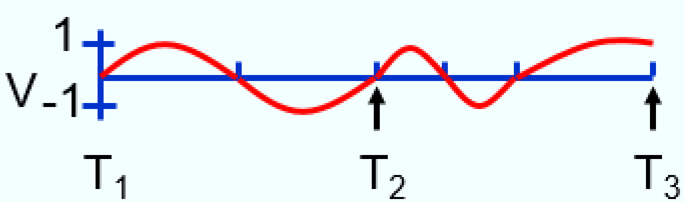

$V(t) = [V_0 + \varepsilon(t)] \sin[2\pi\nu_0 t + \phi(t)]$

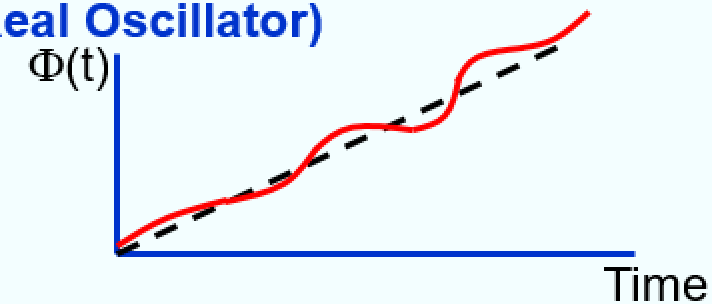

$\Phi(t) = 2\pi\nu_0 t + \phi(t)$

Instantaneous frequency, $\nu(t) = \frac{1}{2\pi}\frac{d\Phi(t)}{dt} = \nu_0 + \frac{1}{2\pi}\frac{d\phi(t)}{dt}$

$V(t)$ = Oscillator output voltage, V_0 = Nominal peak voltage amplitude

$\varepsilon(t)$ = Amplitude noise, ν_0 = Nominal (or "carrier") frequency

$\Phi(t)$ = Instantaneous phase, and $\phi(t)$ = Deviation of phase from nominal (i.e., the ideal)

Allan Deviation

Allan variance)

$$\sigma_y^2(\tau) = \frac{1}{2}\langle(\bar{y}_{t+\tau} - \bar{y}_t)^2\rangle$$

Allan standard deviation (ADEV)

$$\sigma_y(\tau) = \sqrt{\frac{1}{2}\langle(\bar{y}_{t+\tau} - \bar{y}_t)^2\rangle}$$

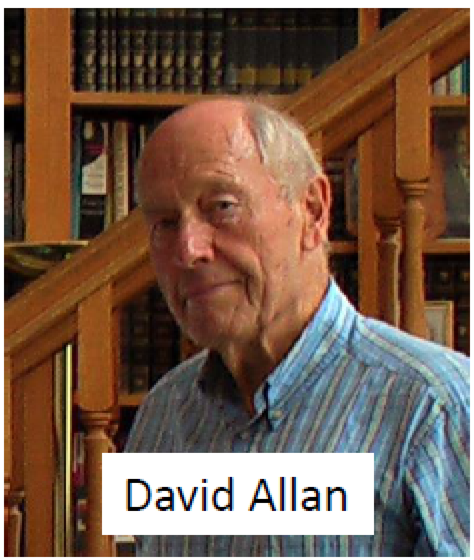

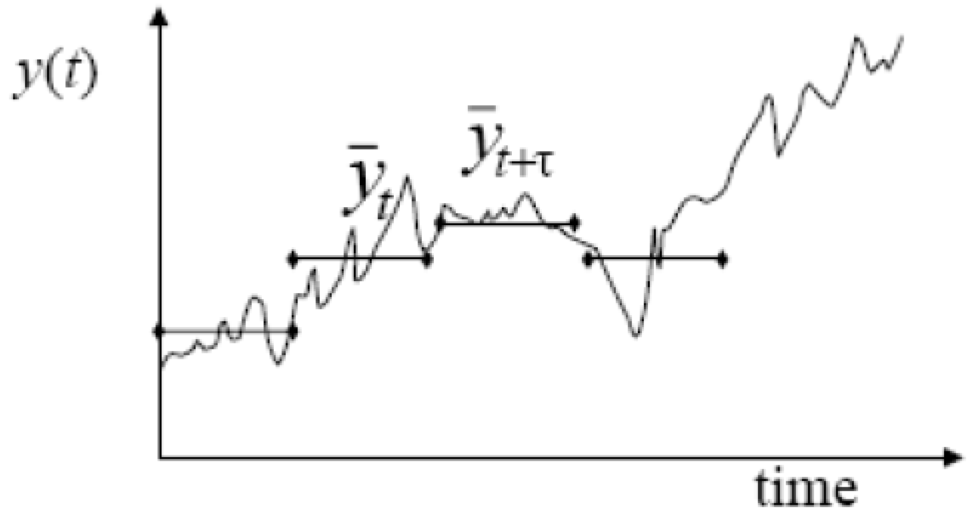

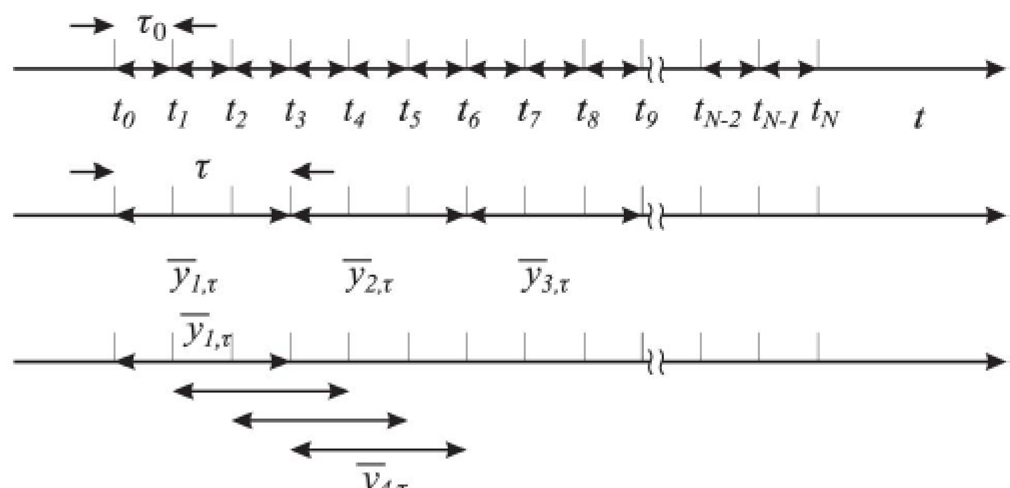

Fritz Riehle – Noise and stability of oscillators

Why Allan Deviation ?

- **Classical variance:** $$\sigma_{y_i}^2 = \frac{1}{m-1}\sum\left(y_i - \bar{y}\right)^2,$$

  diverges for some commonly observed noise processes, such as random walk, i.e., the variance increases with increasing number of data points.

- **Allan variance:**
  - Converges for all noise processes observed in precision oscillators.
  - Has straightforward relationship to power law spectral density types.
  - Is easy to compute.
  - Is faster and more accurate in estimating noise processes than the Fast Fourier Transform.

Allan Deviation and Frequency Noise

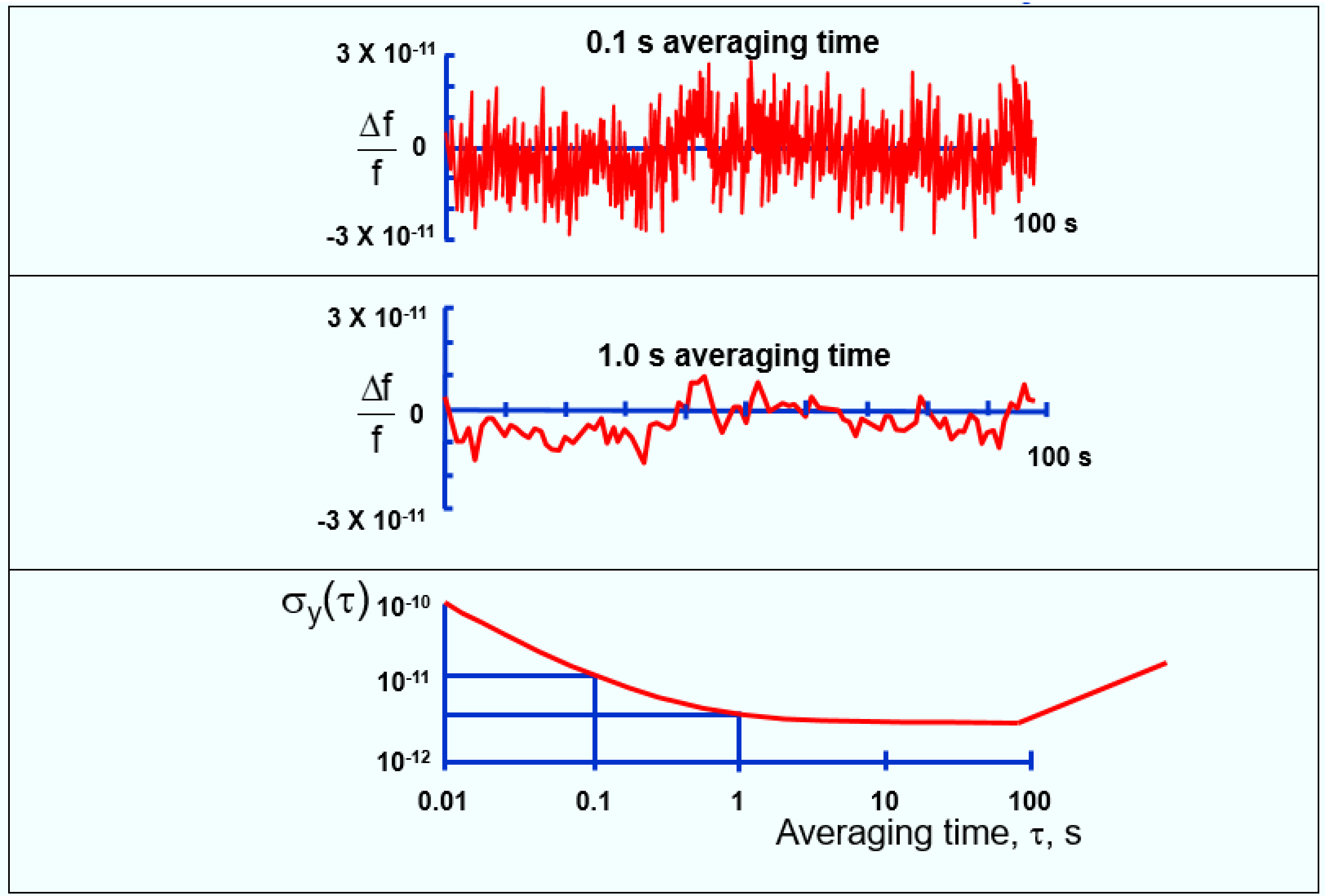

Allan Deviation – Power Law Dependence

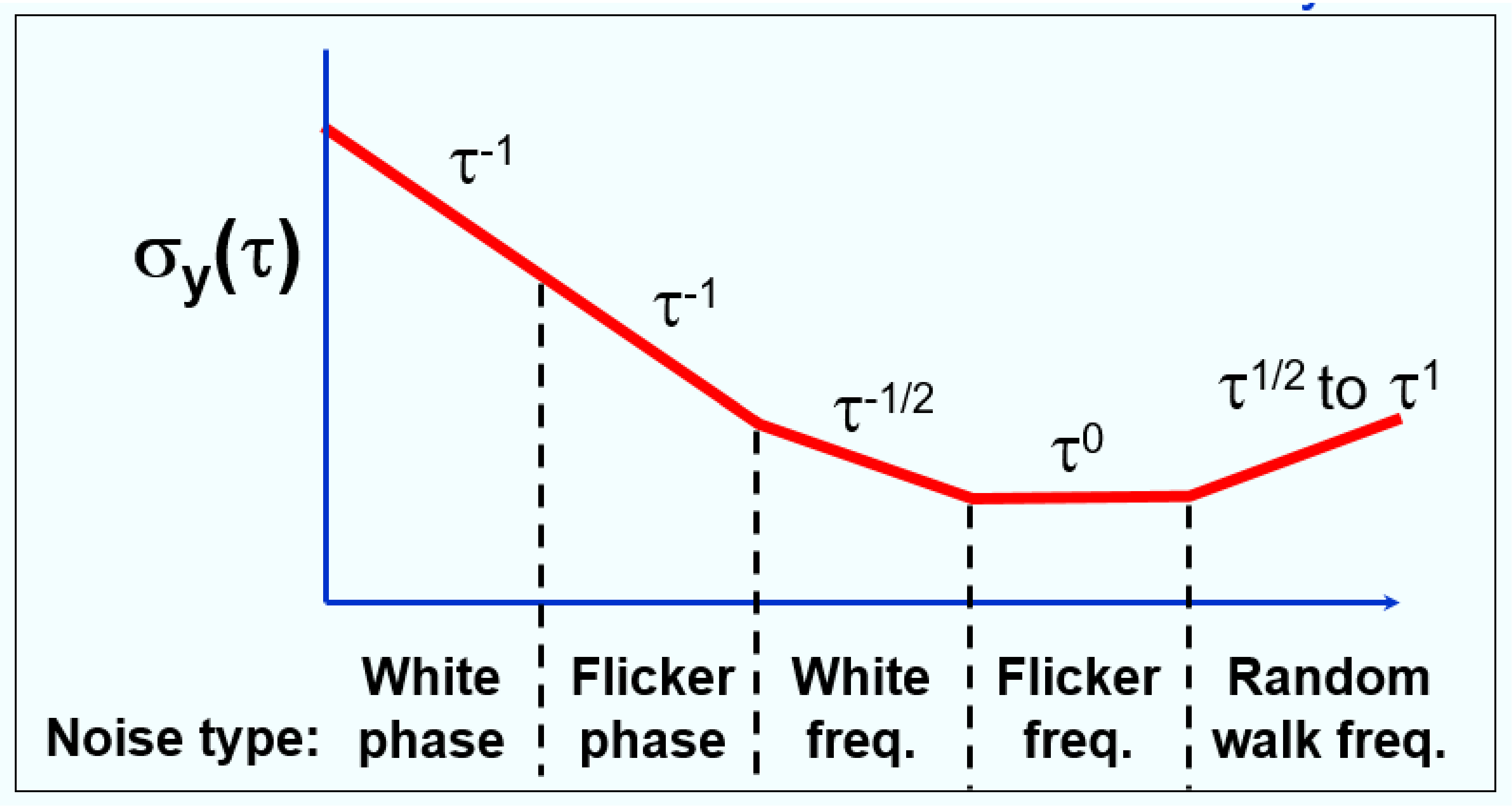

Short-term 안정도의 world-record

PRL 118, 263202 (2017) PHYSICAL REVIEW LETTERS week ending 30 JUNE 2017

1.5 μm Lasers with Sub-10 mHz Linewidth

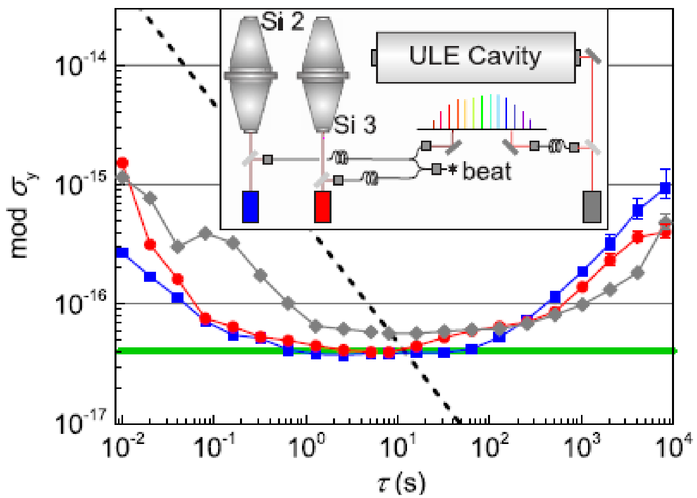

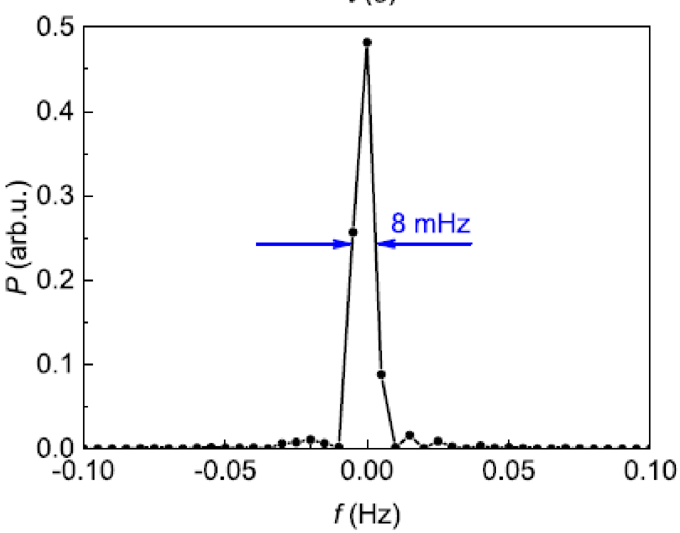

nature photonics ARTICLES
PUBLISHED ONLINE: 9 SEPTEMBER 2012 | DOI: 10.1038/NPHOTON.2012.217

A sub-40-mHz-linewidth laser based on a silicon single-crystal optical cavity

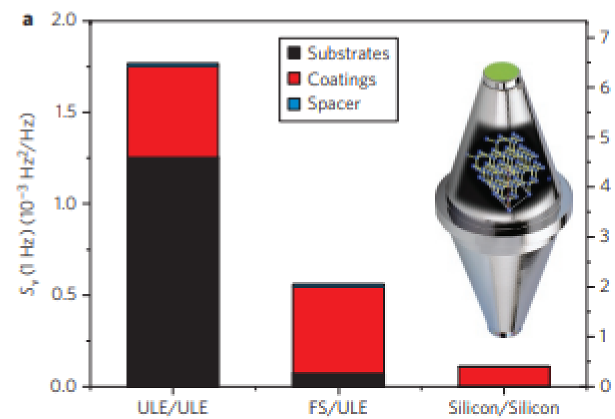

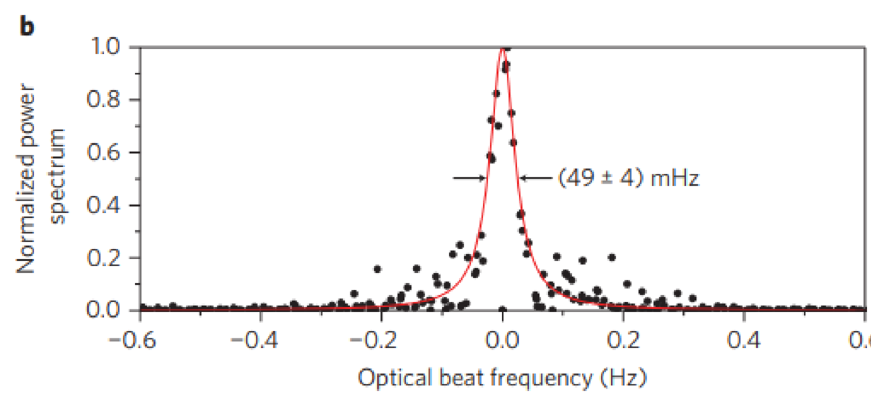

[1] PhysRevLett.118.263202(2017)1.5 μm Lasers with Sub-10 mHz Linewidth
[2] Nat. Photon. 6, 687(2012) A sub-40 mHz linewidth laser based on a silicon single-crystal optical cavity

Long-term 안정도, 정확도의 world-record

LETTER

https://doi.org/10.1038/s41586-018-0738-2

Atomic clock performance enabling geodesy below the centimetre level

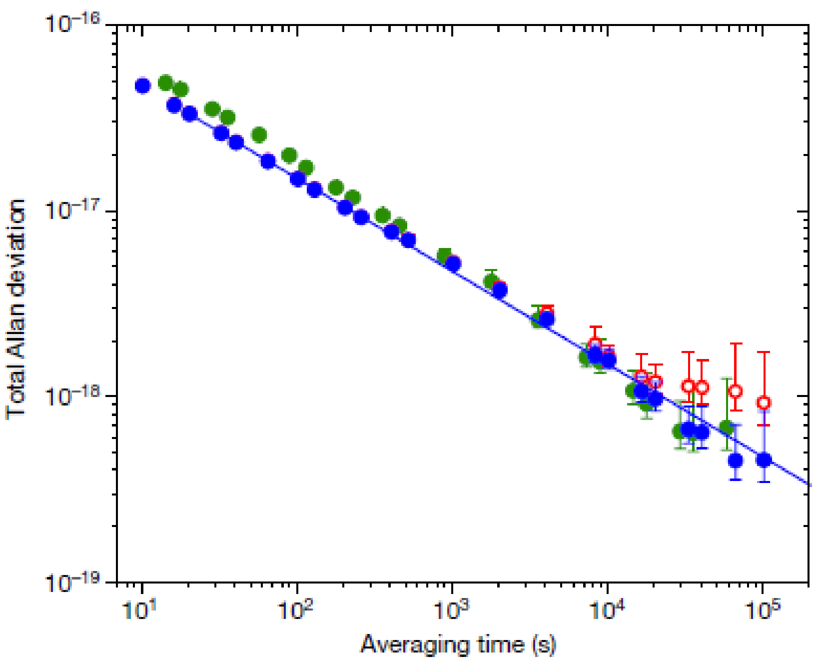

Measurement instability of 3.2 × 10^{-19}

Table 1 | Characteristic clock uncertainty budget

Shift	Yb-1 shift	Yb-1 uncertainty
Background gas collisions	−5.5	0.5
Spin polarization	0	<0.3
Cold collisions[a]	−0.21	0.07
Doppler	0	<0.02
BBR[a]	−2,361.2	0.9
Lattice light (model)	0	0.3
Travelling wave contamination	0	<0.1
Lattice light (experimental)	−1.5	0.8
Second-order Zeeman[a]	−118.1	0.2
DC Stark	0	<0.07
Probe Stark	0.02	0.01
Line pulling	0	<0.1
Tunnelling	0	<0.001
Servo error	0.03	0.05
Optical frequency synthesis	0	<0.1
Total	**−2,486.5**	**1.4**
Gravity shift from TT reference surface	180,819	6
Total shift from TT reference surface	**178,333**	**6**

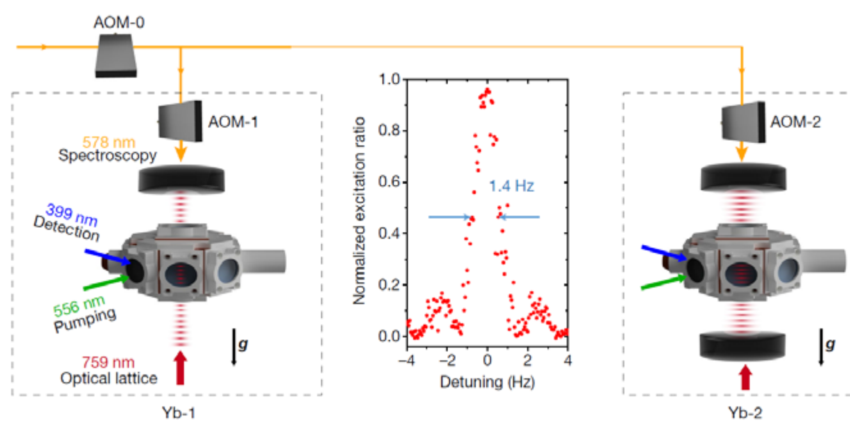

[1] nature564-87(2018)Atomic clock performance enabling geodesy below the centimetre level

Power Spectral Density

$$V(t) = [V_0 + \varepsilon(t)] \sin[2\pi\nu_0 t + \phi(t)]$$

In the frequency domain, due to the phase deviation, $\phi(t)$, some of the power is at frequencies other than ν_0. The stabilities are characterized by "spectral densities." The spectral density, $S_V(f)$, the mean-square voltage $\langle V^2(t) \rangle$ in a unit bandwidth centered at f, is not a good measure of frequency stability because both $\varepsilon(t)$ and $\phi(t)$ contribute to it, and because it is not uniquely related to frequency fluctuations (although $\varepsilon(t)$ is often negligible in precision frequency sources.)

The spectral densities of phase and fractional-frequency fluctuations, $S_\phi(f)$ and $S_y(f)$, respectively, are used to measure the stabilities in the frequency domain. The spectral density $S_g(f)$ of a quantity g(t) is the mean square value of g(t) in a unit bandwidth centered at f. Moreover, the RMS value of g^2 in bandwidth BW is given by $g^2_{RMS}(t) = \int_{BW} S_g(f)df$.

Frequency - Phase - Time Relationships

$$\nu(t) = \nu_0 + \frac{1}{2\pi}\frac{d\phi(t)}{dt} = \text{"instantaneous" frequency;} \quad \phi(t) = \phi_0 + \int_0^t 2\pi[\nu(t') - \nu_0]dt'$$

$$y(t) \equiv \frac{\nu(t) - \nu_0}{\nu_0} = \frac{\dot{\phi}(t)}{2\pi\nu_0} = \text{normalized frequency;} \quad \phi_{RMS}^2 = \int S_\phi(f)dt$$

$$S_\phi(f) = \frac{\phi_{RMS}^2}{BW} = \left(\frac{\nu_0}{f}\right)^2 S_y(f); \qquad \mathcal{L}(f) \equiv 1/2\ S_\phi(f), \text{ per IEEE Standard 1139} - 1988$$

$$\sigma_y^2(\tau) = 1/2 < \left(\bar{y}_{k+1} - \bar{y}_k\right)^2 > = \frac{2}{(\pi\nu_0\tau)^2}\int_0^\infty S_\phi(f)\sin^4(\pi f\tau)\,df$$

The five common power-law noise processes in precision oscillators are:

$$S_y(f) = \underset{\text{(White PM)}}{h_2 f^2} + \underset{\text{(Flicker PM)}}{h_1 f} + \underset{\text{(White FM)}}{h_0} + \underset{\text{(Flicker FM)}}{h_{-1} f^{-1}} + \underset{\text{(Random-walk FM)}}{h_{-2} f^{-2}}$$

$$\text{Time deviation} = x(t) = \int_o^t y(t')dt' = \frac{\phi(t)}{2\pi\nu}$$

Phase noise power spectral density

$$S_y(f) = \frac{1}{\nu_0^2} S_\nu(f) \qquad S_\nu(f) = f^2 S_\phi(f) \qquad S_y(f) = \frac{f^2}{\nu_0^2} S_\phi(f)$$

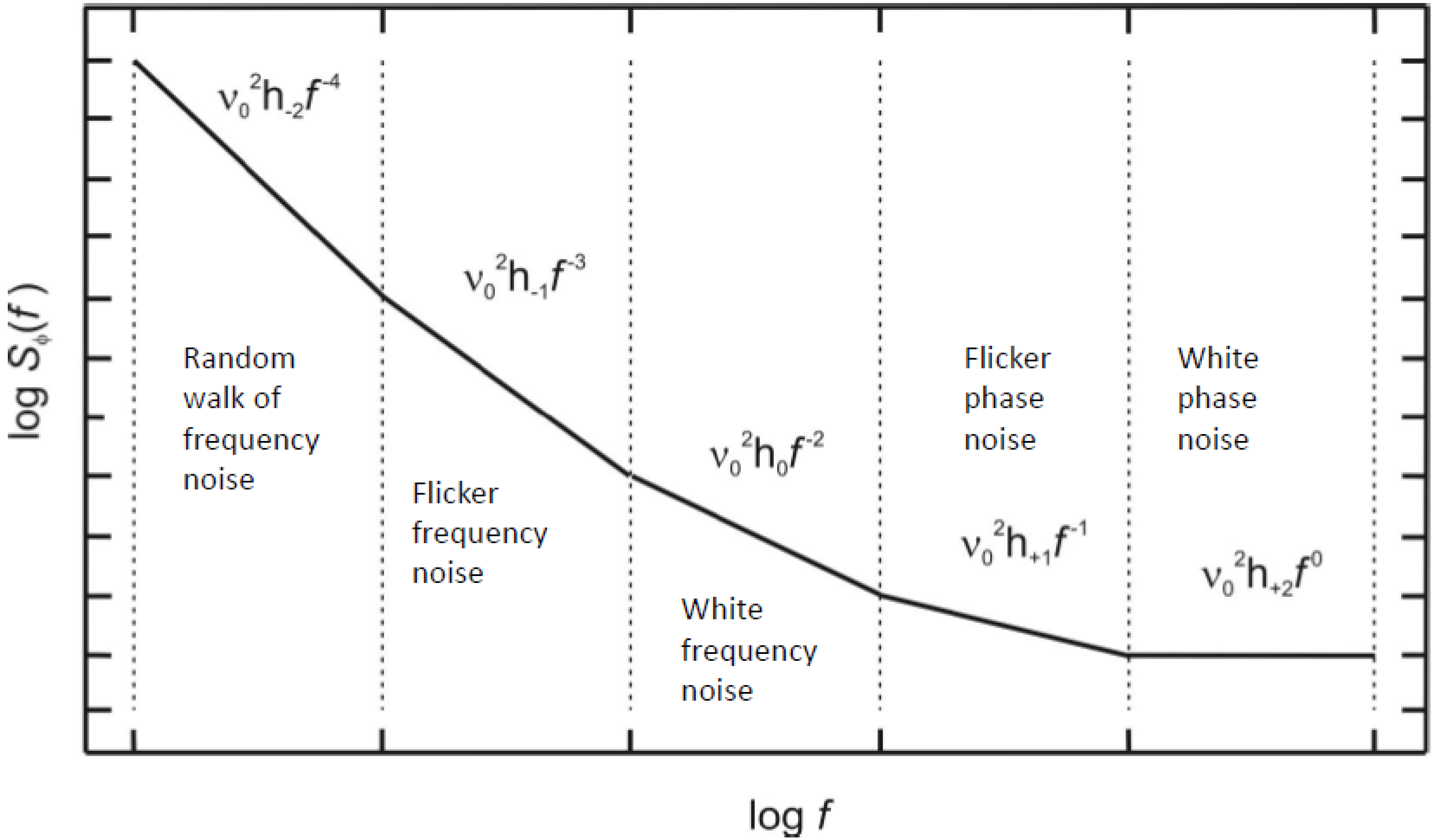

Fritz Riehle – Noise and stability of oscillators

frequency noise power spectral density

$$S_y(f) = \sum_{\alpha=-2}^{2} h_\alpha f^\alpha \qquad S_y(f) = \frac{S_\phi(f)}{f^2}$$

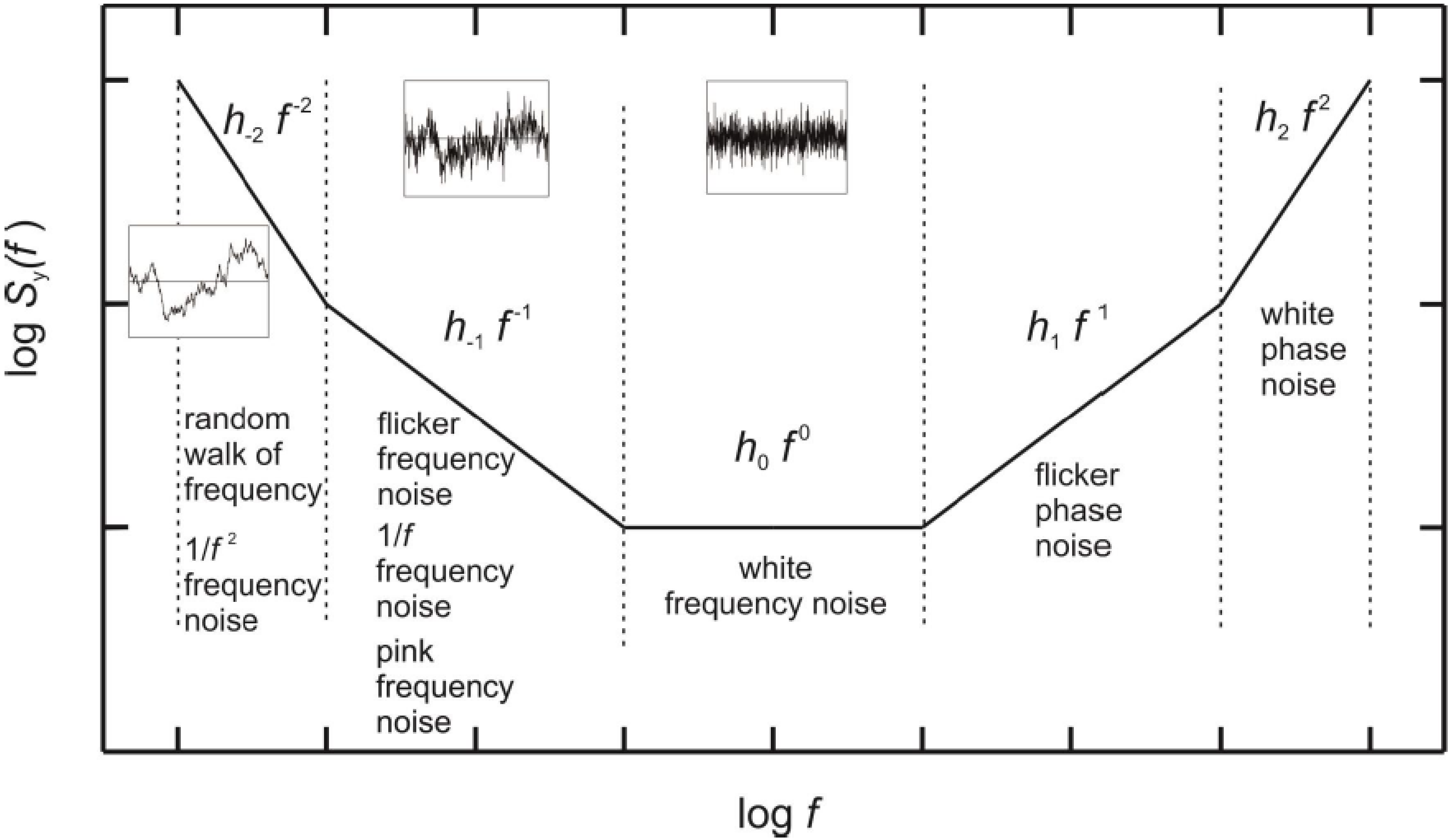

Fritz Riehle – Noise and stability of oscillators

Phase noise and friends

random phase fluctuation

$$S_\varphi(f) = \text{PSD of } \varphi(t)$$

power spectral density

it is measured as

$$S_\varphi(f) = \mathbb{E}\left\{\Phi(f)\Phi^*(f)\right\} \quad \text{(expectation)}$$

$$S_\varphi(f) \approx \left\langle \Phi(f)\Phi^*(f) \right\rangle_m \quad \text{(average)}$$

$$\mathcal{L}(f) = \frac{1}{2} S_\varphi(f) \ \ \text{dBc}$$

random fractional-frequency fluctuation

$$y(t) = \frac{\dot{\varphi}(t)}{2\pi\nu_0} \quad \Rightarrow \quad S_y = \frac{f^2}{\nu_0^2} S_\varphi(f)$$

Allan variance
(two-sample wavelet-like variance)

$$\sigma_y^2(\tau) = \mathbb{E}\left\{ \frac{1}{2}\left[\overline{y}_{k+1} - \overline{y}_k\right]^2 \right\} .$$

approaches a half-octave bandpass filter (for white noise), hence it converges for processes steeper than 1/f

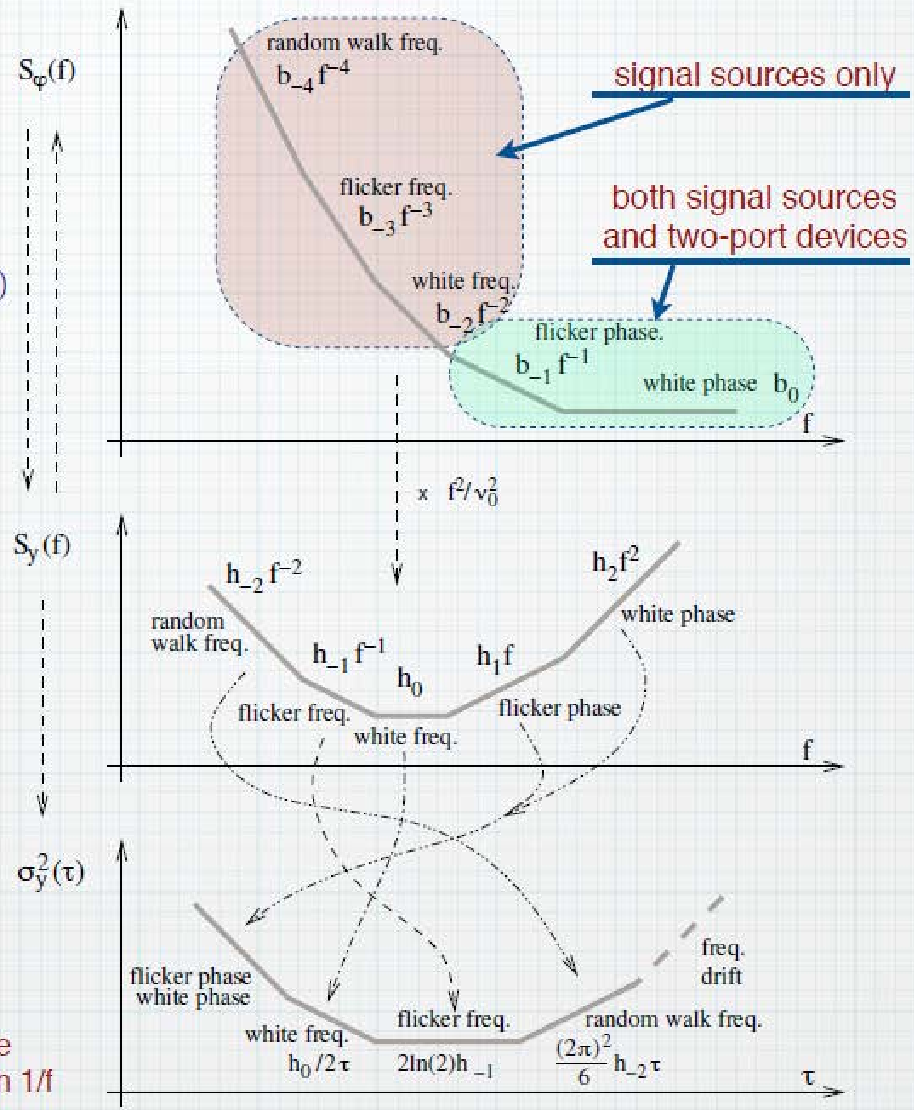

Modified Allan variance

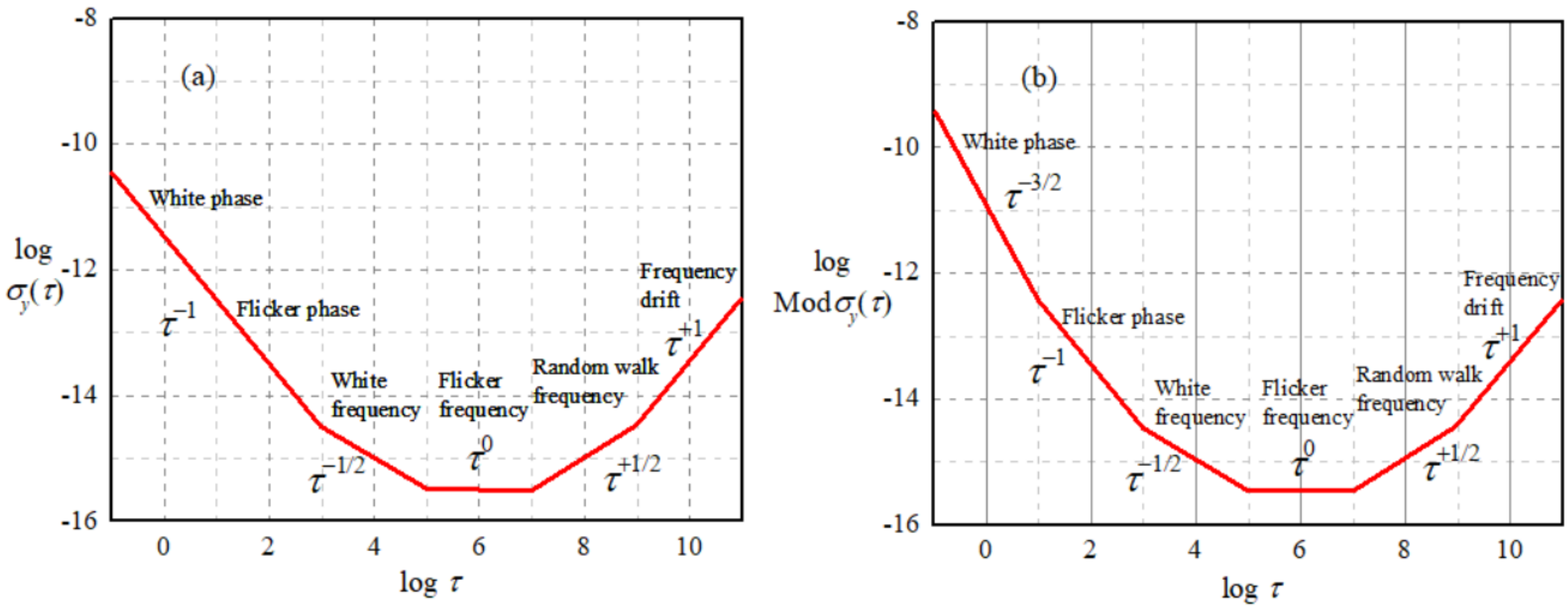

W. J. Riley, "Handbook of frequency stability analysis," (2008)

Relationships between spectra and variances

noise type	$S_\varphi(f)$	$S_y(f)$	$S_\varphi \leftrightarrow S_y$	$\sigma_y^2(\tau)$	mod $\sigma_y^2(\tau)$
white PM	b_0	$h_2 f^2$	$h_2 = \frac{b_0}{\nu_0^2}$	$\frac{3 f_H h_2}{(2\pi)^2} \tau^{-2}$ $2\pi\tau f_H \gg 1$	$\frac{3 f_H \tau_0 h_2}{(2\pi)^2} \tau^{-3}$
flicker PM	$b_{-1} f^{-1}$	$h_1 f$	$h_1 = \frac{b_{-1}}{\nu_0^2}$	$[1.038 + 3\ln(2\pi f_H \tau)] \frac{h_1}{(2\pi)^2} \tau^{-2}$	$0.084\, h_1 \tau^{-2}$ $n \gg 1$
white FM	$b_{-2} f^{-2}$	h_0	$h_0 = \frac{b_{-2}}{\nu_0^2}$	$\frac{1}{2} h_0 \tau^{-1}$	$\frac{1}{4} h_0 \tau^{-1}$
flicker FM	$b_{-3} f^{-3}$	$h_{-1} f^{-1}$	$h_{-1} = \frac{b_{-3}}{\nu_0^2}$	$2\ln(2)\; h_{-1}$	$\frac{27}{20} \ln(2)\; h_{-1}$
random walk FM	$b_{-4} f^{-4}$	$h_{-2} f^{-2}$	$h_{-2} = \frac{b_{-4}}{\nu_0^2}$	$\frac{(2\pi)^2}{6} h_{-2} \tau$	$0.824\, \frac{(2\pi)^2}{6} h_{-2} \tau$
linear frequency drift $\dot{y}$				$\frac{1}{2} (\dot{y})^2 \tau^2$	$\frac{1}{2} (\dot{y})^2 \tau^2$

f_H is the high cutoff frequency, needed for the noise power to be finite.

Short-Term Stability Measures

Measure	Symbol
Two-sample deviation, also called "Allan deviation"	$\sigma_y(\tau)$*
Spectral density of phase deviations	$S_\phi(f)$
Spectral density of fractional frequency deviations	$S_y(f)$
Phase noise	$\mathcal{L}(f)$*
* Most frequently found on oscillator specification sheets	

$$f^2 S_\phi(f) = \nu^2 S_y(f);\ \ \mathcal{L}(f) \equiv ½\,[S_\phi(f)] \qquad \text{(per IEEE Std. 1139),}$$

and

$$\sigma_y^2(\tau) = \frac{2}{(\pi\nu\tau)^2}\int_0^\infty S_\phi(f)\sin^4(\pi f\tau)\,df$$

Where τ = averaging time, ν = carrier frequency, and f = offset or Fourier frequency, or "frequency from the carrier".

http://rubiola.org/

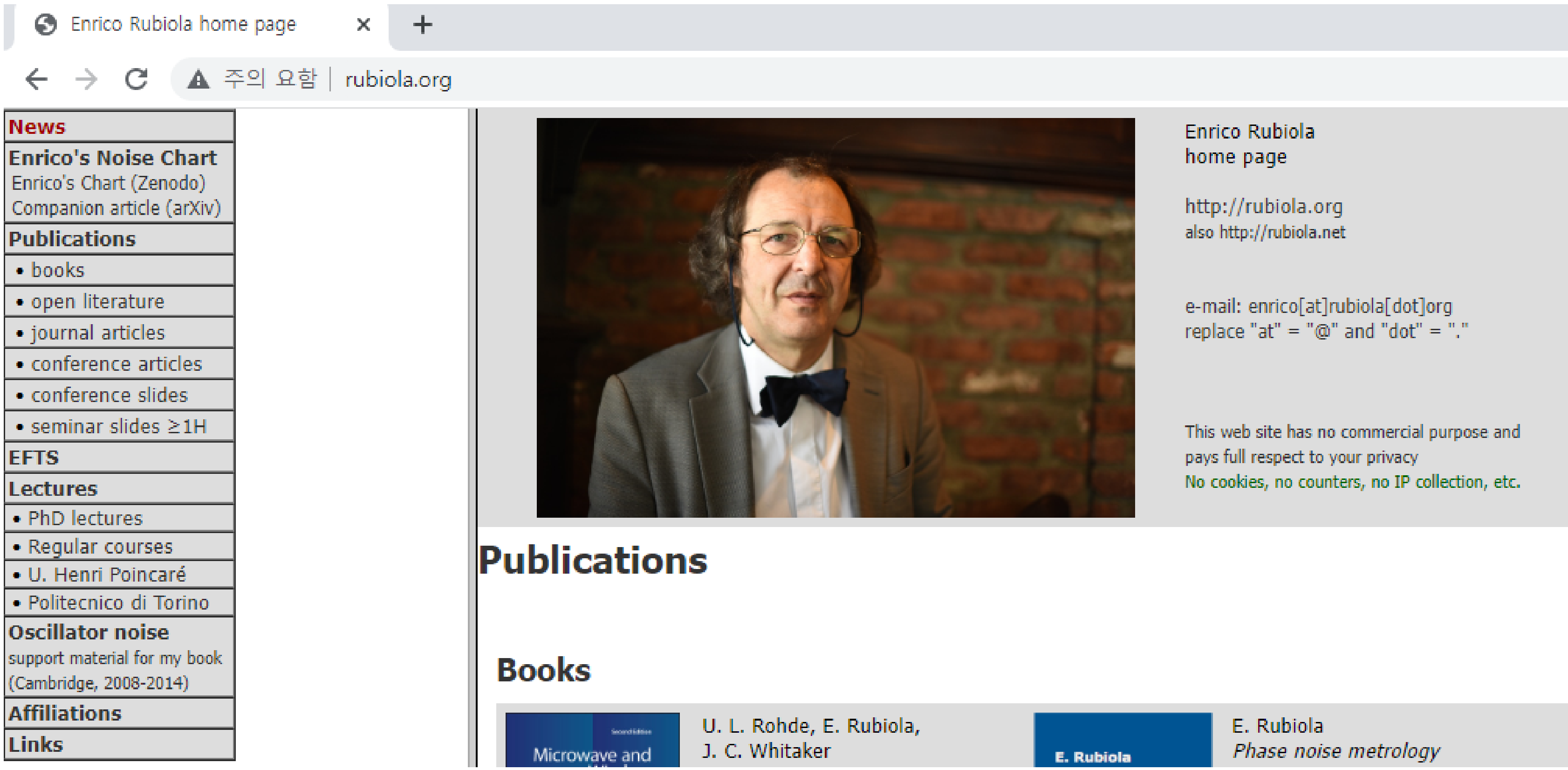

Stable32

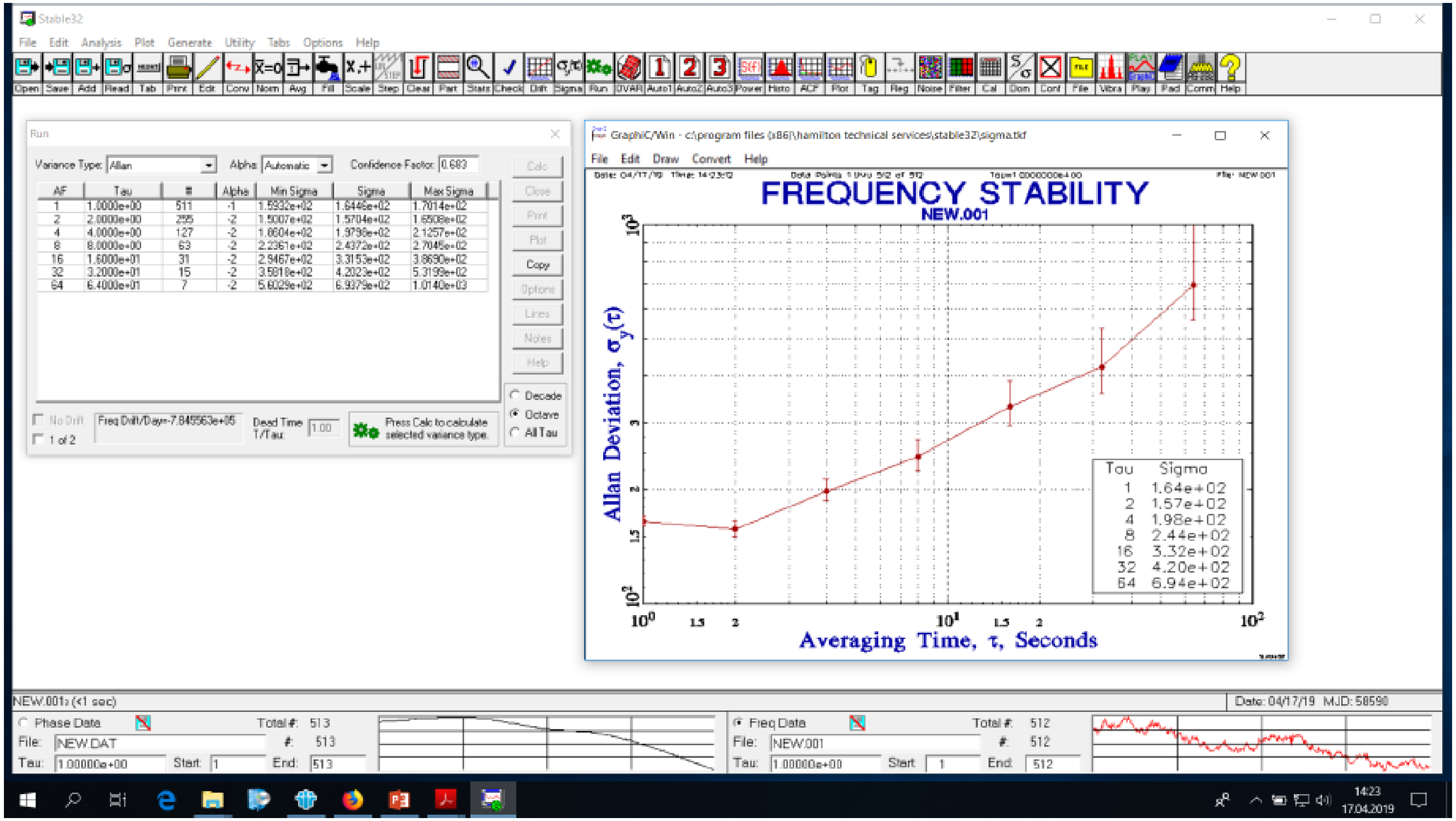

The Stable32 program for frequency stability analysis is freely available from the IEEE UFFC-S

http://www.stable32.com/

Stable32

https://github.com/IEEE-UFFC/stable32

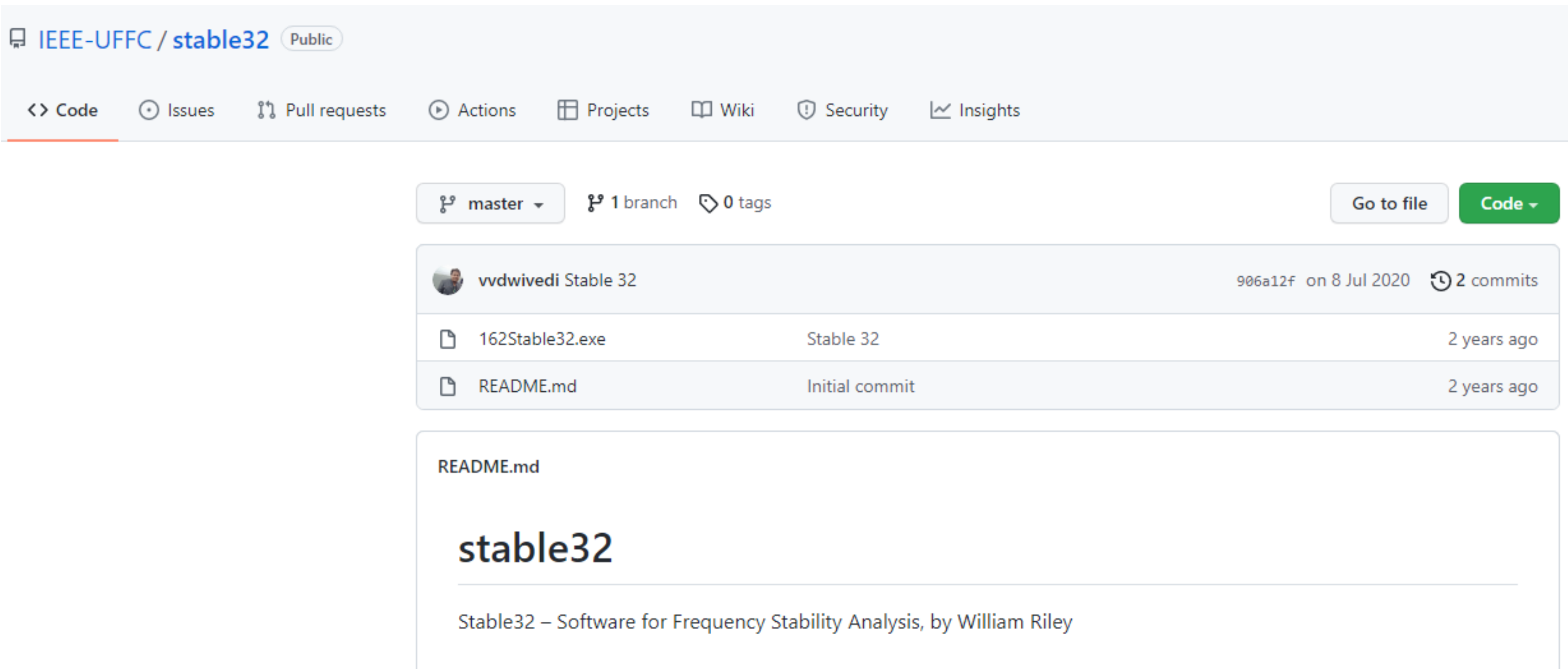

Linewidth

NKT Photonics Koheras ADJUSTIK low noise single-frequency lasers

Rack mountable benchtop, low noise fiber laser featuring ultra-low phase noise and Hz-range linewidth. Standard systems are available at 1550.12nm and 1064.00nm and we offer special systems anywhere in the 1535–1580nm and 1030–1120nm ranges. Depending on the model, output powers are 10-40mW.

The benchtop ADJUSTIK models are based on the Koheras BASIK Module seed technology but supplied in a 19" rack mounted unit with front panel control interface. The standard ADJUSTIK is availabel at powers from 10-40mW, and the ADJUSTIK HP in powers up to 2 W output power

Linewidth specification < <1 kHz@120us

Simple approach to the relation between laser frequency noise and laser line shape

Appl. Opt. **49**, 4801(2010)

<질문하나>

선폭이 1 MHz인 레이저의 선폭을 줄이려면 feedback servo의 control bandwidth는 최소한 얼마라야 할까?

1. 100 kHz
2. 570 kHz
3. 1 MHz
4. 3 MHz

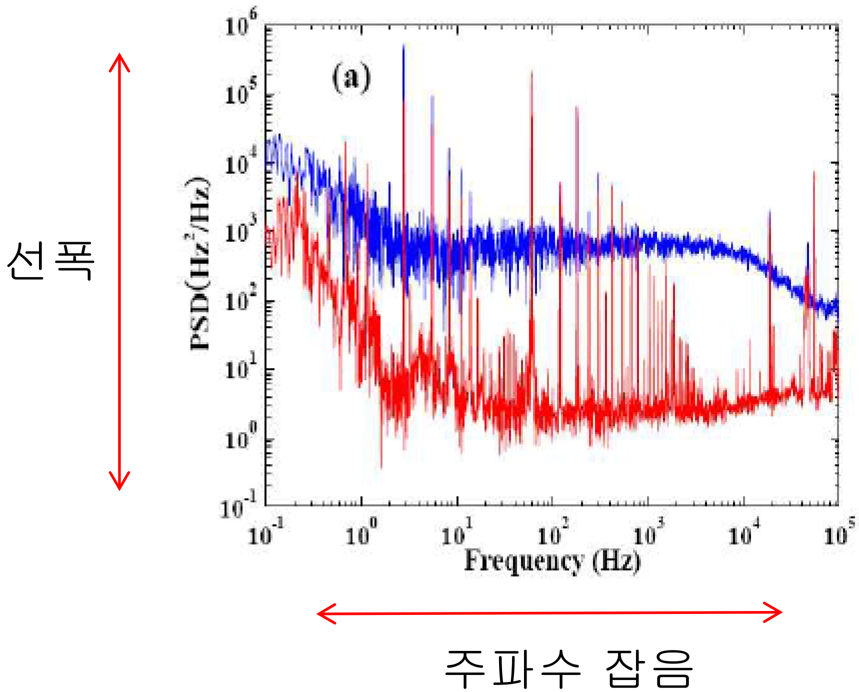

Linewidth, drift, and measurement time

❖ Processes faster than the measurement time broaden the spectrum or the linewidth of the laser.

❖ Processes slower than the measurement time cause the spectrum drift between measurements.

❖ Typical measurement time lie between us and s.

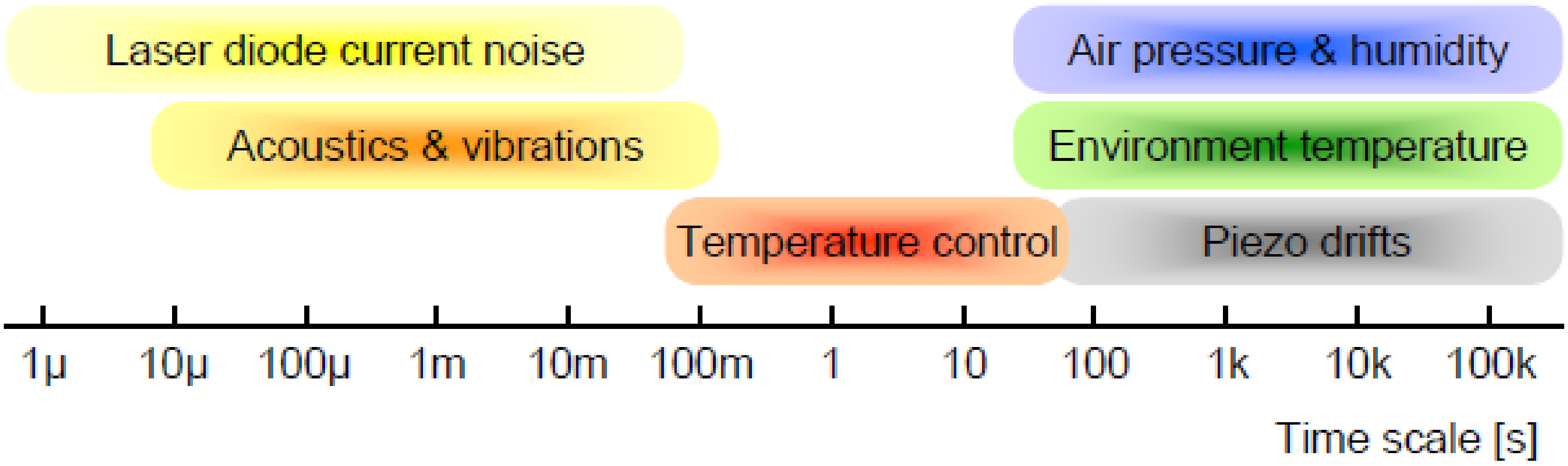

Linewidth vs. Frequency Noise Spectum

<Linewidth>

❖ Simple parameter
❖ Optical line shape
❖ Time scale should be given
❖ By heterodyning with an independent laser source
❖ By self-homodyne/heterodyne interferometry using a long delay line

<Freq. Noise Spectral Density>

<(FNSD)>

❖ More complete information
❖ Spectrum of laser freq. fluctuation
❖ By using a frequency discriminator

$$E(t) = E_0 \exp[i(2\pi\nu_0 t + \phi(t))]$$

$$S_E \quad \underset{\not\longrightarrow}{\longleftarrow} \quad S_{\delta\nu}$$

Linewidth derivation from FNSD

- Laser light field; $E(t) = E_0 \exp[i(2\pi\nu_0 t + \phi(t))]$
- Frequency; $\nu(t) = \nu_0 + \delta\nu = \nu_0 + \dfrac{d\phi(t)}{2\pi dt}$
- FNSD; $S_{\delta\nu}(f) = \dfrac{1}{BW}\left\langle \left| \int_f^{f+BW} \int_{-\infty}^{\infty} \dfrac{d\phi(t)}{2\pi dt} e^{-i2\pi ft} dtdf \right|^2 \right\rangle$
- Autocorrelation function;

$$\Gamma_E(\tau) = < E^*(t)E(t+\tau) >= E_0^2 \exp[i2\pi\nu_0\tau] < \exp[i\{\phi(t) - \phi(t+\tau)\}] >$$

$$= E_0^2 \exp[i2\pi\nu_0\tau] \exp\left\{ -\frac{1}{2} < [\phi(t) - \phi(t+\tau)\}]^2 > \right\}$$; Gaussian momentum theorem

$$= E_0^2 \exp[i2\pi\nu_0\tau] \exp\left\{ -2\int_0^{\infty} S_{\delta\nu}(f) \frac{\sin^2(\pi f\tau)}{f^2} df \right\}$$

Wiener-Khinchin theorem (power spectrum is the Fourier transform of the corresponding autocorrelation function)

- Laser line shape; $\boxed{S_E(f) = 2\int_{-\infty}^{\infty} \exp[-i2\pi f\tau]\Gamma_E(\tau) d\tau}$

Linewidth derivation from FNSD

<in case of pure white frequency noise>

Analytic solution exists.

$$S_{\delta\nu}(f) = h_0$$

$$S_E(\nu) = E_0^2 \frac{h_0}{(\nu-\nu_0)^2 + (\pi h_0/2)^2}$$; Lorentzian with FWHM = πh_0

<Example>

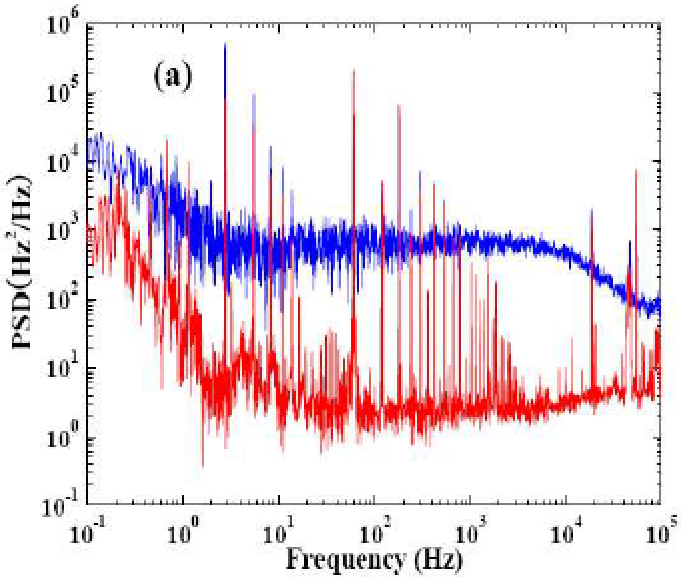

The white noise level was approximately 540 Hz^2/Hz,

inherent linewidth of $\pi S_f(f)$ = 1.7 kHz (full widths at half-maximum)

Linewidth derivation from FNSD

<in case of Low-Pass filtered white frequency noise>

$$S_{\delta\nu}(f) = \begin{cases} h_0 & \text{if } f \le f_c \\ 0 & \text{if } f > f_c \end{cases}.$$

$$\Gamma_E(\tau) = E_0^2 e^{i2\pi\nu_0\tau} e^{2\frac{h_0}{f_c}(\sin^2(\pi f_c\tau) - \pi f_c \tau \mathrm{Si}(2\pi f_c \tau))},$$

❖ Analytic solution exists in the two extreme conditions $f_c \to \infty$ $f_c \to 0$

- When $f_c \to \infty$:

$$S_E(\nu) = E_0^2 \frac{h_0}{(\nu - \nu_0)^2 + (\pi h_0/2)^2}, \qquad (5)$$

and the line shape is Lorentzian with a width FWHM $= \pi h_0$ (this corresponds to the white noise previously mentioned).

- When $f_c \to 0$:

$$S_E(\nu) = E_0^2 \left(\frac{2}{\pi h_0 f_c}\right)^{1/2} e^{-\frac{(\nu-\nu_0)^2}{2h_0 f_c}}, \qquad (6)$$

and the line shape is Gaussian with a width FWHM $= (8\ln(2) h_0 f_c)^{1/2}$ that depends on the cutoff frequency f_c.

❖ Numerical evaluation is required otherwise.

Linewidth derivation from FNSD

<in case of Low-Pass filtered white frequency noise>

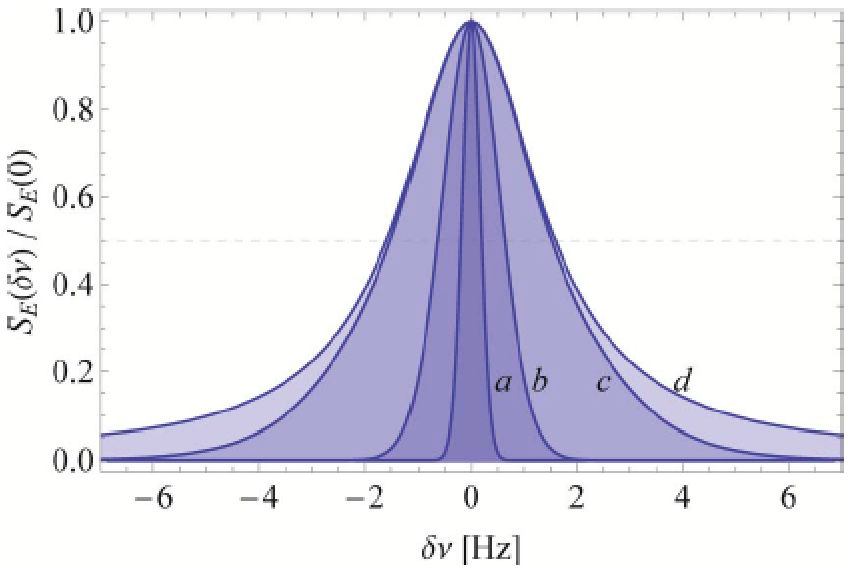

Fig. 1. (Color online) Numerical calculation of the laser line shape $S_E(\delta\nu)$ for a fixed frequency noise level $h_0 = 1\,\mathrm{Hz}^2/\mathrm{Hz}$ and different values of the cutoff frequency: a, $f_c = 0.03\,\mathrm{Hz}$; b, $f_c = 0.3\,\mathrm{Hz}$; c, $f_c = 3\,\mathrm{Hz}$; and d, $f_c = 30\,\mathrm{Hz}$. The line shapes are normalized to help the comparison of their full width at half-maximum (FWHM). The line shape evolves from a Gaussian when $f_c \ll h_0$ and to a Lorentzian when $f_c \gg h_0$.

observes that when $f_c \ll h_0$, the line shape is Gaussian and the linewidth increases with f_c. However, when $f_c \gg h_0$, the line shape becomes Lorentzian and the linewidth stops to increase (it will be shown later that the noise at high Fourier frequencies contributes only to the wings of the line shape). In order

Linewidth derivation from FNSD

<in case of Low-Pass filtered white frequency noise>

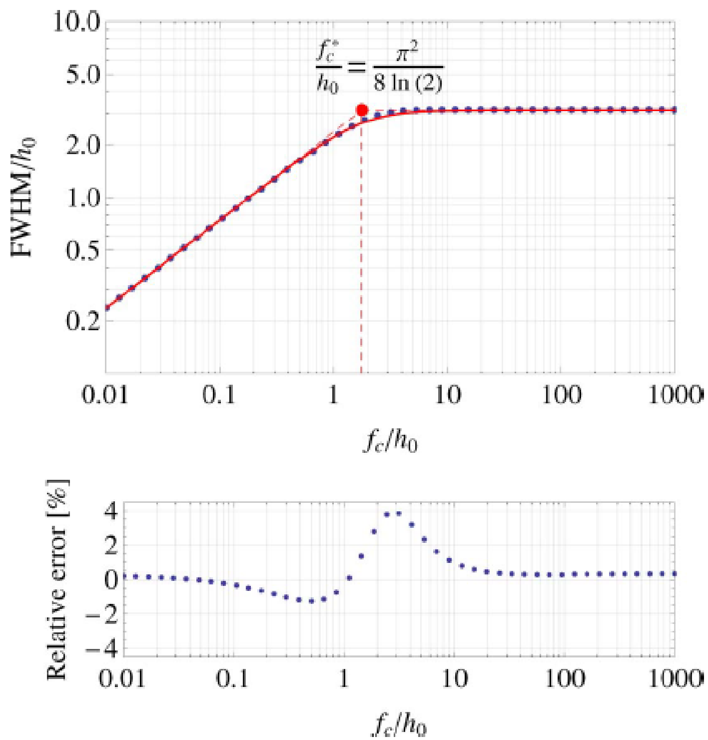

Fig. 2. (Color online) Upper graph: Numerical computation showing the evolution of the linewidth (FWHM) with the cutoff frequency f_c in the case of low-pass filtered white noise. The dots have been calculated by numerical integration of the exact relations Eqs. (1) and (2). The continuous line is given by our approximate formula Eq. (7). Both horizontal and vertical scales have been normalized to the noise level h_0. The behavior at low and high cutoff frequencies is indicated by the asymptotic response (red dashed lines). Lower graph: Relative error between the exact and approximate values.

sented in Fig. 2. We found that a good approximation valid for any f_c is given by the following expression:

$$\mathrm{FWHM} = h_0 \frac{(8\ln(2) f_c/h_0)^{1/2}}{\left[1 + \left(\frac{8\ln(2)}{\pi^2}\frac{f_c}{h_0}\right)^2\right]^{1/4}}, \qquad (7)$$

with a relative error smaller than 4% over the entire range of the cutoff frequency f_c as shown in the lower

$$\boxed{f_c^* = \frac{\pi^2}{8\ln(2)} h_0 \approx 1.78 h_0}$$

Simple Formula to Estimate the Laser Linewidth

<in case of arbitrary frequency noise>

β-separation line $\quad S_{\delta\nu}(f) = 8\ln(2)f/\pi^2$

$$S_{\delta\nu}(f) = f/1.78 \quad or\ Log[S_{\delta\nu}(f)] = Log[f] - 0.25$$

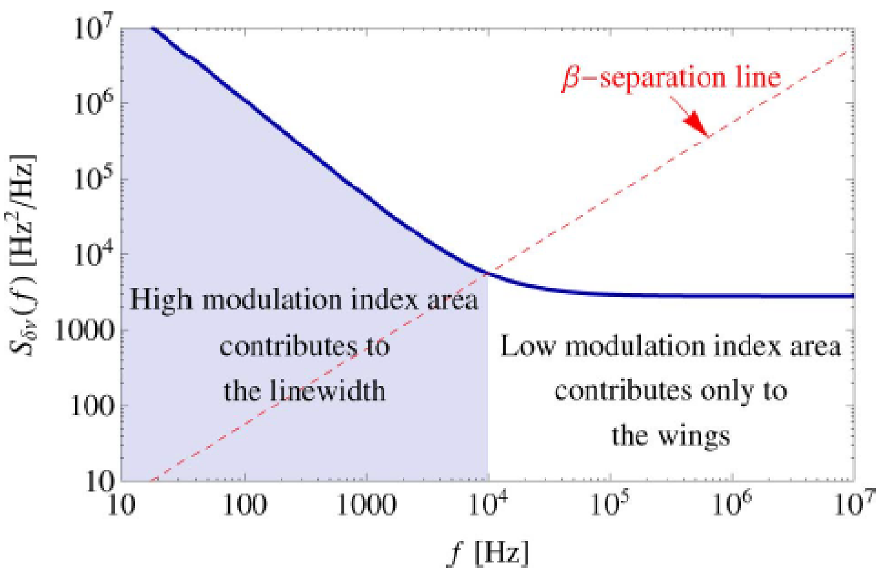

Fig. 3. (Color online) A typical laser frequency noise spectral density composed of flicker noise at low frequencies and white noise at high frequencies. The dashed line given by $S_{\delta\nu}(f) = 8\ln(2)f/\pi^2$ separates the spectrum into two regions whose contributions to the laser line shape is very different: the high modulation index area contributes to the linewidth, whereas the low modulation index area contributes only to the wings of the line shape (see the text for details).

tended to arbitrary noise spectra. Indeed, noise components in the high modulation index area with a spectral density higher than their Fourier frequency ($S_{\delta\nu}(f) > f$) give rise to Gaussian autocorrelation functions, which are multiplied together and then Fourier transformed to give the laser line shape. As a result, the line shape is a Gaussian function whose variance is the sum of the contributions of all high modulation index noise components. Therefore, one can obtain a good approximation of the laser linewidth by the following simple expression:

$$\boxed{\mathrm{FWHM} = (8\ln(2)A)^{1/2},} \qquad (9)$$

where A is the surface of the high modulation index area, i.e., the overall surface under the portions of $S_{\delta\nu}(f)$ that exceed the β-separation line (see Fig. 3)

$$A = \int_{1/T_o}^{\infty} H(S_{\delta\nu}(f) - 8\ln(2)f/\pi^2)S_{\delta\nu}(f)\mathrm{d}f, \qquad (10)$$

with $H(x)$ being the Heaviside unit step function ($H(x) = 1$ if $x \geq 0$ and $H(x) = 0$ if $x < 0$) and T_o being the measurement time that prevents the observation of low frequencies below $1/T_o$. This low frequency

❖Cf. recall Gaussian line shape

$$\mathrm{FWHM} = (8\ln(2)h_0 f_c)^{1/2}$$

Linewidth estimation from FNSD

<in case of pure flicker frequency noise>

$$S_{\delta\nu}(f) = af^{-\alpha}, \text{ with } 1 \le \alpha \le 2$$

$$\frac{S_{\delta\nu}(f)}{f_m} = \frac{8\ln(2)}{\pi^2}\left(\frac{f}{f_m}\right)^{-\alpha}$$

integrating Eq. (10), one obtains for $\alpha = 1$

$$\mathrm{FWHM} = f_m \frac{8\ln(2)}{\pi}[\ln(f_m T_o)]^{1/2}, \qquad (12)$$

and for $\alpha > 1$,

$$\mathrm{FWHM} = f_m \frac{8\ln(2)}{\pi}\left[\frac{(f_m T_o)^{\alpha-1} - 1}{\alpha - 1}\right]^{1/2}. \qquad (13)$$

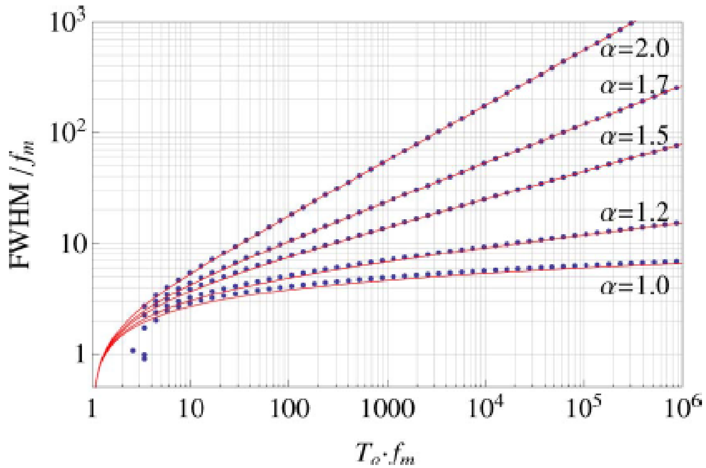

Fig. 5. (Color online) Evolution of the laser linewidth with respect to the measurement time in the case of a frequency noise spectrum composed of flicker noise as shown in Fig. 4. The dots have been obtained by numerical integration of the exact relation between the frequency noise and the line shape given by Eqs. (1) and (2). The red lines are the values given by the approximate formulas Eqs. (12) and (13).

the linewidth is a function of the observation time To

Application to laser linewidth reduction

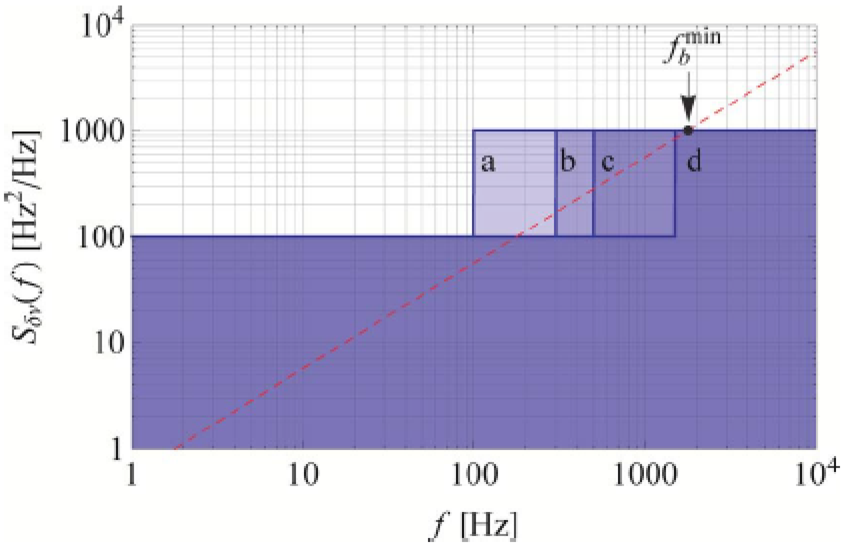

Fig. 6. (Color online) Frequency noise model used to study laser linewidth reduction using a servo loop. We assume that the free-running laser noise level $h_b = 1000\text{Hz}^2/\text{Hz}$ is reduced to $h_a = 100\text{Hz}^2/\text{Hz}$ with a servo loop having a bandwidth f_b of a, 100 Hz; b, 300 Hz; c, 500 Hz; and d, 1500 Hz. The dashed line represents the β-separation line. The minimum servo-loop bandwidth necessary to efficiently reduce the laser linewidth is $f_b^{\min} = \pi^2 h_b/(8\ln(2))$.

$$\Gamma_E(\tau) = E_0^2 e^{i2\pi\nu_0\tau} e^{-h_b\pi^2|\tau| - \frac{h_a - h_b}{f_b}\left(\omega_b\tau \mathrm{Si}(\omega_b\tau) - 2\sin^2\left(\frac{\omega_b\tau}{2}\right)\right)}$$

❖ Notice that this simplified noise model may also result from a laser showing initial **flicker** noise in free-running mode if the servo loop contains an **integral** part that reduces the flicker noise at low frequencies.

Application to laser linewidth reduction

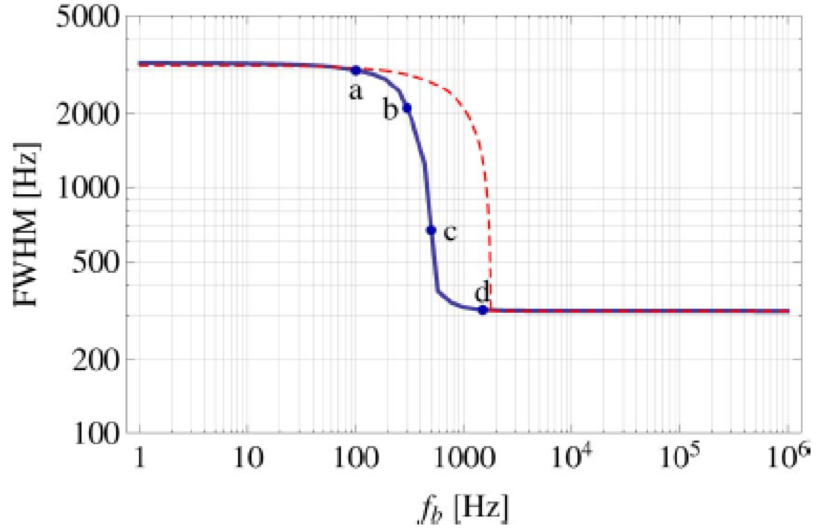

Fig. 7. (Color online) Evolution of the laser linewidth (FWHM) with the servo-loop bandwidth f_b for the frequency noise model presented in Fig. 6. Special values of the servo bandwidth, for which the line shape is represented in Fig. 8, are indicated by the following points: a, $f_b = 100$ Hz; b, $f_b = 300$ Hz; c, $f_b = 500$ Hz; and d, $f_b = 1500$ Hz. The continuous line has been obtained by numerical integration of the exact relation Eqs. (1) and (2), and the dashed line has been obtained with our approximate formula Eqs. (9) and (10).

sented in Figs. 7 and 8. We observe that the laser linewidth tends toward πh_b when the bandwidth f_b tends toward zero. This can be understood because the noise spectrum tends toward a white-type noise of spectral density h_b, leading to a Lorentzian profile of width πh_b. On the other hand, the linewidth drops down to πh_a when the bandwidth f_b tends toward infinity, since in this case, the noise spectrum approaches a white-type noise of spectral density h_a. In Fig. 7, we

Application to laser linewidth reduction

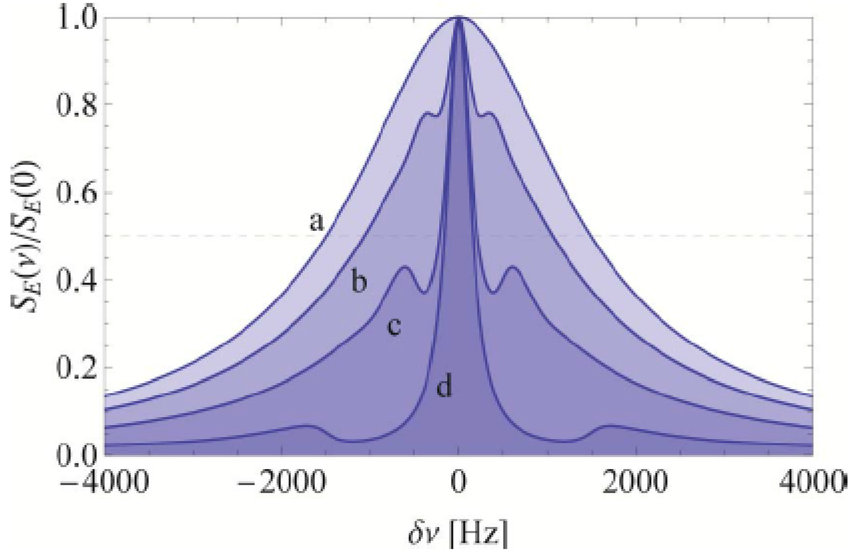

Fig. 8. (Color online) Evolution of the laser line shape with the servo-loop bandwidth for the frequency noise model presented in Fig. 6. We chose the following values of the servo bandwidth: a, $f_b = 100\,\text{Hz}$; b, $f_b = 300\,\text{Hz}$; c, $f_b = 500\,\text{Hz}$; and d, $f_b = 1500\,\text{Hz}$, which correspond to the points indicated in Fig. 7.

two sidebands appear outside of the servo bandwidth, i.e., at δv > f b, while the central part strongly narrows and becomes Lorentzian. Because of this radical change of line shape, the different linewidths at half-maximum are not similar in this range, and comparison with the Gaussian linewidth approximation Eqs. (9) and (10) loses its significance, which explains the observed discrepancy.

Application to laser linewidth reduction

explains the observed discrepancy. Nevertheless, our approximate formula is able to predict the minimum servo-loop bandwidth necessary to efficiently reduce the laser linewidth, which is given by $f_b^{\min} = \pi^2 h_b / (8 \ln(2))$. It depends on the free-running laser noise level h_b and corresponds to the situation in which the noise level h_b is entirely below the β-separation line for frequencies outside of the servo bandwidth

width, which is given by πh_a. Note that the final laser linewidth depends on the noise level h_a, and thus on the servo-loop gain at low frequency, but is independent of the servo bandwidth, provided that $f_b > f_b^{\min}$.

선폭이 1 MHz인 레이저의 선폭을 줄이려면 feedback servo의 control bandwidth는 최소한 얼마라야 할까?

1. 100 kHz
2. 570 kHz
3. 1 MHz
4. 3 MHz

$$f_b^{\min} = \frac{\pi^2 h_b}{8\ln(2)} = 1.78 h_b = \frac{1.78}{\pi}(\pi h_b) = 0.57\pi h_b$$

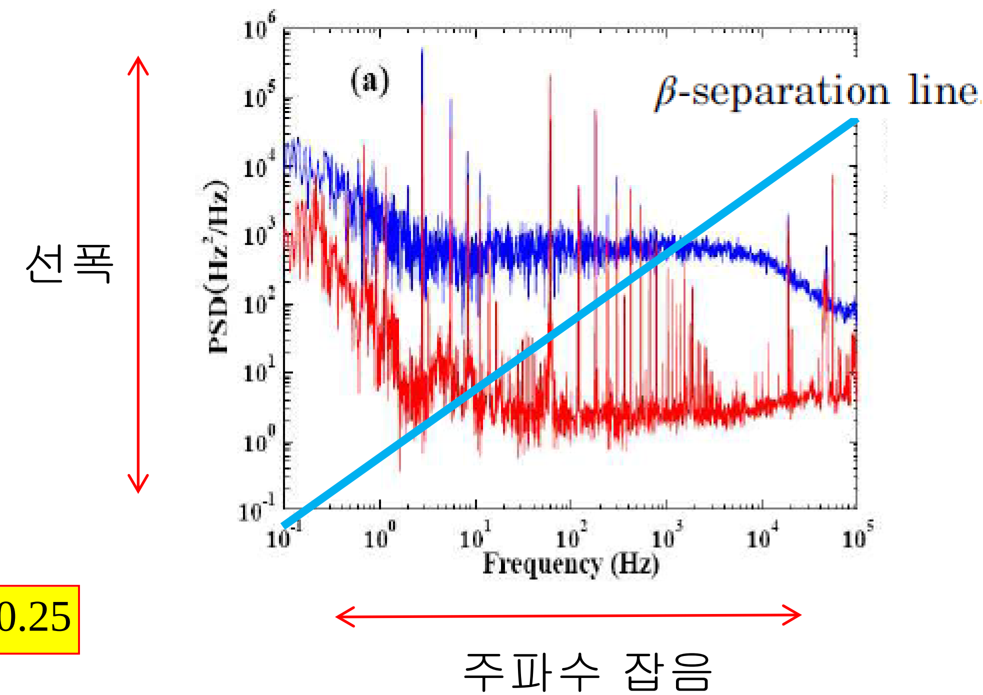

$S_{\delta\nu}(f) = f/1.78 \quad or\ Log[S_{\delta\nu}(f)] = Log[f] - 0.25$